U.S. DEPARTMENT OF COMMERCE / Environmental Science Services Administration
National Environmental Satellite Center

DIRECT TRANSMISSION SYSTEM
USERS GUIDE

APT

DRIR

U.S. DEPARTMENT OF COMMERCE
Maurice H. Stans, Secretary

ENVIRONMENTAL SCIENCE SERVICES ADMINISTRATION
Robert M. White, Administrator

ESSA DIRECT TRANSMISSION SYSTEM USERS GUIDE

prepared by the
National Environmental Satellite Center

Supersedes APT Users Guide (1965)

WASHINGTON, D.C.
1969

For sale by the Superintendent of Documents, U.S. Government Printing Office
Washington, D.C. 20402 - Price $2.25

FOREWORD

The APT Users Guide published in 1965 by the U.S. Department of Commerce, Environmental Science Services Administration (ESSA), National Weather Satellite Center, adequately described the existing techniques for acquiring, geographically locating and interpreting pictures transmitted by the Automatic Picture Transmission (APT) System of the ESSA and Nimbus spacecraft. The Nimbus research and development spacecraft also were used to flight test a real-time* infrared data system. Data formats and gridding procedures for this system were described in special National Aeronautics and Space Administration (NASA) publications provided to all of the APT stations known to ESSA and NASA. The launch of the first Improved TIROS Operational Satellite (ITOS) is expected in 1969; this spacecraft will carry the first operational infrared data system ever flown. This development emphasized the necessity for rewriting the 1965 APT Users Guide to include information about the acquisition and use of data from this new infrared system. In addition, research and daily use during the past few years have increased our understanding of the cloud patterns seen in pictures from the satellites. Therefore, the brief section on data interpretation has also been revised to include this newer information. For more detailed publications on interpretation, the reader is referred to the open literature.

---

* real-time: Time in reporting on events or recording of the events is simultaneous or nearly simultaneous with the events. For example, the real-time of a satellite is that time in which it simultaneously reports its environment as it encounters it.

ACKNOWLEDGMENTS

Credit is due to many people for the material presented in the ESSA Direct Transmission Systems Users Guide. Most of the information has been authored by the staff of the National Environmental Satellite Center. Details concerning the system design and technical procedures have been prepared by Mr. Arthur Schwalb. Chapter 8 on Meteorological Interpretation has been prepared under the direction of Mr. Vincent J. Oliver, Chief, Applications Group, NESC, with extensive assistance by Messrs. R. K. Anderson and Edward W. Ferguson, and Mrs. Frances C. Parmenter. Substantive review has been provided by Mr. Lee M. Mace and the staff of the Analysis Branch, NESC, Maj. Alfred C. Molla of the Air Weather Service Liaison Office, Cdr. William E. Willingham, U. S. Navy, and the staff of Project FAMOS (Fleet Applications of Meteorological Observations from Satellites). Illustrations were prepared by Mr. Larue F. Amacher. Finally, Mr. Paul E. Lehr, Planning and Coordination Group, NESC, has provided technical guidance concerning all aspects of the publication.

CONTENTS

LIST OF FIGURES

LIST OF TABLES

1. REAL-TIME DATA SYSTEMS FOR LOCAL USERS

During 1969 the Improved TIROS Operational Satellite System will be inaugurated. The spacecraft for this system - ITOS - will have two instrument packages that will broadcast real-time data for receipt by local ground stations now equipped to receive APT data. These subsystems are the now familiar APT (Automatic Picture Transmission) camera system which takes and immediately transmits pictures during daylight, and the Scanning Radiometer which may acquire and transmit data during both the daylight and dark portions of the orbit. The scanning radiometer concept was successfully flight-tested on Nimbus II and III by means of the Direct Readout Infrared (DRIR) system. Although the DRIR test transmissions were not universally accepted because of problems in presentation of the data, the tests did prove the feasibility of the system, and the data were considered useful at a number of receiving stations. Both systems are described below.

1.1 The Automatic Picture Transmission (APT) System.

The APT subsystem consists of a camera and an FM transmitter designed to broadcast television pictures of the cloud cover below the spacecraft during daylight. Transmission is automatic and immediate. A ground station with appropriate antenna, receiver and recorder can receive and display these pictures when the spacecraft is within acquisition range during the day.

The basic picture taking and transmission sequence is divided into two periods. During the first eight seconds, a "start" tone and horizontal phasing pulses are transmitted. The picture is taken during this period. During the interval that follows, the vidicon (TV tube) is scanned at four lines per second; the signals transmitted will produce a picture with scan lines essentially perpendicular to the orbit track.

From an altitude of 790 nautical miles (the altitude planned for operational use through 1970) the successive APT pictures will overlap almost 30 percent along the track. Pictures on successive orbits will be contiguous at the equator; overlap will increase with increasing latitude north or south. Mid latitude APT stations can expect to receive pictures from two to three (on rare occasions four) consecutive passes each day.

1.2 Direct Readout Infrared (DRIR)* Sensor

The DRIR system for real-time data transmission consists of a scanning radiometer and transmitter combination designed to transmit (in real-time) slow scan energy profiles (of reflected or emitted radiation) which can be converted to cloud cover pictures.

As the spacecraft moves along its orbit the radiometer scans the earth's surface from horizon to horizon, essentially perpendicular to the orbital track. The scan is generated by using the forward motion of the spacecraft to displace the sensing beam along the spacecraft track. The scan across the track is generated by a mirror continuously rotating (through 360 degrees) and reflecting energy to the sensor. Data as sensed are converted to electrical signals which are transmitted in real-time. The horizon to horizon scan of the earth uses approximately one third of the time for one revolution of the radiometer mirror. The remaining time is used to transmit synchronizing signals and calibration data.

---

*DRIR as used in this Users Guide refers to the signal output of a scanning "radiometer" system which may have a channel sensitive to energy from wave lengths outside the infrared region. For example, one channel of a two channel instrument may be sensitive in the visible range (0.5 to 0.7 microns) while the second channel is sensitive to infrared window (10.5 to 12.5 micron) radiation.

The following table lists the basic differences between APT and DRIR data significant to real-time data transmission users:

TABLE 1

APT	DRIR
Frame Format: Entire picture taken at one time	Individual lines of data generated and transmitted in real-time
Start tone and horizontal phasing transmitted before each picture	No start tone or horizontal phasing possible
Full scan line contains usable earth view data	Approximately 1/3 of scan line contains usable earth view data
Visible data only	Infrared or visible data possible
Fiducial reference marks on each picture	No reference marks in data area
Field of view limited by lens and vidicon	Full horizon to horizon view - may be limited on one side by a sun shield
Approximately 30% overlap (along track) between successive frames	Overlap between successive lines only. Depends on line width, mirror rotation rate and spacecraft altitude.

1.3 Transmission Frequencies

The ESSA and experimental Nimbus real-time data systems have made use of 3 assigned transmission frequencies. The Nimbus spacecraft have broadcast on 136.95 MHZ* while the ESSA series have alternated between 137.50 MHZ and 137.62 MHZ to eliminate possible interference between operating spacecraft in similar orbits. The specific frequency for a particular spacecraft is published in Part IV of the Daily Predict Message (Appendix A) routinely sent on meteorological communications networks.

* Megahertz

2. ORBITAL CONSIDERATIONS

2.1 General Aspects of Orbits and Their Effects:

When plans are made to place a meteorological satellite in orbit, three factors must be considered. In deciding how best to meet the mission requirement of daily global coverage these factors are: (1) the area of view of each sensor; (2) the orbital period and its relationship to the frequency and spatial continuity of observations; (3) the resolution of detail within the field of view of each sensor.

2.1.1 Coverage

Computing the area that can be seen by a sensor is a relatively simple geometric problem. APT pictures are taken by a camera lens and shutter combination which focuses an image on a vidicon tube. The angular field of view seen by the lens and then scanned from the tube can be determined from calibration data. It is not important from a geometric point of view if the entire 800 line picture or a portion (ex.600 lines) of it is reproduced; it is important that relative dimensions at equal distances from the picture center be the same. The diagram and equations below illustrate the method used for determining the distance on the earth from the satellite subpoint to any point in the picture. An angle, W_c for any point in the picture is determined from system calibration; lens and electronic distortions are considered in these computations. If nominal values are assumed, no distortion is considered.

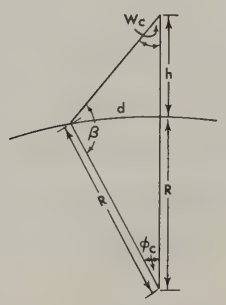

Figure 2-1 Geometry Diagram

W_c = angle of view

$\emptyset_c$ = geocentric angle to intersection of W_c on earth

R = radius of earth

h = spacecraft altitude

d = distance on earth from subpoint to picture point for viewing angle W_c

(1) $\sin \beta = \frac{(R+h)}{R} \sin W_c$

(2) $\phi_c = 180 - (W_c + \beta)$

(3) $d = \phi_c \times 60$ (nautical miles)

When a fixed lens camera is pointed normal to the earth's surface the area covered by each picture depends on spacecraft height alone (refer to Figure 2-1 and equations 1 & 2). The higher the spacecraft the larger the area viewed by the camera system. For example, the picture taken by an APT camera ($W_c = 45°$) at 750 nautical miles is approximately 867 nautical miles from center to side; at 400 nautical miles it is approximately 425 nautical miles. This factor forms the basis for the use of "universal" grids for geographic orientation of pictures from the APT camera system.

Computation of the area of view for a line scan system is equivalent to that above with the exception that angle W_c is limited to the area at right angles to the satellite heading line. The area viewed by a single scan line is essentially perpendicular to the direction in which the spacecraft is moving and has a component in the direction of movement equal to the line width on the earth.

Swath length is equal to the distance traveled by the spacecraft over the earth in the time given.

2.1.2 Orbital Period

The orbits of earth satellites, whether natural or man-made, are controlled by the same physical laws. A satellite in orbit follows a path that is the result of balanced forces; the acceleration of gravity on the satellite is exactly balanced by the outward component of the tangential linear velocity. The requirement for the existence of this balance permits the computation of the orbital speed and hence the orbital period of a satellite for any given height. The orbit period T, for a near circular orbit is:

$T = 84.4 \left(1 + \frac{h}{R}\right)^{3/2}$ minutes, where h is the altitude of the satellite and R is the radius of the earth. Thus, as h increases, T increases, as shown in Table 2:

TABLE 2

ALTITUDE/ORBIT PERIOD

Altitude		Orbit Period
h (Km)	h (n.mi.)	T (minutes)
371	200	91.9
834	450	101.5
1,112	600	107.4
1,390	750	113.5
1,462	790	115.1
-	-	-
35,790	19,312	1,440 (Synchronous altitude)

Since the orbit plane is essentially "fixed" in space for short-time periods, and the earth rotates within the orbit, the orbit period (T) determines the longitudinal distance between successive equatorial crossings. Thus, for a satellite orbit of 100 minutes this longitudinal distance is 25 degrees (one degree per four minutes). For example, if equator crossing "n" takes place at 75° W the next crossing (n + 1), 100 minutes later, will be at 100° W. This fact provides the basis of orbital position computations used in tracking and gridding procedures discussed later.

The altitude of the satellite thus determines the time difference and the longitudinal distance (ϕ_E) between successive equatorial crossings. If the data acquired on successive orbits are to be contiguous (just touch) at the equator, the swath width measured in geocentric angles ϕ_e-(ϕ_c at edge of picture) must equal the longitudinal distance between successive equator crossings. If contiguity is not possible at the equator ($\phi_e < \phi_E$), the lowest latitude (λo) at which contiguity occurs is where $\lambda o = \cos^{-1} \frac{\phi_e}{\phi_E}$. Data swaths that just touch

at the equator overlap by about 30 percent at 45 degrees of latitude.

2.1.3 Resolution

The resolution of elements in a television picture is determined basically by the number of scan (or raster) lines making up the image, and the picture width.

For example, if a picture represents an area 500 miles on a side, 500 scan lines will provide an average resolution of one mile over the picture; actual resolution decreases away from the picture center. When the picture is taken from 750 n. mi., using 800 scan lines and a 108-degree lens, the resolution of the APT pictures is roughly 1.47 n.mi. at the picture center and 4.67 n.mi. at the edge of the picture. Resolution of a line scan device is determined primarily by the instantaneous field of view of the sensor (spot size on the earth).

2.2 Selection of Orbit

A near polar, sun-synchronous orbit has been chosen for meteorological satellites with real-time transmission systems because it offers the best geometry for routine coverage on a regular basis. A sun synchronous orbit maintains the satellite in a relatively constant relationship to the sun so that the ascending node (northbound equator crossing) remains at a constant solar time, thus permitting receipt of data at approximately the same local time each day. The choice of time of day is based on meteorological and spacecraft operating considerations; no change is possible once the spacecraft has been launched.

2.3 Effects of Precession of Orbital Plane

2.3.1 Sun-synchronous Orbits with Earth-oriented Sensors

A satellite traveling in a sun-synchronous orbit can take pictures of any given area at the same local sun time each day. To maintain this sun-synchronous operation from week to week, it is necessary that precession $-\dot{\Omega}-$ of the orbital plane be 360 degrees in

354-645 O - 69 - 2

365 days to compensate for the earth's seasonal travel around the sun. Precession is a function of satellite altitude and orbital inclination and is given by the expression

$$\dot{\Omega} = 10.0\ a^{-3.5} \cos i \text{ (degrees/24 hours)}$$

where i is the orbital inclination to the equator, $a = (1 + h/R)$, $R = 3440$ n. mi., and h is average satellite height. The desired precession is achieved when the sun-synchronous inclination i_{ss} is such that:

$$\cos i_{ss} = 0.0986 \left(1 + \frac{h}{R}\right)^{3.5}$$

NOTE:
If the standard sign convention is followed, sun-synchronous precession is achieved when $\dot{\Omega}$ has the negative value - .986 and i_{ss} is greater than 90 degrees (a retrograde orbit). However, sun-synchronous may be taken to be positive, and the symbols i and i_{ss} for inclination are then defined to be the acute angle between the equatorial and orbital planes for a retrograde orbit.

The orbital inclination also defines the maximum geocentric latitude (north and south) reached by the satellite subpoint on each orbital pass. The maximum poleward excursions for sun-synchronous inclination for various satellite altitudes are:

TABLE 3

h (n.mi.)	i_{ss} (degrees)
450	81.1
600	79.9
750	78.6
1,000	75.9

2.4 Spacecraft Track Over the Earth

In the early 1600's Johann Kepler discovered the physical laws which control the paths and motions of satellites in orbit. Those laws which form the basis of computations at the local site are:

a. The orbit of each planet (satellite) is an ellipse with the sun (earth) always located at one focus.

b. Each planet (satellite) moves in an orbit so that an imaginary line drawn between the planet (satellite) and the sun (earth) sweeps out equal areas in equal times. (See figure below).

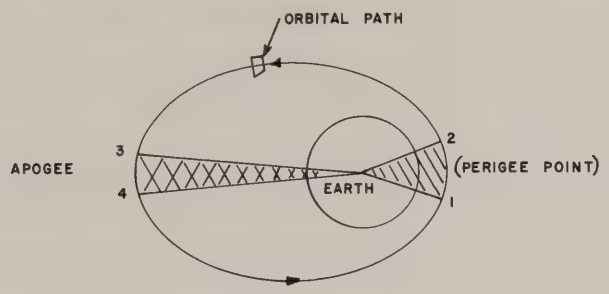

XXX TRIANGLE A
" B

FIGURE 2-2

Area of A will equal the Area of B when the time to move from 1 to 2 is equal to the time to move from 3 to 4.

In a perfectly circular orbit at any given altitude, a spacecraft moves above the surface of the earth at a constant velocity. In actual practice no earth orbit is perfectly circular; some may approach this condition. In an earth satellite's orbital ellipse, the point of closest approach to the earth is called perigee while the point farthest from the earth is the apogee. The initial position of apogee and perigee is determined by the launch characteristics; the gravity effect of the equatorial bulge of the earth has the effect of causing the positions of apogee and perigee to advance gradually around the orbit.

The motion of perigee and apogee cause the height at which the spacecraft passes over a given region of the earth to vary with time. (See Figure 2-3). Daily messages will reflect changes in the position of apogee and perigee.

For convenience and ease of computations, the time the spacecraft passes over a given geographical location is frequently expressed as the elapsed time between the northbound equator crossing (ascending node) and the time it reaches the particular location. In this way, time is considered zero when the spacecraft passes the equator northbound and

increases through a complete orbital period.

The time for a spacecraft to move through a given geocentric angle of its ellipse is considered to be constant for any particular day so that the time necessary for the spacecraft to reach a particular latitude is the same for every circuit of the earth on that day. For example, if it reaches latitude 30 degrees North ten minutes after the northbound equator crossing (ascending node) on one circuit of the earth, it will reach the same latitude (30° N) at ten minutes after the ascending node on each succeeding circuit of the earth during that day. The movement of apogee and perigee causes a very gradual change in the time necessary to reach this latitude on each circuit. These changes are included in the Daily Messages.

DIAGRAM SHOWING EFFECT OF THE MOVEMENT OF PERIGEE AND APOGEE POSITION

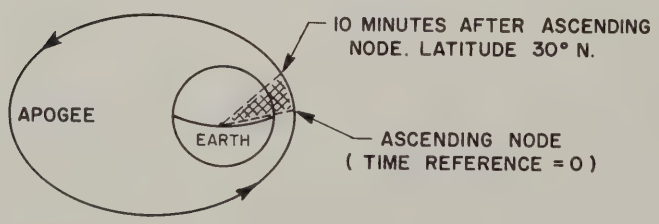

DAY I CONDITION : PERIGEE IS LOCATED AT THE EQUATOR.

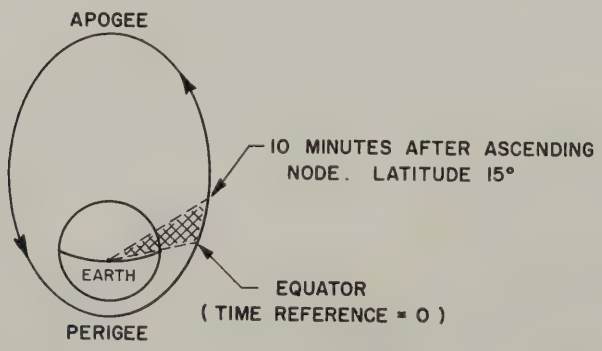

DAY N CONDITION : PERIGEE IS NEAR THE SOUTH POLE.

FIGURE 2-3

3. TRACKING PROCEDURES FOR DIRECTIONAL ANTENNAS USED TO ACQUIRE DATA FROM REAL-TIME TRANSMISSION SYSTEM SENSORS 1)

3.1 Introduction

A directional antenna is frequently used to receive signals from the real-time transmission system of meteorological satellites. These directional antennae combine high gain signal reception with minimum noise and are capable of acquiring data from a longer (line of sight) range. It is necessary to keep a directional antenna pointed at the spacecraft while data are being acquired. Though the required pointing accuracy is a function of antenna design and must be determined locally, the procedure explained here provides pointing data of sufficient accuracy for antennae usually used for this purpose.

To track the spacecraft properly, its location in relation to the receiving antenna must be known for the period when the spacecraft is within range of the station. The usual ground based tracking information is in terms of azimuth and elevation relative to the antenna location. This section describes procedures for determining those orbits where acquisition of data is possible, and the procedure for computing necessary tracking data.

3.2 Materials Needed

a.* Plotting Board - Polar Diagram (Figures 3-1 and 3-2)

b.* Tracking Diagram - Azimuth Great Circle Arc Length Diagram (Figure 3-3)

---

(1) Procedures outlined here may be useful for planning purposes even for stations using a non-directional antenna for data acquisition.

---

* Full size copies of the Plotting Board and Tracking Diagram are available on request for stations developing the capacity to receive real-time transmissions from meteorological satellites. The user should specify the latitude of his antenna when requesting these aids. Address: APT Coordinator, National Environmental Satellite Center, Environmental Science Services Administration, Washington, D.C. 20233

APT SYSTEM

METEOROLOGICAL SATELLITE

PLOTTING BOARD

AND

TRACKING DIAGRAM

APT STATION: _____

LOCATION: ____LAT.,____LONG.

ARACON LABORATORIES

A DIVISION OF ALLIED RESEARCH ASSOCIATES, INC
CONCORD MASSACHUSETTS

APRIL 1963

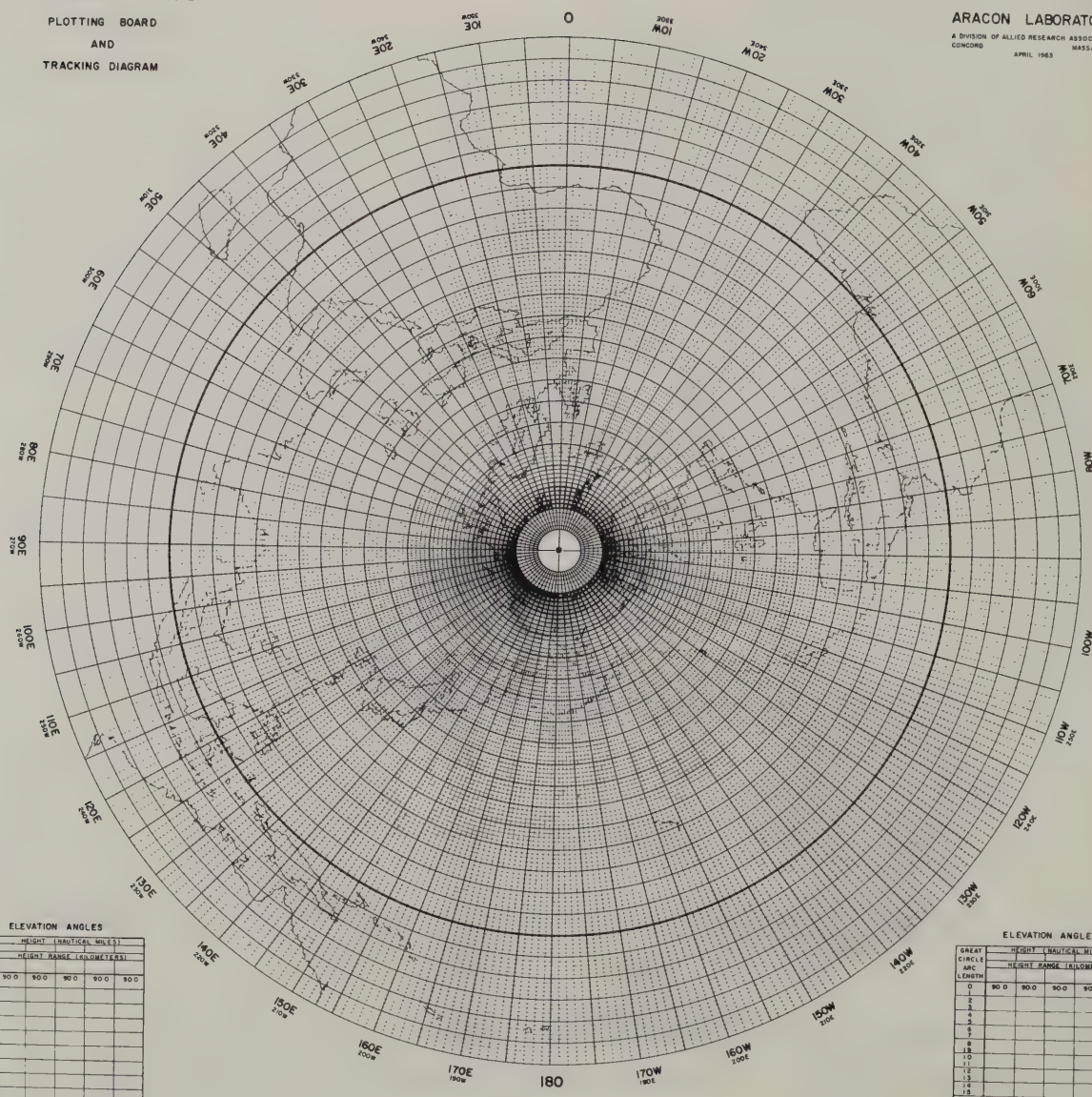

ELEVATION ANGLES

GREAT CIRCLE ARC LENGTH	HEIGHT (NAUTICAL MILES) / HEIGHT RANGE (KILOMETERS)				
0	90.0	90.0	90.0	90.0	90.0
1					
2					
3					
4					
5					
6					
7					
8					
9					
10					
11					
12					
13					
14					
15					
16					
17					
18					
19					
20					
21					
22					
23					
24					
25					
26					
27					
28					
29					
30					
31					
32					
33					
34					

ELEVATION ANGLES

GREAT CIRCLE ARC LENGTH	HEIGHT (NAUTICAL MILES) / HEIGHT RANGE (KILOMETERS)				
0	90.0	90.0	90.0	90.0	90.0
1					
2					
3					
4					
5					
6					
7					
8					
9					
10					
11					
12					
13					
14					
15					
16					
17					
18					
19					
20					
21					
22					
23					
24					
25					
26					
27					
28					
29					
30					
31					
32					
33					
34					

FIGURE 3-1

PLOTTING BOARD
NORTHERN HEMISPHERE

APT SYSTEM

METEOROLOGICAL SATELLITE
PLOTTING BOARD
AND
TRACKING DIAGRAM

APT STATION: _____

LOCATION: ____ LAT., ____ LONG.

ARACON LABORATORIES
A DIVISION OF ALLIED RESEARCH ASSOCIATES, INC.
CONCORD MASSACHUSETTS
APRIL 1963

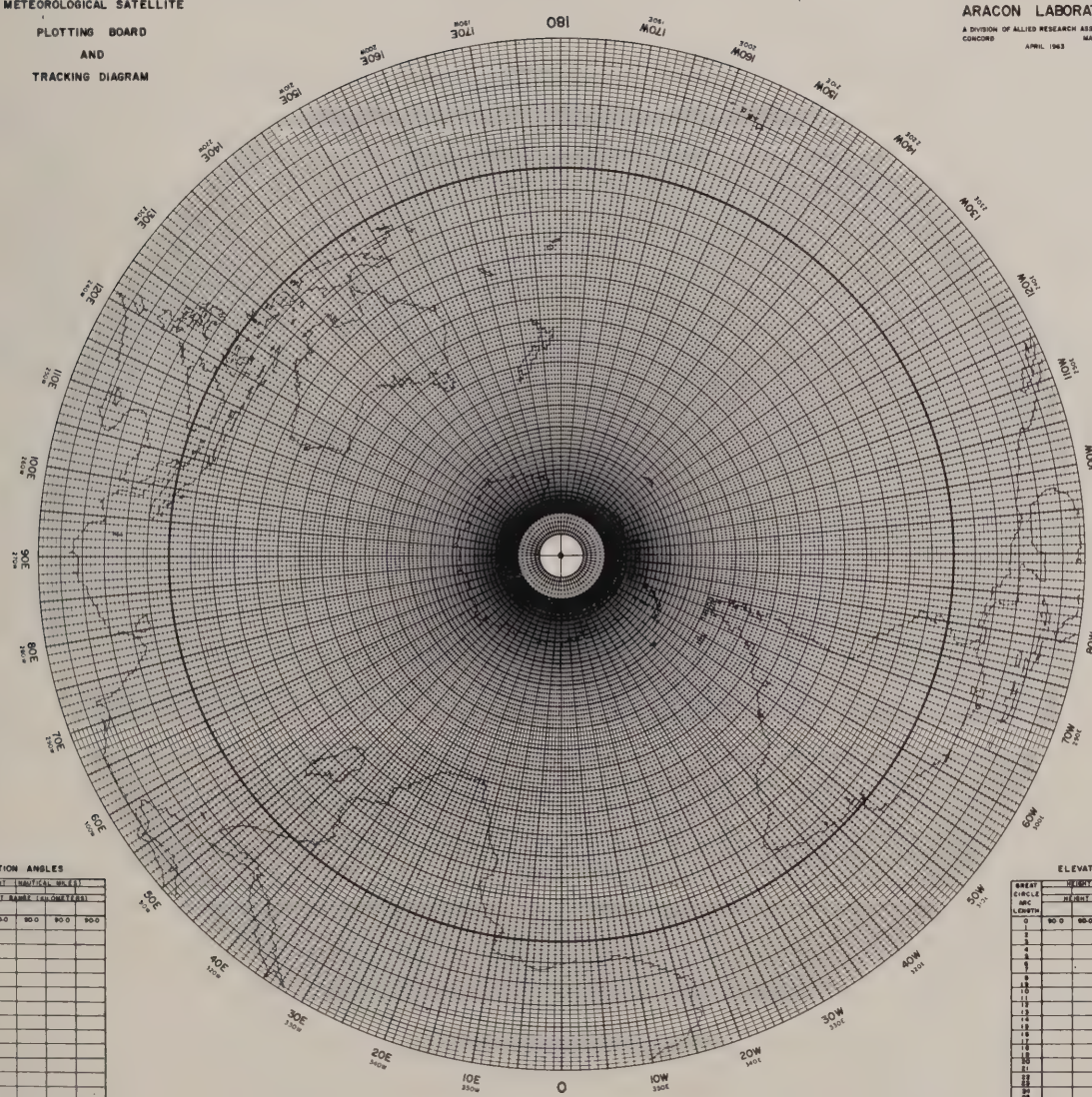

ELEVATION ANGLES

GREAT CIRCLE ARC LENGTH	HEIGHT (NAUTICAL MILES) HEIGHT RANGE (KILOMETERS)				
0	90.0	90.0	90.0	90.0	90.0
1					
2					
3					
4					
5					
6					
7					
8					
9					
10					
11					
12					
13					
14					
15					
16					
17					
18					
19					
20					
21					
22					
23					
24					
25					
26					
27					
28					
29					
30					
31					
32					
33					
34					
35					

ELEVATION ANGLES

GREAT CIRCLE ARC LENGTH	HEIGHT (NAUTICAL MILES) HEIGHT RANGE (KILOMETERS)				
0	90.0	90.0	90.0	90.0	90.0
1					
2					
3					
4					
5					
6					
7					
8					
9					
10					
11					
12					
13					
14					
15					
16					
17					
18					
19					
20					
21					
22					
23					
24					
25					
26					
27					
28					
29					
30					
31					
32					
33					
34					
35					

FIGURE 3-2

PLOTTING BOARD
SOUTHERN HEMISPHERE

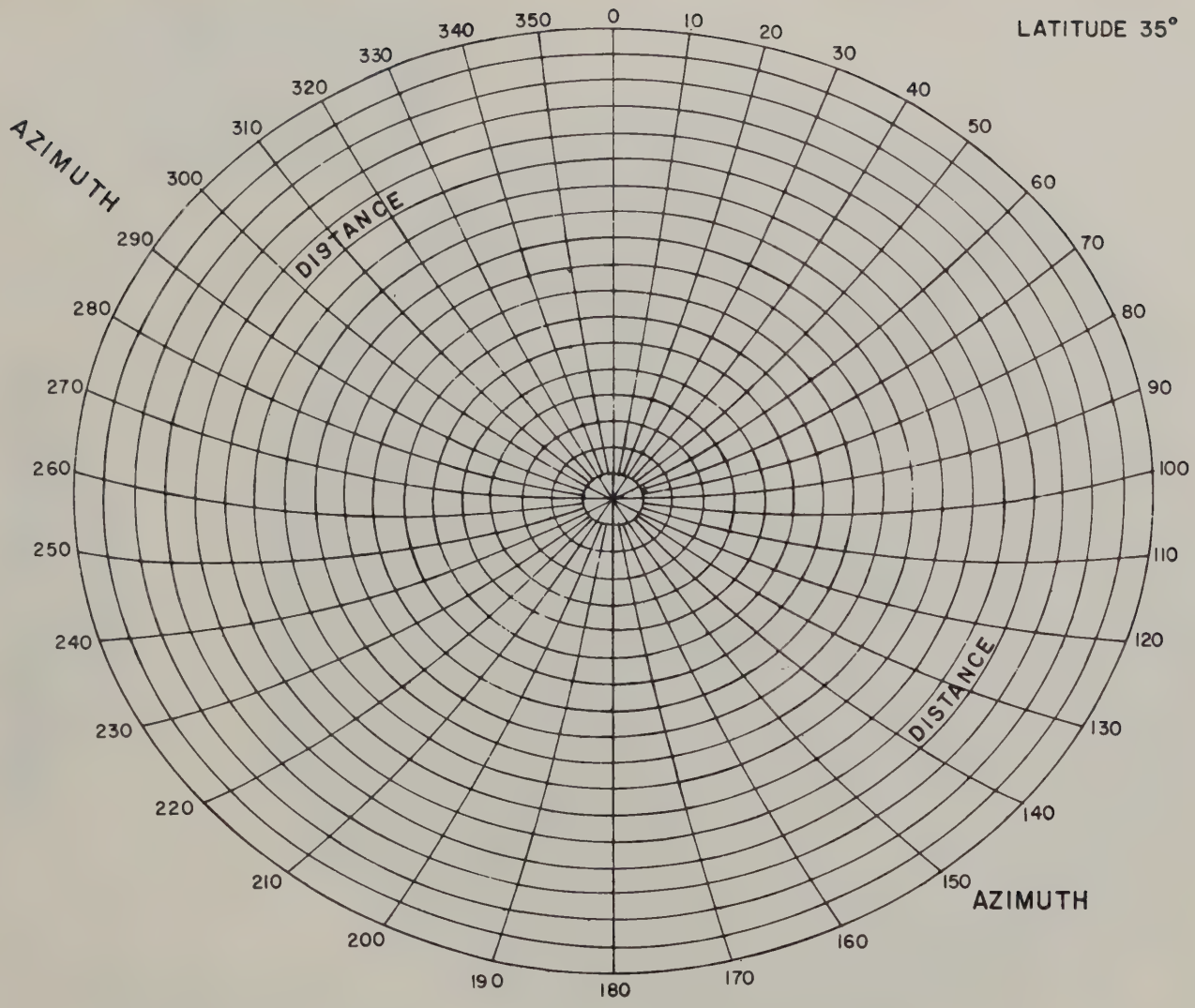

TRACKING DIAGRAM
AZIMUTH GREAT CIRCLE ARC LENGTH DIAGRAM
FOR LATITUDE 35 DEGREES

EACH ELLIPSE REPRESENTS A GREAT CIRCLE CENTERED AT THE STATION LOCATION (FOR THIS CASE NEAR 35 DEGREES LATITUDE).
INTERVAL OF ARC: 120 NAUTICAL MILES

FIGURE 3-3

c. Orbital Plot on Transparent Overlay

To be procured by and plotted at the local station from data in the Ephemeris Predict Message.

d. Ephemeris Predict (Daily) Message (Appendix A)

e. Clock. Accurate to one second

3.3 Description of Materials

3.3.1 Plotting Board (Figure 3-1 and 3-2)

The APT Plotting Board is a polar projection diagram of the earth centered at either pole and extending 30 degrees of latitude past the equator into the other hemisphere. The Board has radials from the pole representing one-degree intervals of longitude; each fifth radial is accentuated. Concentric circles on the projection represent latitudes. The equatorial latitude (zero degrees) is represented by a heavier circle for clarity.

3.3.2 Tracking Diagram (an example for latitude 35 degrees is shown in Figure 3-3)

3.3.2.1 Theory

Azimuth is a function of the direction of the spacecraft from the antenna site and can be measured on any convenient map upon which the station and spacecraft location can be plotted.

Spacecraft elevation angle is a function of the spatial location (position and height) of the spacecraft and the ground station antenna (see Figure 3-4 below).

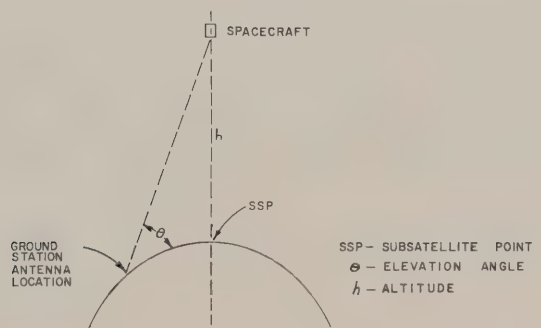

FIGURE 3-4

If the spacecraft altitude (h) and the distance from the ground station antenna to the spacecraft subpoint are known the elevation angle (θ) of the spacecraft can be computed.

3.3.2.2 Application

The Tracking Diagram (Figure 3-3) was designed for use with the Plotting Board and is constructed to show azimuth and distance of the spacecraft from the antenna site for a given subpoint position. The concentric curves (near ellipses) are isopleths of great circle arc distance drawn at two-degree (120 nautical mile) intervals.

Azimuth is used directly in tracking; arc distance (geocentric degrees) must be converted to elevation angle. Table 4 and 5 provide a convenient conversion from arc length to elevation angle. It should be noted here that the arc distance on the diagram can be converted to and labeled directly as elevation angles. This is particularly desirable if a circular orbit is achieved since, once labeled, the diagram need not be changed during the lifetime of the spacecraft. An elliptical orbit requires frequent changes of labels so use of the tables is recommended in place of labeling.

A Tracking Diagram is available for each five-degree latitude belt. The diagram drawn for the latitude closest to the antenna location should be used since the scale changes significantly with latitude.

3.3.3 Orbital Plot on Transparent Overlay

A transparent overlay is centered at the pole on the Plotting Board. The subpoint track for the spacecraft from which data are to be acquired is plotted on this overlay.

3.3.4 Ephemeris Predict Message*

Data required by the ground stations for tracking and picture gridding purposes will be provided routinely in a Daily Message transmitted over world wide meteorological teletype circuits.

---

* The schematic message format and code explanation is contained in Appendix A.

3.3.4.1 Daily Message

The Daily Message is divided into four basic parts. Part I contains the following information:

a. Equator crossing time and longitude for every fourth orbit through an orbital day. The first equator crossing data pertain to the reference orbit for which detailed spatial locations are given in Parts II and III of the message.

b. Nodal Period (the time between successive equator crossings).

c. Nodal longitudinal increment (degrees of longitude between successive equator crossings).

Part II (Day) contains predicted subpoint and height data at two-minute intervals for the portion of the orbit that is sunlit north of the equator.

Part II (Night) contains predicted subpoint and height data at two-minute intervals for the portion of the orbit in darkness north of the equator.

Part III (Day) contains predicted subpoint and height data at two-minute intervals for the portion of the orbit that is sunlit south of the equator.

Part III (Night) contains predicted subpoint and height data at two-minute intervals for the portion of the orbit in darkness south of the equator.

Part IV is reserved for "remarks" pertinent to the operational aspects of the system. For example, spacecraft real time data transmitting frequency is given here routinely.

3.3.5 Clock

It is necessary to have a station clock readily available when tracking (if a directional antenna is used) and when acquiring data. This clock should be accurate to ± one second and easily read if accurate data location is to result. Since the spacecraft moves over the earth at approximately 180 nautical miles per minute, a one second time error results in a location error of 3 nautical miles.

3.4 Procedures

3.4.1 Initial Preparation*

* An example is included as Appendix B & C.

Center the appropriate tracking diagram on the Plotting Board at the location (latitude and longitude) of the antenna site. The zero degree azimuth line must always point toward the pole and the 0-180 radial must be parallel to a longitude line.

NOTE: Southern Hemisphere stations must re-label azimuth lines after the diagram is in place so that the zero-degree azimuth refers to North.

3.4.2 Post Launch Preliminary Preparation

3.4.2.1 Transparent Orbital Overlay:

a. Plot the orbital path on the Plotting Board overlay using the data in the first valid Daily Message. Subdivide the track into one-minute intervals starting with minute zero at the equator. All points, therefore, will be plotted at a time relative to the ascending node (northbound equator crossing).

NOTE: Spacecraft of the operational meteorological system beginning in 1969 are expected to have real time transmission systems operating both by day and by night. Stations with the capability of receiving and displaying both types of transmissions should plot the orbital subpoint track for both times of day as indicated in the Daily Message.

b. Subdivide the equatorial line (on the orbital overlay) into divisions equal to the nodal increment. Begin at the reference orbit and progress in a westward direction through 360 degrees numbering sequentially from the reference orbit. Since the equator crossing for every fourth orbit is given in Part I of the Daily Message, with the reference orbit set properly, these points may be plotted directly to eliminate possible error.

3.4.2.2 Equator Line on Plotting Board

Determine and indicate on the equator line of the Plotting Board the acquisition zone of equator crossings (ascending nodes) that will bring the spacecraft within range of the antenna site.* There will be two zones - one for the sunlit portion of the orbit and one for the night portion. These should be labeled appropriately:

---

* Example, Appendix B

a. From the data in Table 4 on page 21, determine the arc distance (refer to theory, page 15) for a zero degree antenna elevation when the spacecraft is at apogee (this provides an estimate of the maximum range from which data acquisition is possible).

b. Indicate the zero degree line directly on the tracking diagram.

c. Rotate the previously plotted orbital overlay diagram until the subpoint track (for the portion of the orbit where the spacecraft is heading northward) until it is tangent to the zero-degree elevation circle east of the antenna site. Indicate the longitude of the equator crossing (ascending node) of the plotted subpoint track. Rotate the orbital overlay until the subpoint track is tangent to the zero-degree elevation circle west of the antenna site. Again, determine longitude of the equator crossing (ascending node). Orbits whose ascending nodes fall between the two longitudes determined are (assuming no local obstruction) generally within line of sight of the spacecraft during the northward portion of these orbits.

d. Repeat the process (b) for the portion of the orbit where the spacecraft is headed southward to determine the corresponding longitudinal range for southbound acquisition.

For practical application, it will be found that the elevation of the spacecraft will have to exceed zero to five degrees above the horizon for at least four to five minutes during a pass before useful data can be expected. Exact limits can be determined by experience, and the longitudinal belts can be adjusted accordingly.

3.4.3 Daily Preparation - Derivation of Tracking Data (Example, Appendix C)

a. Determine from the Daily Message the exact equator crossing (longitude and time) of the orbits from which data are to be acquired.

a.1 Place the ascending node of the plotted subpoint track overlay for the Plotting Board at the longitude of the ascending node of the reference orbit.

a.2 Read directly the longitude of the ascending nodes and the number of orbital increments from the reference orbit to the equator

crossings within the acquisition zone determined in 3.4.2.2

a.3 Mathematically determine the equator crossing time of those orbits from which data is to be acquired by adding the proper number (as determined above) of nodal periods (Daily Message) to the equator crossing time of the reference orbit. The exact longitude of the equator crossings may be determined in a similar manner if desired. For most purposes, however, the graphical solution will prove to be of sufficient accuracy.

b. Rotate the transparent orbital overlay until the ascending node of the plotted subpoint track is at the exact longitude of the orbit from which data are to be acquired.

c. Read directly the azimuth and arc distance* of the satellite (from the station) at the plotted points (one-minute intervals) along the track when the track is within the zero-degree elevation circle. The point of maximum elevation angle (minimum arc distance) may be included as a supplementary datum point.

d. Convert arc distance* to elevation angle.

e. Convert the time for each minute (which is relative to the equator crossing time) to GMT.

f. Check the accuracy of the clock. Set to be accurate within one second.

NOTE: When a relatively circular orbit is achieved and absolute pointing accuracy is not required, antenna predicts (with time relative to the equator crossing) may be re-used for future orbits with similar equator crossing longitudes. It has been found for instance that it is entirely feasible to use a single antenna predict for ESSA 6 equator crossings within ± 1 degree of the nominal predict. GMT (clock) time must be up-dated for the actual equator crossing time as determined from the daily message.

---

* Refer to section 3.3.2.2. If a relatively circular orbit has been achieved, the great circle arc lengths should have been converted to and labeled with their equivalent elevations for ease of computation.

TABLE 4

GREAT CIRCLE ARC LENGTH AT
ZERO DEGREE ELEVATION

Orbit Height (Nautical Miles)	Arc Length	Height (Kilometers)	Arc Length
100	13.6	200	14.2
125	15.2	250	15.8
150	16.6	300	17.3
175	17.9	350	18.6
200	19.1	400	19.8
225	20.2	450	20.9
250	21.2	500	22.0
275	22.2	550	23.0
300	23.1	600	23.9
325	24.0	650	24.9
350	24.8	700	25.7
375	25.6	750	26.5
400	26.4	800	27.3
425	27.1	850	28.1
450	27.8	900	28.8
475	28.5	950	29.5
500	29.2	1000	30.2
525	29.8	1050	30.9
550	30.4	1100	31.5
575	31.0	1150	32.1
600	31.6	1200	32.7
625	32.2	1250	33.3
650	32.7	1300	33.9
675	33.3	1350	34.4
700	33.8	1400	34.9
725	34.3	1450	35.5
750	34.8	1500	36.0
775	35.3	1550	36.5
800	35.8	1600	36.9
825	36.2	1650	37.4
850	36.7	1700	37.9
875	37.1	1750	38.3
900	37.6	1800	38.8

TABLE 5

ELEVATION ANGLE AS FUNCTION OF GREAT CIRCLE ARC LENGTH AND ALTITUDE

GREAT CIRCLE ARC LENGTH	Altitude (Nautical Miles) 200	225	250	275	300	325	350	375	400
	Altitude Range (Kilometers) 348 /393	394 /439	440 /486	487 /532	533 /578	579 /625	626 /671	672 /717	718 /764
0	90.0	90.0	90.0	90.0	90.0	90.0	90.0	90.0	90.0
1	71.5	73.3	74.8	76.0	77.1	78.0	78.7	79.5	80.0
2	57.9	60.8	63.2	65.1	66.9	68.3	69.6	70.8	71.8
3	46.2	49.4	52.2	54.7	56.9	58.8	60.5	62.0	63.4
4	37.3	40.6	43.5	46.1	48.4	50.6	52.5	54.3	55.9
5	30.7	33.7	36.5	39.1	41.5	43.7	45.7	47.6	49.3
6	25.5	28.3	31.0	33.4	35.8	37.9	39.9	41.8	43.6
7	21.4	24.0	26.4	28.8	31.0	33.1	35.0	36.9	38.6
8	18.1	20.5	22.8	24.9	27.0	28.9	30.8	32.6	34.3
9	15.3	17.5	19.6	21.6	23.5	25.4	27.2	28.9	30.5
10	12.9	15.0	16.9	18.8	20.6	22.3	24.0	25.7	27.2
11	10.9	12.7	14.5	16.3	18.0	19.6	21.2	22.8	24.3
12	9.1	10.8	12.5	14.1	15.7	17.3	18.8	20.2	21.7
13	7.4	9.0	10.6	12.2	13.7	15.1	16.6	18.0	19.3
14	6.0	7.5	8.9	10.4	11.8	13.2	14.5	15.9	17.1
15	4.6	6.0	7.4	8.8	10.1	11.4	12.7	14.0	15.2
16	3.4	4.7	6.0	7.3	8.6	9.8	11.0	12.2	13.4
17	2.2	3.5	4.7	5.9	7.1	8.3	9.5	10.6	11.7
18	1.1	2.3	3.5	4.6	5.8	6.9	8.0	9.1	10.1
19	.1	1.2	2.3	3.4	4.5	5.6	6.6	7.7	8.7
20	*	.2	1.2	2.3	3.3	4.4	5.4	6.3	7.3
21	*	*	.2	1.2	2.2	3.2	4.1	5.1	6.0
22	*	*	*	.2	1.1	2.1	3.0	3.9	4.8
23	*	*	*	*	.1	1.0	1.9	2.7	3.6
24	*	*	*	*	*	*	.8	1.7	2.5
25	*	*	*	*	*	*	*	.6	1.4
26	*	*	*	*	*	*	*	*	.4

TABLE 5 Continued

ELEVATION ANGLE AS FUNCTION OF GREAT CIRCLE ARC LENGTH AND ALTITUDE

	ALTITUDE (NAUTICAL MILES)							
	425	450	475	500	525	550	575	600
	ALTITUDE RANGE (KILOMETERS)							
	765 /810	811 /856	857 /903	904 /949	950 /995	996 /1042	1043 /1088	1089 /1134
0.	90.0	90.0	90.0	90.0	90.0	90.0	90.0	90.0
1.	80.5	81.0	81.4	81.8	82.1	82.5	82.7	83.0
2.	72.7	73.5	74.2	74.9	75.5	76.0	76.5	77.0
3.	64.6	65.7	66.8	67.7	68.5	69.3	70.0	70.7
4.	57.3	58.7	59.9	61.0	62.0	63.0	63.9	64.7
5.	50.9	52.3	53.7	54.9	56.1	57.2	58.2	59.1
6.	45.2	46.7	48.1	49.5	50.7	51.9	53.0	54.0
7.	40.2	41.8	43.2	44.6	45.9	47.1	48.2	49.4
8.	35.9	37.4	38.9	40.3	41.6	42.8	44.0	45.1
9.	32.1	33.6	35.0	36.3	37.6	38.9	40.0	41.2
10.	28.7	30.1	31.5	32.8	34.1	35.3	36.5	37.6
11.	25.7	27.1	28.4	29.7	30.9	32.1	33.3	34.4
12.	23.0	24.3	25.6	26.9	28.1	29.2	30.4	31.4
13.	20.6	21.9	23.1	24.3	25.5	26.6	27.6	28.7
14.	18.4	19.6	20.8	21.9	23.0	24.1	25.2	26.2
15.	16.4	17.5	18.7	19.8	20.8	21.9	22.9	23.9
16.	14.5	15.6	16.7	17.8	18.8	19.8	20.8	21.7
17.	12.8	13.8	14.9	15.9	16.9	17.9	18.8	19.7
18.	11.2	12.2	13.2	14.2	15.1	16.1	17.0	17.9
19.	9.7	10.7	11.6	12.6	13.5	14.4	15.3	16.1
20.	8.3	9.2	10.1	11.0	11.9	12.8	13.6	14.5
21.	6.9	7.8	8.7	9.6	10.4	11.3	12.1	12.9
22.	5.7	6.5	7.4	8.2	9.0	9.8	10.6	11.4
23.	4.5	5.3	6.1	6.9	7.7	8.5	9.3	10.0
24.	3.3	4.1	4.9	5.7	6.4	7.2	7.9	8.7
25.	2.2	3.0	3.7	4.5	5.2	6.0	6.7	7.4
26.	1.1	1.9	2.6	3.3	4.1	4.8	5.5	6.2
27.	.1	.8	1.5	2.3	2.9	3.6	4.3	5.0
28.	*	*	.5	1.2	1.9	2.5	3.2	3.8
29.	*	*	*	.2	.8	1.5	2.1	2.7
30.	*	*	*	*	*	.4	1.1	1.7

354-645 O - 69 - 3

TABLE 5 Continued

ELEVATION ANGLE AS FUNCTION OF GREAT CIRCLE ARC LENGTH AND ALTITUDE

	ALTITUDE (NAUTICAL MILES)							
	625	650	675	700	725	750	775	800
	ALTITUDE RANGE (KILOMETERS)							
	1135 /1181	1182 /1227	1228 /1273	1274 /1320	1321 /1366	1367 /1413	1414 /1459	1460 /1505
0.	90.0	90.0	90.0	90.0	90.0	90.0	90.0	90.0
1.	83.2	83.5	83.7	83.8	84.0	84.2	84.3	84.5
2.	77.4	77.8	78.2	78.6	78.9	79.2	79.4	79.7
3.	7.13	71.9	72.4	72.9	73.4	73.8	74.2	74.6
4.	65.5	66.2	66.9	67.5	68.1	68.6	69.1	69.7
5.	60.0	60.9	61.7	62.4	63.1	63.7	64.3	64.9
6.	55.0	55.9	56.8	57.6	58.3	59.1	59.8	60.4
7.	50.4	51.3	52.3	53.1	53.9	54.8	55.5	56.2
8.	46.1	47.1	48.1	49.0	49.9	50.7	51.5	52.3
9.	42.2	43.3	44.2	45.2	46.1	46.9	47.7	48.5
10.	38.7	39.7	40.7	41.7	42.6	43.3	44.3	45.1
11.	35.5	36.5	37.5	38.4	39.3	40.2	41.0	41.8
12.	32.5	33.5	34.4	35.4	36.3	37.1	38.0	38.8
13.	29.7	30.7	31.7	32.6	33.5	34.3	35.2	36.0
14.	27.2	28.2	29.1	30.0	30.9	31.8	32.6	33.4
15.	24.8	25.8	26.7	27.6	28.5	29.3	30.1	30.9
16.	22.7	23.6	24.5	25.4	26.2	27.0	27.8	28.6
17.	20.6	21.5	22.4	23.2	24.1	24.9	25.7	26.4
18.	18.8	19.6	20.5	21.3	22.1	22.8	23.6	24.4
19.	17.0	17.8	18.6	19.4	20.2	21.0	21.7	22.4
20.	15.3	16.1	16.9	17.7	18.4	19.2	19.9	20.6
21.	13.7	14.5	15.2	16.0	16.7	17.4	18.2	18.8
22.	12.2	13.0	13.7	14.4	15.1	15.8	16.5	17.2
23.	10.8	11.5	12.2	12.9	13.6	14.3	15.0	15.6
24.	9.4	10.1	10.8	11.5	12.2	12.8	13.5	14.1
25.	8.1	8.8	9.4	10.1	10.8	11.4	12.0	12.7
26.	6.8	7.5	8.2	8.8	9.4	10.1	10.7	11.3
27.	5.6	6.3	6.9	7.5	8.2	8.8	9.4	10.0
28.	4.5	5.1	5.7	6.3	6.9	7.5	8.1	8.7
29.	3.3	4.0	4.6	5.1	5.7	6.3	6.9	7.4
30.	2.3	2.8	3.4	4.0	4.6	5.1	5.7	6.2
31.	1.2	1.8	2.3	2.9	3.5	4.0	4.5	5.1
32.	.2	.7	1.3	1.8	2.4	2.9	3.4	4.0
33.	*	*	.3	.8	1.3	1.9	2.4	2.9
34.	*	*	*	*	.3	.8	1.3	1.8
35.	*	*	*	*	*	*	.3	.8

TABLE 5 Continued

ELEVATION ANGLE AS FUNCTION OF GREAT CIRCLE ARC LENGTH AND ALTITUDE

	ALTITUDE (NAUTICAL MILES)							
	825	850	875	900	925	950	975	1000
	ALTITUDE RANGE (KILOMETERS)							
	1506 /1551	1552 /1598	1599 /1644	1645 /1690	1691 /1736	1737 /1783	1784 /1829	1830 /1875
0.	90.0	90.0	90.0	90.0	90.0	90.0	90.0	90.0
1.	84.6	84.8	84.9	85.0	85.1	85.2	85.3	85.4
2.	80.0	80.2	80.4	80.6	80.8	81.0	81.2	81.4
3.	75.0	75.3	75.6	75.9	76.2	76.5	76.7	77.0
4.	70.1	70.5	71.0	71.4	71.7	72.1	72.5	72.8
5.	65.5	66.0	66.5	67.0	67.4	67.9	68.3	68.7
6.	61.1	61.7	62.2	62.8	63.3	63.8	64.2	64.7
7.	56.9	57.5	58.2	58.7	59.3	59.9	60.4	60.9
8.	53.0	53.7	54.3	55.0	55.6	56.1	56.7	57.3
9.	49.3	50.0	50.7	51.4	52.0	52.6	53.2	53.8
10.	45.8	46.6	47.3	48.0	48.6	49.3	49.9	50.5
11.	42.6	43.4	44.1	44.8	45.5	46.1	46.8	47.4
12.	39.6	40.4	41.1	41.8	42.5	43.2	43.8	44.5
13.	36.8	37.5	38.3	39.0	39.7	40.4	41.0	41.6
14.	34.2	34.9	35.6	36.3	37.0	37.7	38.4	49.0
15.	31.7	32.4	33.1	33.9	34.5	35.2	35.9	36.5
16.	29.3	30.1	30.8	31.5	32.2	32.8	33.5	34.1
17.	27.2	27.9	28.6	29.3	30.0	30.6	31.3	31.9
18.	25.1	25.8	26.5	27.2	27.8	28.5	29.1	29.7
19.	23.2	23.8	24.5	25.2	25.8	26.5	27.1	27.7
20.	21.3	22.0	22.6	23.3	23.9	24.6	25.2	25.8
21.	19.5	20.2	20.8	21.5	22.1	22.7	23.3	23.9
22.	17.9	18.5	19.1	19.8	20.4	21.0	21.6	22.2
23.	16.3	16.9	17.5	18.1	18.7	19.3	19.9	20.5
24.	14.7	15.4	16.0	16.6	17.2	17.7	18.3	18.9
25.	13.3	13.9	14.5	15.1	15.6	16.2	16.8	17.3
26.	11.9	12.5	13.0	13.6	14.2	14.7	15.3	15.8
27.	10.5	11.1	11.7	12.2	12.8	13.3	13.8	14.4
28.	9.2	9.8	10.3	10.9	11.4	11.9	12.5	13.0
29.	8.0	8.5	9.1	9.6	10.1	10.6	11.1	11.6
30.	6.8	7.3	7.8	8.4	8.9	9.4	9.9	10.3
31.	5.6	6.1	6.6	7.1	7.6	8.1	8.6	9.1
32.	4.5	5.0	5.5	6.0	6.5	6.9	7.4	7.9
33.	3.4	3.9	4.3	4.8	5.3	5.8	6.2	6.7
34.	2.3	2.8	3.2	3.7	4.2	4.6	5.1	5.5
35.	1.3	1.7	2.2	2.6	3.1	3.5	4.0	4.4
36.	.2	.7	1.1	1.6	2.0	2.5	2.9	3.3

3.4.4 Tracking - Step Tracking

As most receiving antennas will have beam widths of 20 to 30 degrees, it is necessary to move the antenna only at one-minute intervals rather than to track continuously. Keep as close to the predetermined values as possible. If, for instance, the computed values were

Time	Azimuth	Elevation
15:50:25Z	150°	10°
15:51:25Z	140°	18°

it would be desirable to have the antenna pointed at 18 degrees elevation 140 degrees azimuth at 15:50:55Z so that the antenna would be "ahead of" the satellite for 30 seconds and "behind" for a like period. The next adjustment would then be at 15:51:55Z. When the elevation angle exceeds 50 degrees, the user may find that the antenna postion must be changed at 30-second intervals since azimuth will be changing rapidly during this period.

4. DATA FORMAT & GEOMETRY

4.1 APT Camera System

The APT camera system is built with a one-inch vidicon tube on which appropriate reference fiducials are etched. Figure 4-1a shows the fiducial pattern used during 1968-69 to transmit pictures with 800 TV lines; Figure 4-1b shows the pattern to be used to transmit pictures with 600 TV line beginning in 1969.

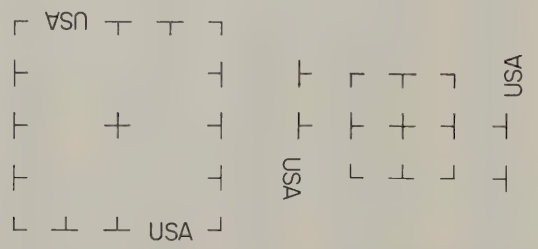

4-1a
APT FIDUCIAL PATTERN

4-1b
NEW 600 LINE PATTERN

FIGURE 4-1

The center fiducial (+) and the camera optical axis (picture geometric center) are coincident. The camera is aligned on the spacecraft so that the vertical portion of the column of fiducials through its center will be oriented along the spacecraft velocity vector in space when the picture is taken. The horizontal portion of the row of fiducials through the center is perpendicular to the velocity vector.

Spacecraft with APT camera systems are designed so that during routine operation pictures are taken when the camera optical axis is perpendicular to the earth. Therefore, the picture center and spacecraft subpoint should be coincident at the time the picture is taken. A line drawn through the vertical portion of the middle column of fiducials represents the projection of the velocity vector on the earth.

In practice, the picture data are scanned and transmitted with the first data showing an area the spacecraft has already passed over. The last line shows the area toward which the spacecraft is heading. As received then, an arrow drawn from top to bottom of the picture represents the direction of movement of the spacecraft over the earth. If the spacecraft is moving from north to south, the first line of data will be the northernmost; if the spacecraft is moving from south to north, the first line of data would be the southernmost.

4.2 The DRIR System

The DRIR display has no fiducial reference marks to aid in data orientation. The data are transmitted line by line as the spacecraft passes over an area. Assuming the spacecraft in proper mission orientation, the instantaneous subpoint position will be at the midpoint of the data line.

5. DATA TIME

The geographical location of real-time transmission data requires an accurate knowledge of data time. Since the operation of camera and line scan systems are different, they require separate

techniques for data time determination.

Briefly, the camera takes a "snap shot" so that the entire picture contains data taken at a single time. A line scan system (such as DRIR) "sees" and transmits data simultaneously so each line of data has a unique time associated with it.

5.1 APT Camera Systems

The APT system, data transmission sequence, is divided into two basic periods. During the first period, start and horizontal phasing pulses are transmitted. Picture data are transmitted during the second period. The start tone (the 2400 Hz subcarrier is modulated with a 300 Hz tone) is generated for the first 3 seconds of the initial period. This is followed by 5 seconds of 12.5 millisecond horizontal phasing pulses occuring at the rate of 1 every 250 milliseconds. The camera shutter is activated and the picture taken 2 1/2 seconds after the tone change between "start" and "phasing". Picture time then is determined by noting the time of the audible tone change between start and phase and adding 2 1/2 seconds. Since the time between pictures is reasonably constant (for each type of spacecraft), a missed picture time can be determined by adding (subtracting) the proper interval to the known time of any picture.

5.2 DRIR Line Scan System

Data time for the line scan system is unique for each line. It is suggested that the time of receipt (display) of several lines of data separated in time by 4-6 minutes be determined during each real time acquisition. For convenience, it will be found helpful to determine the particular lines displayed at exact minutes after the ascending node rather than exact minutes of local clock time - (or before the ascending node in the southern hemisphere). It is left for the user to determine the method of identifying particular data lines since no universal method can be developed.

6. GEOGRAPHIC ORIENTATION PROCEDURES

6.1 APT Picture Data

6.1.1 Introduction

This section provides a detailed procedure for the geographic referencing techniques unique to APT system photographs taken when the camera axis is perpendicular to the earth. The basic system makes use of a library of grids and requires a knowledge of picture time and satellite spatial location. The procedure is independent of whether the spacecraft is northbound or southbound during the daylight portion of the orbit.

6.1.2 Grid Library

A series of special grids (see example, Figure 6-1 and 6-2) have been prepared for the APT analysis procedure and are available on 35mm film.*

To prepare these grids, a spacecraft was assumed to be in a sun-synchronous orbit at an altitude of 750 nautical miles. The grids of latitude and longitude lines were determined mathematically, drawn, and reproduced on film. Latitude lines are solid, longitude lines are dashed.

To fit the APT picture received on a station display, these grids must be enlarged to the scale of the picture.

6.1.2.1 Grid Labels

The latitude line most closely approximating the grid center is indicated by a dotted zero at a latitude, longitude intersection near the center of each grid. The value of this latitude line is indicated in the legend (Figure 6-2). Longitude lines are not labeled since the grids are universal around a latitude circle. In use, the longitude lines on the enlarged, projected grid must be labeled to agree with the spacecraft location at picture time. Directly south of the "dotted zero" reference, along the longitude line, are two numbers

*Available at cost from: The National Weather Records Center, Environmental Science Services Administration. Federal Bldg., Asheville, North Carolina 28801. Current 1969 price $8.50 (U.S. Currency)

which indicate the spacing, in degrees, of the latitude and longitude lines. These numbers always appear to the south of the central latitude line regardless of how the grid is oriented when projected for enlargement (see Figure 6-2). Two sets of grids are provided, one for south to north picture taking orbits, the other for north to south orbits. Care should be taken to use the correct set to avoid serious gridding errors. The grid is positioned on the film so that the orientation is proper for the picture as recorded on facsimile display equipment. North will not necessarily appear toward the top of the grid as it would on a map.

6.1.2.2 Grid Magnification Factors

The proper magnification factor for the APT grids is determined from a knowledge of camera field-of-view (which may vary slightly from camera to camera), picture display size, and spacecraft orbital height. Camera field-of-view is determined from data acquired during sensor calibration, display size is determined locally, and orbital height is given in the daily message. Grid magnification factors for seven possible field-of-view values are given in Table 6. The correct portion of the table for use with particular camera systems to be flown, will be indicated in the Daily Predict Message after launch and in an Information Note sent to all stations immediately before launch. It is necessary that all users keep the National Environmental Satellite Center advised of address changes if they desire to receive this information.

Four marks representing the projection of the cone of view of the lens on the earth are provided on each grid in the pattern shown below and in Figure 6-2.

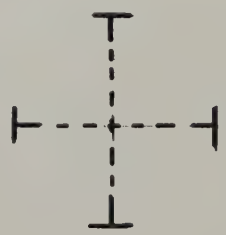

APT GRID
NORTH TO SOUTH
PICTURE TAKING ORBIT
CENTRAL LATITUDE
39° N

APT
LAT +39

FIGURE 6-1

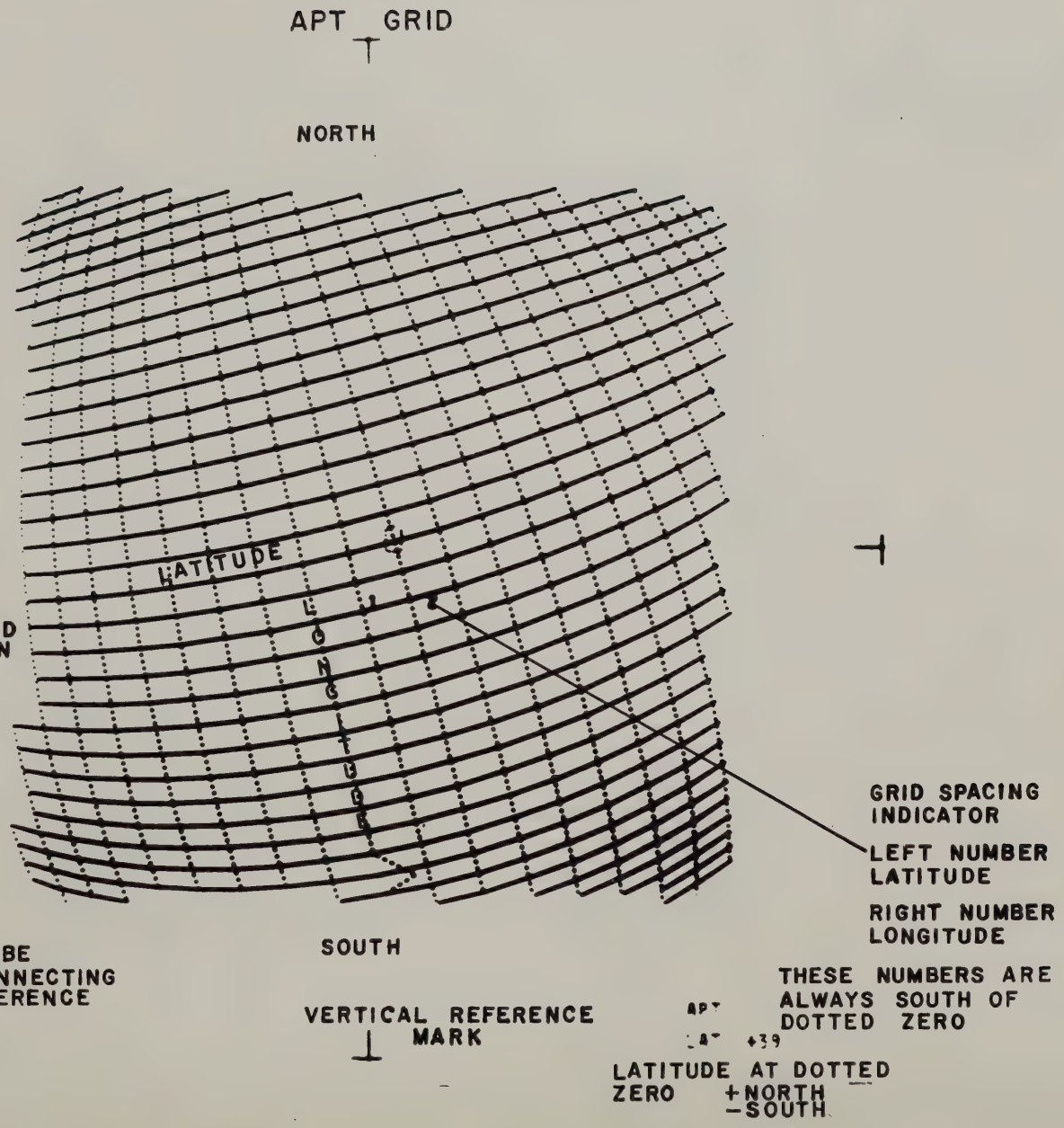
APT GRID
NORTH
LATITUDE
LONGITUDE
HORIZONTAL REFERENCE MARK FOR GRID MAGNIFICATION
GRID SPACING INDICATOR
LEFT NUMBER LATITUDE
RIGHT NUMBER LONGITUDE
HEADING LINE CAN BE CONSTRUCTED BY CONNECTING THE VERTICAL REFERENCE MARKS
SOUTH
VERTICAL REFERENCE MARK
THESE NUMBERS ARE ALWAYS SOUTH OF DOTTED ZERO
LATITUDE AT DOTTED ZERO +NORTH -SOUTH

FIGURE 6-2

A line drawn through the horizontal reference marks will intersect a line through the vertical reference marks at the geometric center of the grid. The grid should be enlarged so that the distances between the pair of horizontal reference marks and the pair of vertical reference marks are equal* and correspond to the distance shown in Table 6 for the spacecraft height at picture time. It will be necessary to interpolate for intermediate values not indicated in the table. When enlarging the grid, care should be taken to assure that the axis of the enlarger (projector) is perpendicular to the surface on which the grid is projected. The table provides data for an eight inch square picture[1] which is standard for many display devices. A proportionate change must be made to the size for any other display, i.e., a grid for a four inch picture would require one half the magnification; a ten inch picture, 1.25 times the magnification.

6.1.2.3 Heading Line

The heading line is the instantaneous projection of the spacecraft velocity vector on the earth and is equivalent to the subpoint track on a non-rotating earth. When pictures are taken, the spacecraft camera system is oriented along this line so that a line connecting the center vertical column of fiducial marks represents the projection of this line on the earth. On the grids a line drawn between the vertical reference marks shows the heading line of the spacecraft relative to the latitude and longitude lines for a sun-synchronous spacecraft at 750 nautical miles.

* Film copies of grids have frequently shown unequal horizontal and vertical shrinkage resulting in grids that are not precisely square. An average between horizontal and vertical dimensions should be used in this case.

(1) ITOS pictures with 600 lines will have a 4 to 3 size ratio when displayed. This table is valid for ITOS pictures 8"x6" in dimension.

TABLE 6

GRID MAGNIFICATION FACTORS

FOR PICTURE DISPLAY 8" x 8" (20.3 cm x 20.3 cm)

Spacecraft Height (KM)	Distance Between Reference Marks Inches						
	A	B	C	D	E	F	G
1000	14.3	14.5	14.6	14.8	15.0	15.2	15.4
1050	13.6	13.8	13.9	14.1	14.3	14.5	14.7
1100	13.0	13.1	13.3	13.5	13.6	13.8	14.0
1150	12.4	12.6	12.7	12.9	13.1	13.2	13.4
1200	11.9	12.1	12.2	12.4	12.5	12.7	12.8
1250	11.4	11.6	11.7	11.9	12.0	12.2	12.3
1300	11.0	11.1	11.2	11.4	11.6	11.7	11.8
1350	10.6	10.7	10.8	11.0	11.1	11.3	11.4
1400	10.2	10.3	10.4	10.6	10.7	10.9	11.0
1450	9.8	10.0	10.1	10.2	10.4	10.5	10.6
1500	9.5	9.6	9.7	9.9	10.0	10.1	10.3
1550	9.2	9.3	9.4	9.6	9.7	9.8	9.9
1600	8.9	9.0	9.1	9.3	9.4	9.5	9.6
1650	8.7	8.8	8.9	9.0	9.1	9.2	9.3
1700	8.4	8.5	8.6	8.7	8.8	9.0	9.1
1750	8.2	8.3	8.4	8.5	8.6	8.7	8.8
1800	7.9	8.0	8.1	8.2	8.3	8.5	8.6
1850	7.7	7.8	7.9	8.0	8.1	8.2	8.3

6.1.3 Fitting of Grids to Pictures (See Appendix D)

a. (Prior Preparation) Extrapolate subpoint data (latitude, longitude and height) for the orbit on which data is to be acquired.

b. Determine picture time accurately during acquisition of data.

c. Place an arrow on the picture indicating the top of the picture as it is recorded on the facsimile equipment. The position of start tone sync bars and the phasing area will also indicate the top of the picture.

d. Convert picture time to minutes and seconds after equator crossing (ascending node) time by subtracting the equator crossing (ascending node) time from picture taking time. For north to south picture taking orbits this time will generally be in excess of 20 minutes. (Note: For south to north picture taking orbits, south of the equator, subtract picture time from equator crossing time to give time before equator crossing time).

e. Interpolate linearly to find the actual subpoint latitude, longitude, and height when picture time is known.

f. Choose the grid with central latitude that most closely approximates the subpoint latitude. Care should be taken here to assure that the grid set is appropriate for direction of spacecraft movement (north to south or south to north).

g. Enlarge the grid to the proper size for the spacecraft height by projecting it on a suitable surface. The legend information should be in the lower right corner of the projected image.

h. Label the projected longitude lines so that the line nearest the center of the grid approximates the longitude of the subpoint.

i. Orient the picture exactly as it was received on the facsimile recorder (sync and phase area to the top). Project the grid on the picture so that the principal point (center fiducial +) is at its exact latitude and longitude and the grid is positioned so that a line through the center line of fiducials (vertical or horizontal) is parallel to a similar line through the comparable grid reference marks. Be sure to keep the center fiducial (+) near the geometric center of the grid (intersection of the lines connecting horizontal and vertical T's).

j. Check latitude and longitude of landmarks, if visible, to determine accuracy of gridding technique. Then trace grid lines onto the picture. Since asymmetrical lens and electronic distortions are neglected in the computation of the grids, a perfect fit between picture and grid will seldom occur over the entire area of the APT picture. These distortions may result in an apparent distortion of landmarks and cloud features.

6.1.4 Grid Preparation for a Circular Orbit

If apogee and perigee differ by no more than 50 kilometers, the grid magnification factor may be considered constant. Grids may then be enlarged and reproduced photographically on foil (film) and used as an overlay rather than a projected image.* Analysis procedures will not be changed by this modification of technique.

6.1.5 Attitude Bias (See Section 7)

Attitude bias may be noted by the analyst when a grid does not fit known geographic features. In this case the grid position should be changed so that the closest fit to these known features is achieved.

6.2 DRIR Picture Data

6.2.1 Introduction

This section provides a detailed procedure for the geographic referencing techniques unique to continuous line scan data systems (DRIR). It is assumed that spacecraft roll, pitch and yaw are all zero. Under these conditions the scan is perpendicular to the heading line and contains the instantaneous subpoint at the bisector of the data line between earth horizons. Thus the subpoint track can be represented by a straight line connecting the mid-point of each line.

The gridding technique involves the use of a library of grids computed for a 48 line per minute, line scan sensor system.**

* Alternatively, several sets of overlays may be prepared to be used in the eleptical orbit case if so desired. Transparent grids can also be used under the picture if a light table is used

** The technique will not change if some other scan rate is used but the grid itself will be different.

The assumption is implicit that the user has a display device with a relative scale factor the same as that used for APT camera data. This requires the use of a linear, rather than a non-linear, rectifying display system, and that the aspect ratio near the subpoint be 1:1. If the distance between contiguous lines of DRIR data as displayed (for example 100 lines per inch) is the same for the line scan system and the APT picture data, the display of information from the full 360 degrees of mirror rotation of the line scan system (earth, space and housing view) will require the full line length of the display device. If only the earth scan and calibration area are displayed, the line spacing must be expanded to maintain the correct aspect ratio and thus allow a proper grid fit.

6.2.2 Grid Library

A series of special grids (see example, Figure 6-3) have been prepared for the DRIR analysis procedure and are available on film strips for enlargement at the local site.

The geometry of a line scan system precludes the possibility of using a single grid (with different magnification) for a wide variation of orbital heights as may be done with the APT camera system. Separate grids are provided for use through the range of orbital heights planned for spacecraft with this system. To prepare these grids, a spacecraft is assumed to be in sun-synchronous orbit at each of these heights.

To fit the line scan display on the ground, the grid for the proper orbital height must be enlarged to the size of the picture.

Figure 6-3 and 6-4 are a reproduction of the grid for an 800 nautical mile orbital height (sun-synchronous orbit, inclination 100.8 degrees). The solid line through the center, parallel to the edges, represents the subpoint track. Earth horizons as seen by the spacecraft are indicated by dashed lines parallel to and at equal distances from the subpoint track. With correct orientation, a single grid drawn for one quarter of the orbit may be used throughout the orbit. Orientation is proper for the orbital segment for which the legend may be read directly. Two copies of the grid may be combined (if desired

by the user) to provide a continuous grid from pole to pole.

6.2.2.1 Grid Labels

Latitude lines are labeled directly; the longitude lines are universal as with the APT grids. The user assigns the proper longitude labels to conform with orbital data computed from the Daily Predict Message. Latitude lines are drawn and labeled for five degree intervals. Longitude interval is a function of latitude, with a spacing of five degrees from the equator to 60 degrees North or South, ten degrees between 60 and 80 degrees, and twenty degrees from 80 to 85 degrees. Longitudes are not indicated above 85 degrees.

a. Longitude Labels:

Longitudes on the DRIR grids are universal, with no fixed values assigned. The user is responsible for assigning correct labels to the longitudes. Unlike the APT grids which may be moved about the picture center with only minor location errors resulting, the DRIR grids must be positioned so that grid and picture horizons (when discernible) match and the individual lines of data are at their proper latitudinal position. It is incorrect to move the grid perpendicular to the track so that longitude values coincide with the grid lines.

Two techniques are available for labeling longitude lines.

1. Determine the longitude of the ascending (descending) node mathematically from information in the Daily Message and label this intersection directly on the grid. Other longitude lines should be labeled relative to this point. (See example, Appendix D Figure D-2).

2. Determine the actual latitude and longitude of the sub-satellite point for several lines of data during acquisition. Label the grid to conform to these points during the gridding procedure.

If an overlay type grid is used for geographical orientation of the DRIR data, technique #1 will probably be the one most readily adaptable to picture gridding. The grid may be prepared easily before acquisition. If a projection method is used for gridding, technique #2 will be most readily adaptable.

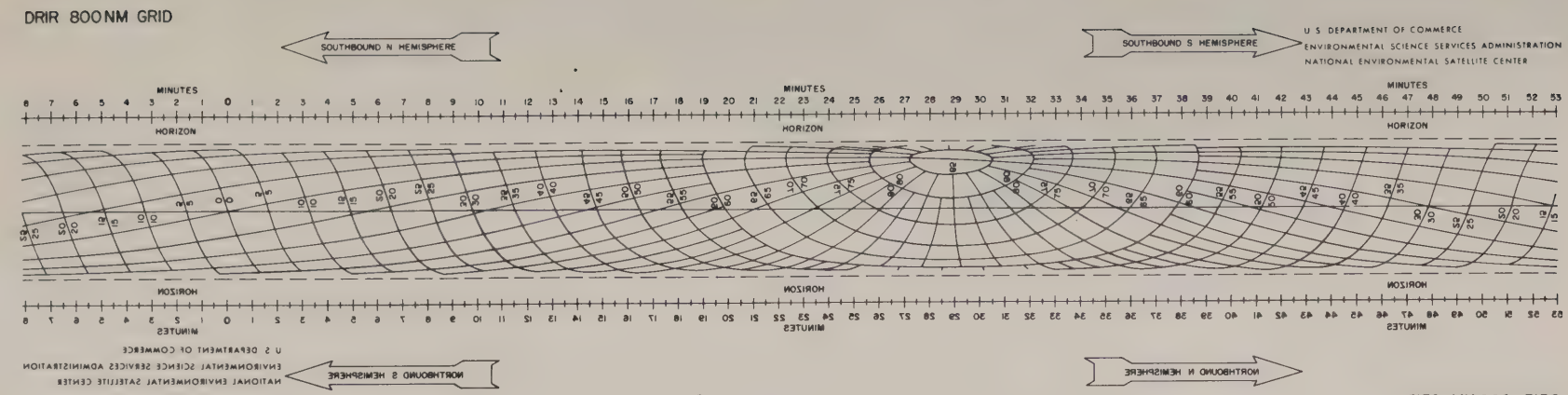

6-3A

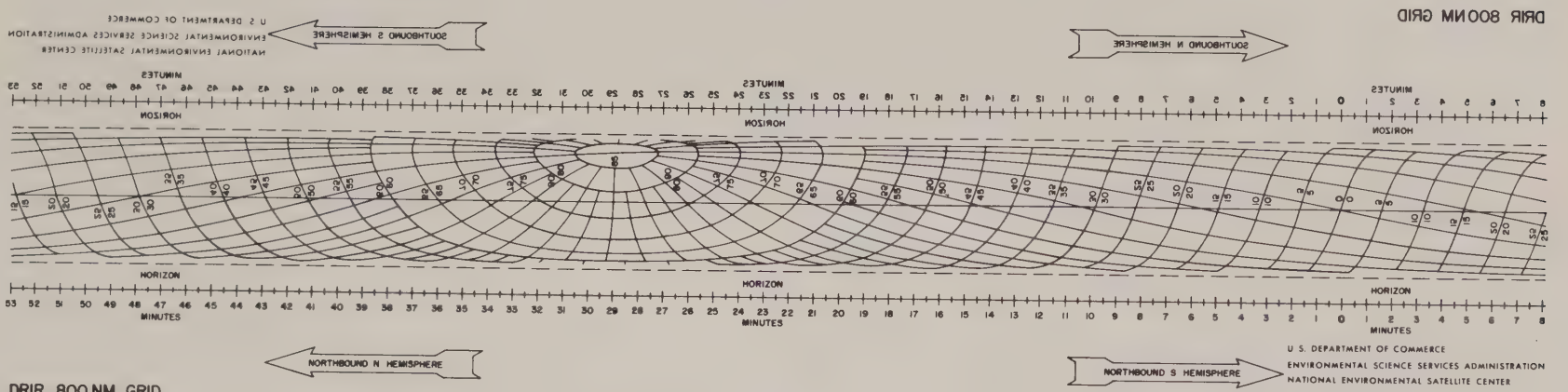

6-3B

FIGURE 6-3

DRIR GRID 800 NAUTICAL MILES

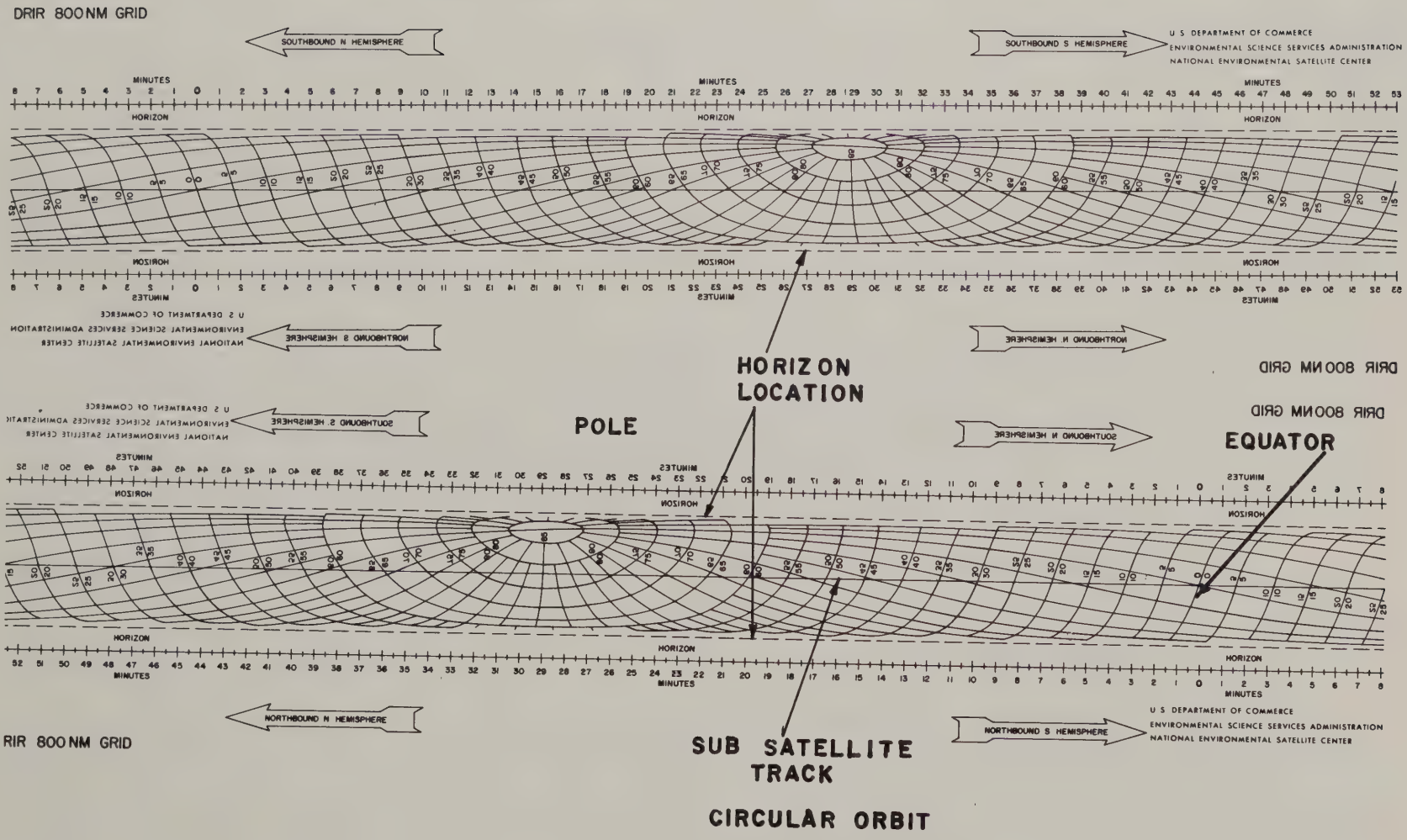
DRIR 800NM GRID
SOUTHBOUND N HEMISPHERE
SOUTHBOUND S HEMISPHERE
U S DEPARTMENT OF COMMERCE
ENVIRONMENTAL SCIENCE SERVICES ADMINISTRATION
NATIONAL ENVIRONMENTAL SATELLITE CENTER
MINUTES
HORIZON
NORTHBOUND S HEMISPHERE
NORTHBOUND N HEMISPHERE
HORIZON LOCATION
POLE
EQUATOR
SOUTHBOUND S. HEMISPHERE
SOUTHBOUND N HEMISPHERE
NORTHBOUND N HEMISPHERE
NORTHBOUND S HEMISPHERE
RIR 800NM GRID
SUB SATELLITE TRACK
CIRCULAR ORBIT

FIGURE 6-4

6.2.2.2 Grid Magnification Factors

Grids for the line scan system must be enlarged to fit the picture as received at the local site. Since the height factor is eliminated by choosing the proper grid, the user need only be sure that the magnification is proper to fit his particular display. The straightforward approach to this problem is the simplest in most cases, and within the degree of accuracy required by most users. It is suggested that the user magnify the proper grid to fit the horizon to horizon size of the image as displayed. Altitude errors, if they exist, will cause minor inaccuracies when using this technique. If, for instance, the horizon of the picture appears to undulate, a spacecraft attitude change may be the cause and a "best fit" should be made for the picture as a whole.

When using this technique, the user should be absolutely certain that both horizons are well defined. In particular, care should be taken where clouds appear on the horizon and mask its appearance. Additionally, some radiometer systems may tend to mask the horizon on one side (particularly at low altitudes) with a sun shield designed to keep the sun from entering the sensor directly during certain portions of the orbit. In this case, users displaying the entire 360 degrees of data (earth, housing space, calibration and synchronization) can compute the grid magnification mathematically and check it against the horizon fit. To determine the perpendicular distance between the two horizon lines, multiply the length of the full scan line (measured on the APT pictures this would include data and the blanking pulse) by the factor shown in the table below:

TABLE 7

DRIR ORBIT HEIGHT	MULTIPLICATION FACTOR
600 Nautical Miles	0.324
650 " "	0.318
700 " "	0.312
750 " "	0.307
800 " "	0.301
850 " "	0.296
900 " "	0.291

A mathematical computation of precise grid magnification factors will also provide the most accurate grid fit for those not displaying the entire 360 degrees of data. Those requiring this accuracy should write to the APT Coordinator, National Environmental Satellite Center, Environmental Science Services Administration, Washington, D.C. 20233, giving full details of the display device used. Include information of length of active data scan line for conventional APT pictures, length of blanking pulse, length of active scan line for DRIR, time to display one full line of DRIR data, inactive time to beginning of next data line and line spacing (scan lines per inch). Again, it must be stressed that subpoint aspect ratio must be 1:1 - the same as provided for the square format APT pictures or the grids cannot fit properly and inaccurate locations will result.

6.2.3 Fitting Grids to Pictures (Overlay Technique)
(See Appendix D)

a. Prior Preparation:

1. Determine subpoint data (latitude and height) directly from the Daily Message and extrapolate the ascending (descending) node longitude for the orbits from which data is to be acquired.

2. Choose the proper height grid (already magnified to the correct size).

3. Label the longitudes to conform to the ascending (descending) node determined in a1.

4. Sketch the even five degree intervals for convenience in using the data.

b. Determine time of receipt of several lines of data separated by 4 to 6 minutes. For convenience, use a time after (before) ascending node found in the Daily Message. (Example: 23 minutes after ascending node).

c. Determine directly latitude of subsatellite point at each of the times in b.

d. Orient the grid properly (based on direction of spacecraft movement) and place it on the picture so that the horizons (grid and pictures) match and the latitude of the subsatellite points determined in c. are correctly located.

6.2.4 Fitting Grids to Pictures (Projection Technique)

a. Prior Preparation:

Determine subpoint data (latitude, longitude, and height) for the orbit on which data is to be acquired.

b. Determine time of receipt of several lines of data separated in time by 4 to 6 minutes. For convenience those lines of data should be found which are acquired at an even minute interval after (before) the ascending node (use a minute value found in the Daily Message).

c. Determine the subsatellite point position of each line of data for which time was determined.

d. Choose the grid drawn for the spacecraft orbital height during receipt of data.

e. Enlarge the grid to the size of the picture display.

f. Orient the grid properly to agree with the direction of motion of the spacecraft.

g. Project the grid onto the picture so that the horizons (grid and picture) match and the latitude of the subsatellite points (c.) are correctly displayed.

h. Assign longitude values to agree with the data determined in c.

NOTE: When using either of these techniques, landmarks should be checked to assure a proper fit. Near the center of the grid, landmarks should appear in the correct location; if they do not the grid should be adjusted to correct the errors. The most common causes of erroneous grid-fit are miscomputations, time or attitude errors.

7. ATTITUDE ERRORS

The gridding techniques discussed so far are based on the assumption that spacecraft roll, pitch and yaw are all zero. In actual practice, with the kinds of spacecraft expected to be operating through

1975, attitude errors of one-half to one degree, measured at the spacecraft, are probable much of the time. Occasional, larger scale, short term attitude deviations are possible. The results of roll, pitch and yaw on APT pictures are shown in Figures 7-1, 7-2 and 7-3. A yaw error (Figure 7-1) causes a rotation of the picture so that picture edges no longer line up with the heading line vector of the satellite. A roll error (Figure 7-3) will cause the picture center to be displaced to the right or left of the subpoint in a direction perpendicular to the heading line. A pitch error (Figure 7-2) will displace the picture center along the heading line either ahead or behind the subpoint.

Minor attitude errors probably will not be apparent in routine use of the pictures received at the local receiving stations. A large error would be more apparent, particularly where geographic features are present in the pictures. The user probably will also see mislocated geographic features when gridding the pictures by routine techniques. Should this occur, it is suggested that the grid fit be adjusted to locate correctly the geographic features. The remainder of the picture will then be located as well as is possible with the grids now used.

Attitude problems with a line scan, real time system are similar to those with a "snap shot" picture (APT) system. Roll, pitch and yaw produce similar effects but on a line to line basis rather than affecting the entire picture at one time. It is possible, with some type of spacecraft, to have an attitude error at the beginning of a data swath which changes as the satellite progresses in its orbit. For example, a "wavy" horizon in the reproduced picture would be indicative of roll variation through the pass. This should be seen rarely.

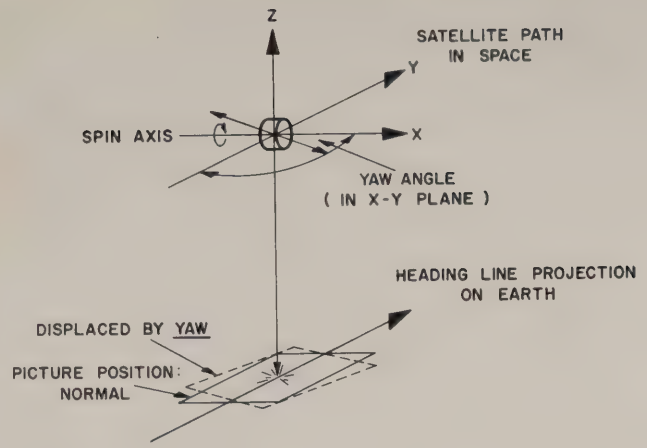

FIGURE 7-1

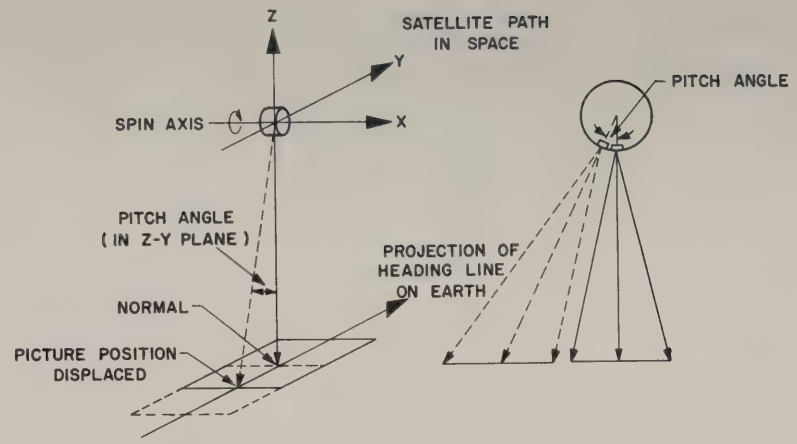

FIGURE 7-2

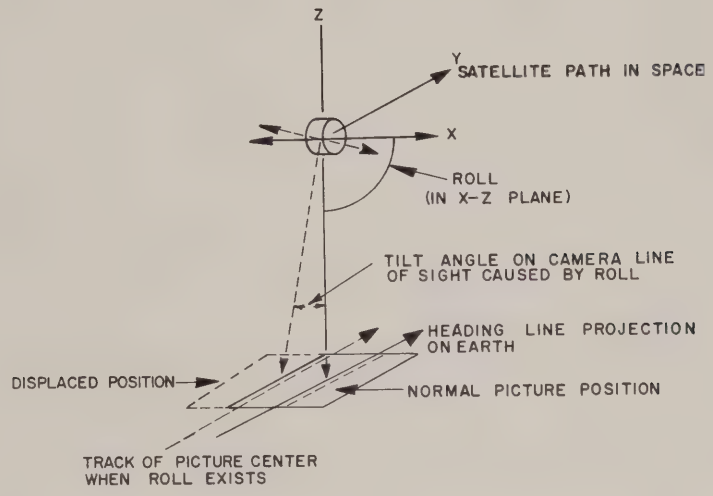

FIGURE 7-3

8. DATA INTERPRETATION

Orbiting satellites provide routine observations of the atmosphere, the land surface, and the sea. Data acquired by these satellites can be applied to many of the geophysical sciences. Meteorologists can observe, in one satellite picture, the complete cloud system associated with a synoptic scale[1/] storm as well as the details of the local mesoscale[2/] cloud distribution within the storm system. Hydrologists can use the pictures to observe snow boundaries directly; oceanographers and hydrographers can chart seasonal changes of polar sea ice boundaries. Oceanographers also can use the infrared data to map the temperature of the sea surface.

To interpret properly the data received from current environmental satellites, analysts must learn to identify the various cloud forms, and to recognize surface features such as areas of snow and ice. Methods for identifying cloud forms, snow and ice patterns, and other features are described in this chapter, as is the meteorological interpretation of some of the more important synoptic and mesoscale cloud formations that appear in the pictures. A selected bibliography on the problems of picture interpretation and the application of satellite data to meteorological analysis appears at the end of this section.

8.1 Appearance of Clouds in Satellite Pictures

Exact identification of the cloud forms seen in satellite photographs is complicated by the fact that one sees only the tops of the clouds from a distance of about 1500 kilometers (about 900 statue miles). The clouds can be readily recognized as cirriform, cumuliform, or stratiform by noting their brightness, texture, size, and general pattern, and by their association with broad scale synoptic patterns.

The analysis of the cloud pictures can yield information on horizontal and vertical motion, atmospheric stability, and to some degree, the vertical extent of individual cloud masses.

8.1.1 Cumuliform Clouds

Cumuliform clouds appear in satellite pictures as irregularly shaped masses with generally rounded edges. These cloud masses vary greatly in size, and occur in many different patterns. They may appear as isolated masses, in bands, or arranged in patterns roughly approximating circles or hexagons (cellular patterns). They also occur as randomly distributed masses in fields of general cloudiness. Cumuliform clouds embedded, but towering above an area completely covered by another deck of clouds, often can be identified by means of shadows cast on the cloud below.

1/ Synoptic scale: Characteristic dimension 300-1500 miles (500-2500 Km).
2/ Mesoscale: Characteristic dimension 30-300 miles (50-500 Km).

Figure 8-1a shows areas of cumuliform clouds arranged in so-called "cellular" patterns. The cells consist of cumuliform clouds arranged in patterns that approximate partial or complete circles, or, when the cells are close together, hexagons. Cellular patterns are classified as <u>open</u> or <u>closed</u>. An <u>open</u> pattern consists of clouds arranged about an open or clear area; a <u>closed</u> pattern tends to have a cloud covered center, and to have a narrow band of relatively clear air surrounding it. The total cloudiness in open patterns is generally much less than with closed cellular patterns. Cellular patterns of cumuliform clouds are most frequently observed over ocean areas. Here, cold unstable air moving equatorward is heated from below by the warm ocean surface.

The area surrounding A in figure 8-1a shows cumulus congestus and cumulonimbus arranged in a pattern of <u>open cells</u> which formed in a deep layer of unstable polar air. This particular pattern formed in the area of cyclonic surface flow is shown at A in figure 8-1b.

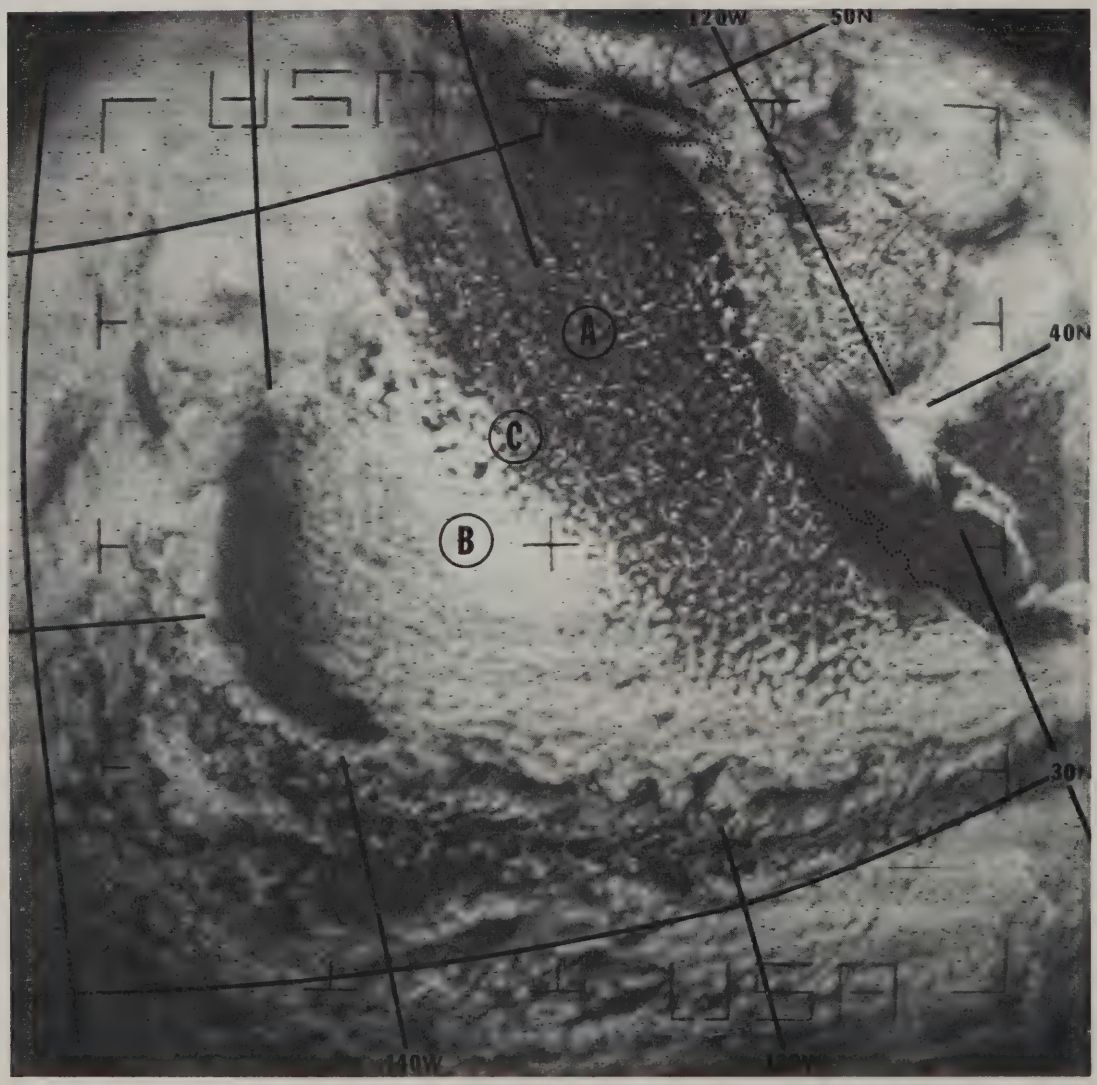

Figure 8-1a. Cumuliform clouds in cellular pattern - Eastern Pacific, 1908 GMT, April 16, 1968, Pass 1981.

At B in figure 8-1a, closed cells have formed under an inversion in the area of anticyclonic surface flow (see B, figure 8-1b). Cumulus activity started below the inversion, and spread out to form the closed cell pattern when the cloud tops reached the base of the inversion. A 200 mb jet stream axis (denoted by arrows) is shown to pass through C in the surface analysis of figure 8-1b. Where a jet stream crosses an area of cellular cumuliform formations, a change in pattern from closed cells to open cells is characteristic. Open cells form on the cold side of the jet stream and closed cells form on the warm side. Thus, where the line marking such a change in pattern is seen in a satellite photograph, it can be useful for locating the axis of the strongest upper level winds.

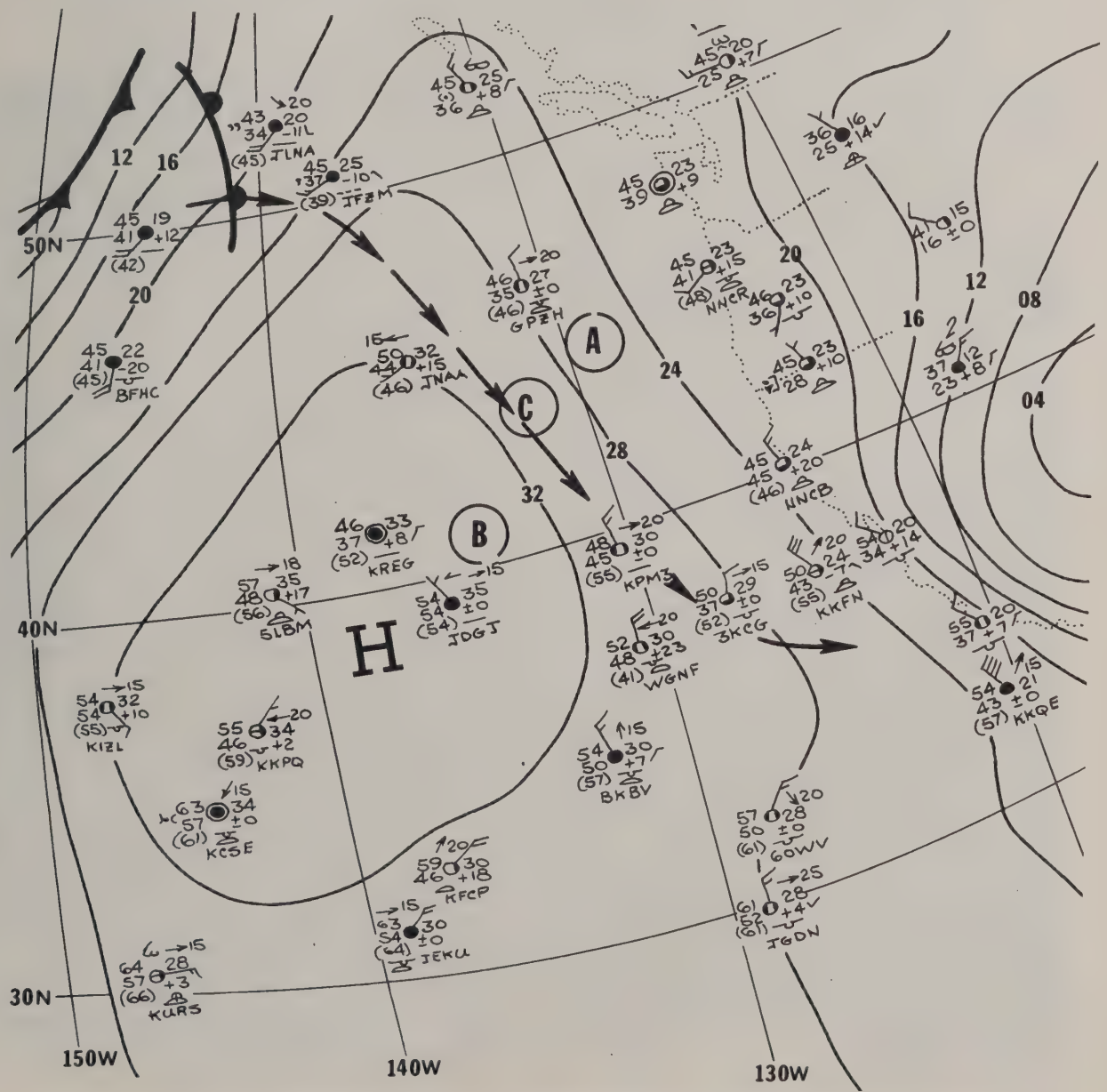

Figure 8-1b. Surface analysis, 1800 GMT and 200 millibar jet stream position, 1200 GMT, April 16, 1968.

A banded pattern composed of lines of cumuliform clouds is shown at G and H in figure 8-2. These cloud lines formed off the eastern shore of North America as cold continental air moved offshore over warmer water. The orientation of convective cloud lines of this type is frequently parallel to the direction of the shear through the layer in which the convective clouds form. In this example, the lines appear narrowest in the area offshore where the clouds first form (G). There is little vertical development in the clouds in this area, and their orientation closely approximates both the surface wind direction and the low level shear. Downstream at H, as the clouds increase in height, the bands grow in width and are parallel to the shear through the convective layer. Further south at I, the banded structure breaks down into a cellular pattern. The frontal cloud band preceding the cold air outbreak is along the eastern edge of the picture between J and K.

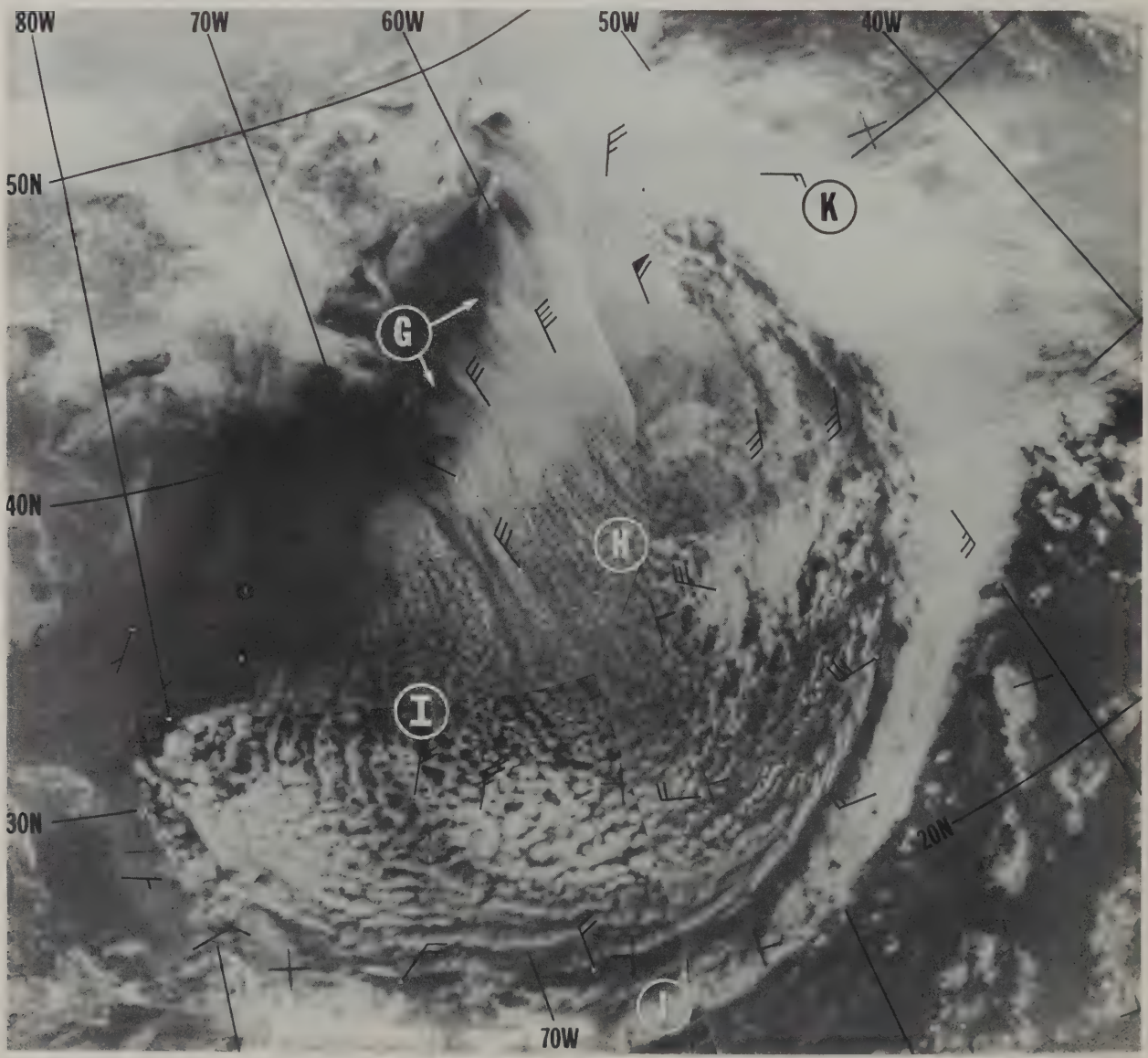

Figure 8-2. Cumuliform cloud lines - Western Atlantic, 1400 GMT, March 8, 1968, Pass 1489-1490.

The satellite picture in figure 8-3 was taken early in the morning when the local sun angle was quite low. The "pebbled" or "bumpy" appearance (A) results from shadows cast by convective cumuliform clouds which protrude above the top of the general overcast cloud shield. Further west, toward the terminator, individual convective elements (B) can be identified clearly. Where sun angles are low, protruding cumuliform cloud elements are highlighted on the side toward the sun and cast a shadow on the upper surface of lower clouds on the side away from the sun. Features such as these indicate the positions of local areas of convection within a synoptic scale system.

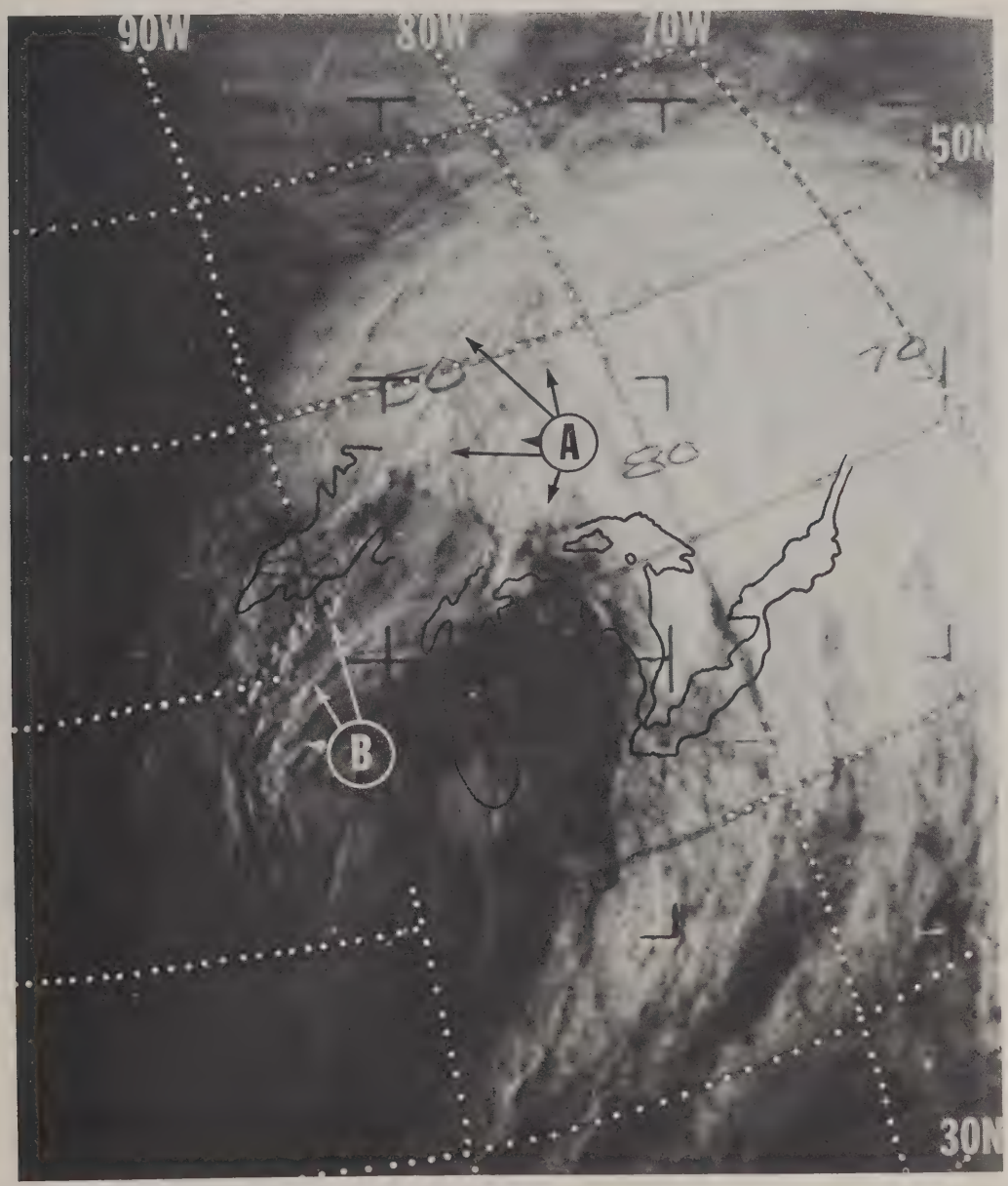

Figure 8-3. Bumpy appearance of convective clouds embedded in a frontal system - United States, 1324 GMT, April 4, 1968, ESSA 2, Pass 9715.

8.1.2 Stratiform Clouds

The upper surface of a stratiform cloud area normally has a smooth and uniform texture (C, figure 8-4). Cloud types which have this appearance in satellite pictures are thick stratus or fog, thick altostratus, and nimbostratus. Cirrostratus, when it occurs above layered altostratus, also can have this appearance.

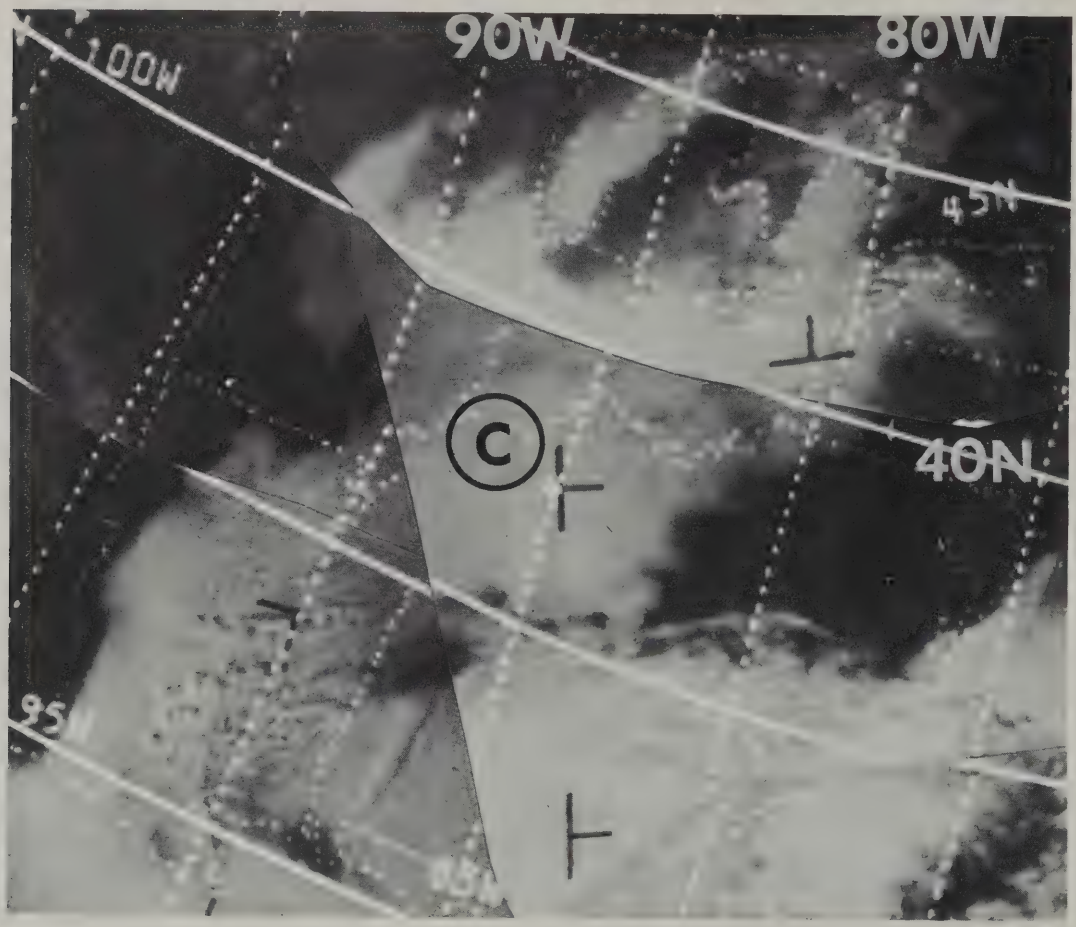

Figure 8-4. Stratiform Clouds - United States, 1900 GMT, December 12, 1966, ESSA 3, Pass 895-896.

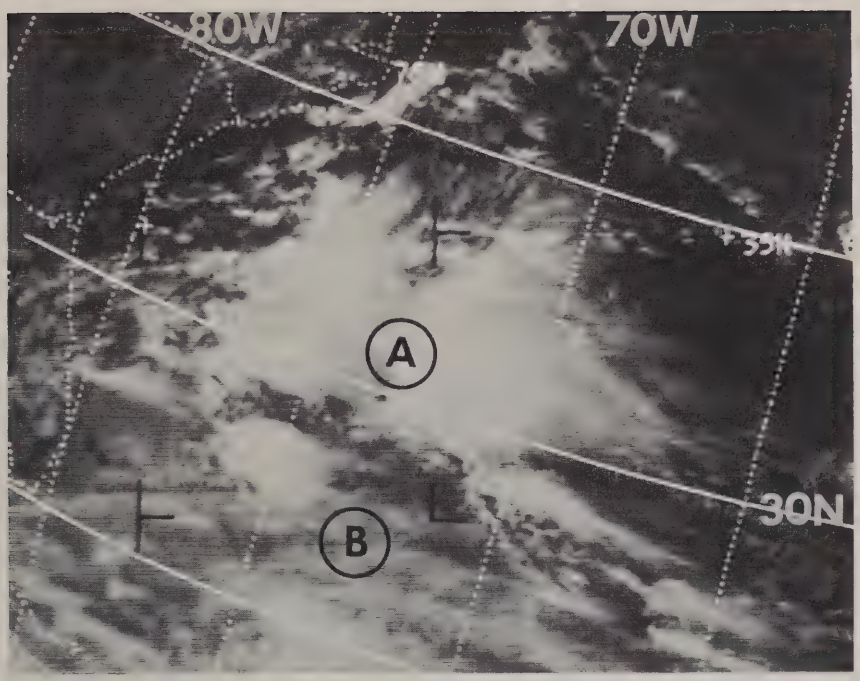

Figure 8-5. Cirriform clouds - Western Atlantic, 1850 GMT, October 14, 1968, ESSA 7, Pass 742.

8.1.3 Cirriform Clouds

The term cirriform is used here to denote cirrus or cirrostratus which is fibrous in appearance. Cirriform cloudiness is most commonly observed along fronts, along the warm side of jet streams, and in association with areas of cumulonimbus activity.

The cumulonimbus clusters around A in figure 8-5 produced the cirrus seen along the right-hand edge of each convective cloud mass. This example shows clearly that cirriform clouds are much darker in appearance than most other clouds and appear white only when there is underlying lower cloudiness. This is particularly evident in the lower portion of the picture around B.

8.2 Extratropical Cloud Systems

8.2.1 Jet Stream

When cirrus cloud formations are associated with the jet stream, they are clearly visible in satellite pictures. An extensive cirrus cloud shield often forms along the tropical side of a jet stream core. The edge of this cirrus shield lies parallel to the jet core and within 100 miles of it.

Often the cirrus shield associated with a jet stream occurs above an area completely covered with lower clouds. Under these circumstances, it is often quite easy to identify the edge of the jet-associated cirrus by the shadow it casts on the upper surface of a lower cloud deck. This shadow is most apparent when the difference in height between the cirrus shield and the top of the lower undercast is great and the local sun angle is low, an effect

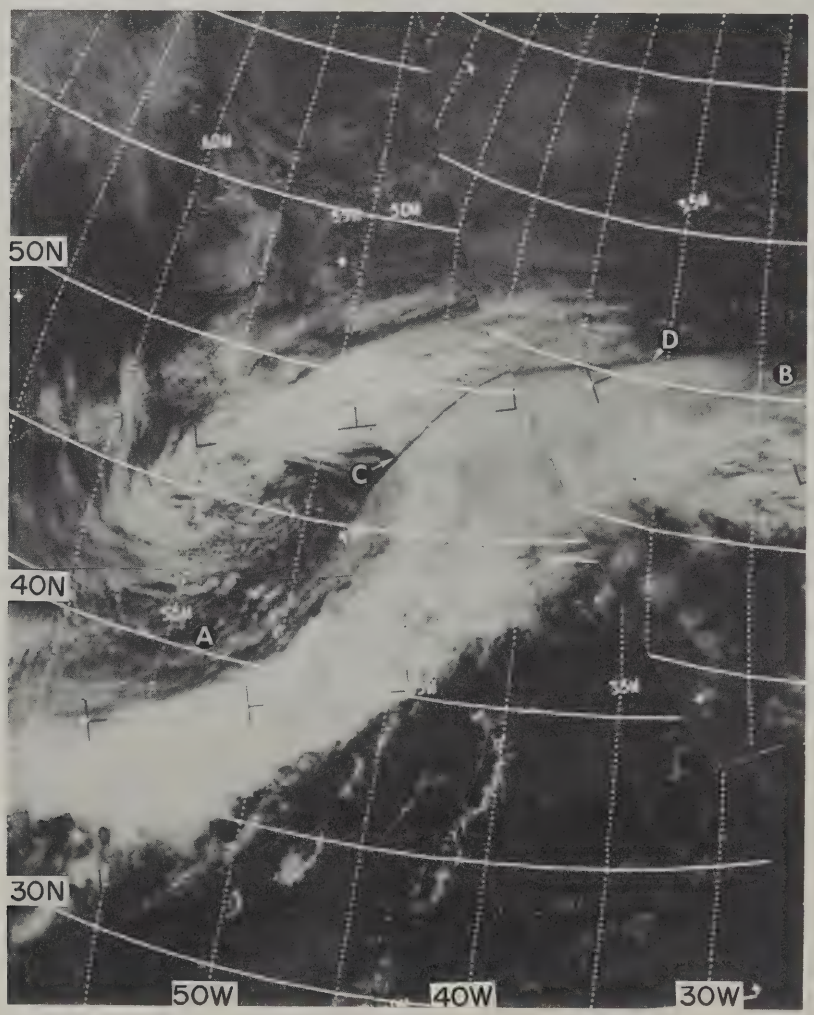

Figure 8-6. Jet stream with cirriform cloud shadow - Atlantic, 1502 GMT, October 23, 1967, ESSA 3, Pass 4849-4850.

most pronounced at higher latitudes. In figure 8-6, the edge of the cirrus extends from A to B. The cirrus cloud edge between C and D casts a well defined shadow on the underlying, more textured cloud deck. The shadow appears as a long thin line to the north of the cirrus shield, and helps to identify the edge of the jet-associated cloud formation. South of C, the edge of the cloud is clearly defined against the dark background of the ocean.

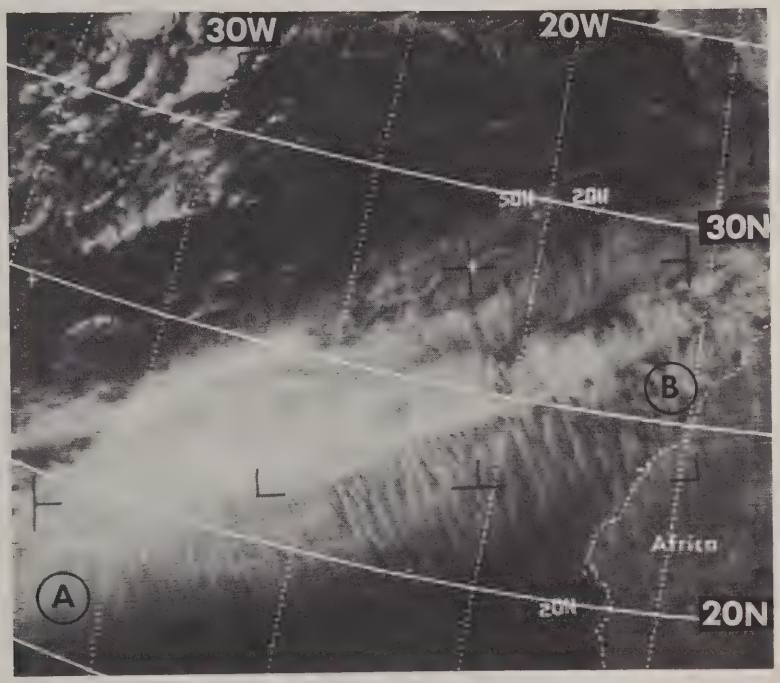

Figure 8-7. Transverse bands, cirriform cloud formation along jet stream - Eastern Atlantic, 1557 GMT, February 3, 1969, ESSA 7, Pass 2143.

Occasionally, cirrus clouds along a jet stream exhibit mesoscale banding nearly perpendicular to the upper level flow. Such transverse banding appears either along the edge or within the cloud shield itself. Figure 8-7 is an example of this type banding which is observed over both land and water; the cloud mass between A and B extends from the Atlantic Ocean into Africa. This type of banding helps to identify a cloud formation as jet-associated.

354-645 O - 69 - 5

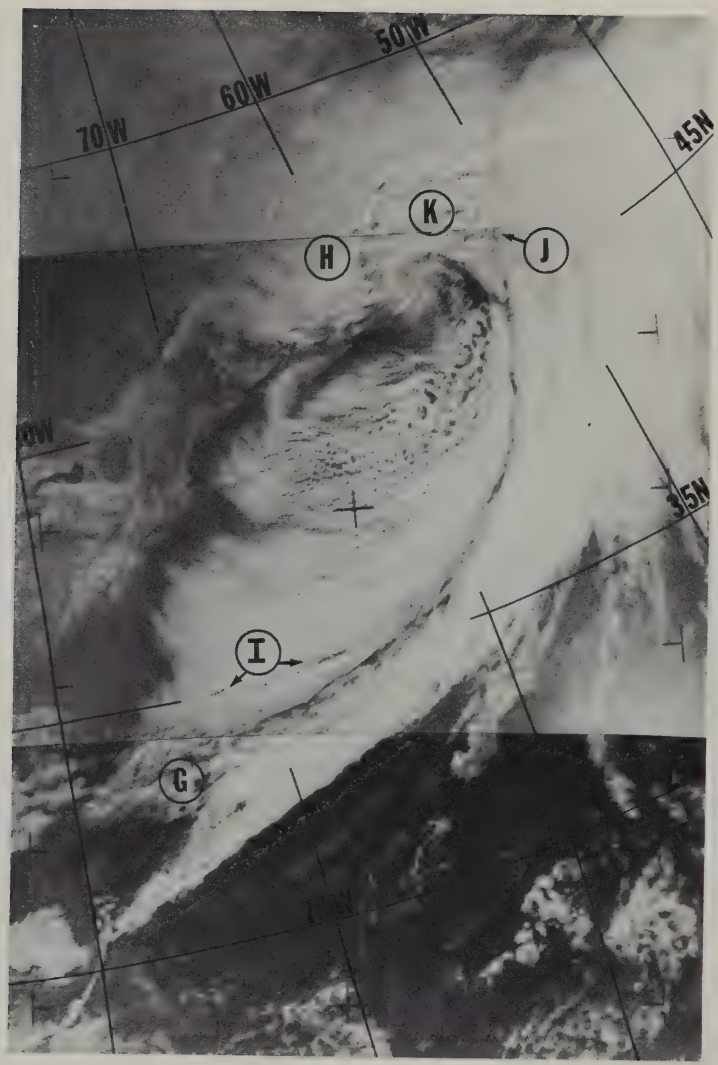

Figure 8-8. Vortex and frontal band - Western Atlantic, 1419 GMT, January 5, 1968, ESSA 6, Pass 700.

8.2.2 Frontal Bands

Frontal bands are characterized by wide multi-layered cloud bands which often spiral into a storm center. Figure 8-8 shows an occluded storm system in the western Atlantic Ocean. A long continuous cloud band spirals from G through J and then to the storm center near H. This cloud band corresponds to the cold (G-J) and occluded (H-J) portions of the frontal system.

Behind the front, a large area of cumuliform cloud lines formed as cold continental air was heated from below by the warmer water. Note how the middle and high clouds along the rear edge of the frontal band (between 35°N and 45°N) cast a long thin shadow on the upper surface of the lower cumuliform clouds.

The jet stream starts north of the cirrus cloud band (I), curves cyclonically along the rear edge of the frontal band between 35°N and 45°N, then crosses the frontal band at J. There is a marked difference in the texture of clouds on either side of the jet stream where it crosses the frontal band. On the right side (east of J) of the jet, the clouds appear smooth while on the left side (K), the lower clouds have a "bumpy" appearance.

Figure 8-9. Mature occluded storm - Eastern Pacific, 1935 GMT, March 10, 1968, ESSA 6, Pass 1517-1518.

8.2.3 Vortices

Cyclonic disturbances produce a variety of spiral cloud patterns which are easily recognized in satellite pictures. The best defined vortical cloud patterns are those associated with storms which have a closed wind circulation from the surface through at least the 500 mb level. Rapidly deepening storms usually have more middle and high cloud than those which are filling. An example of a mature occluded storm is shown in figure 8-9. The circula-

tion center near A is well defined by the spiral cloud bands. Deep storms such as this are usually quasi-stationary or moving slowly with a major cloud band arrayed in one or more complete loops around the storm center. Fully developed storms of this type tilt little with height, so the center of the cloud spiral closely corresponds to the center of the three-dimensional wind circulation. The middle and high clouds dissipate when a low is filling, then the circulation is defined only in the low level clouds. The cloud spiral at A in figure 8-10 marks the remnant of the deep cyclone in the Gulf of Alaska. The clouds forming the center of circulation near A are primarily cumuliform.

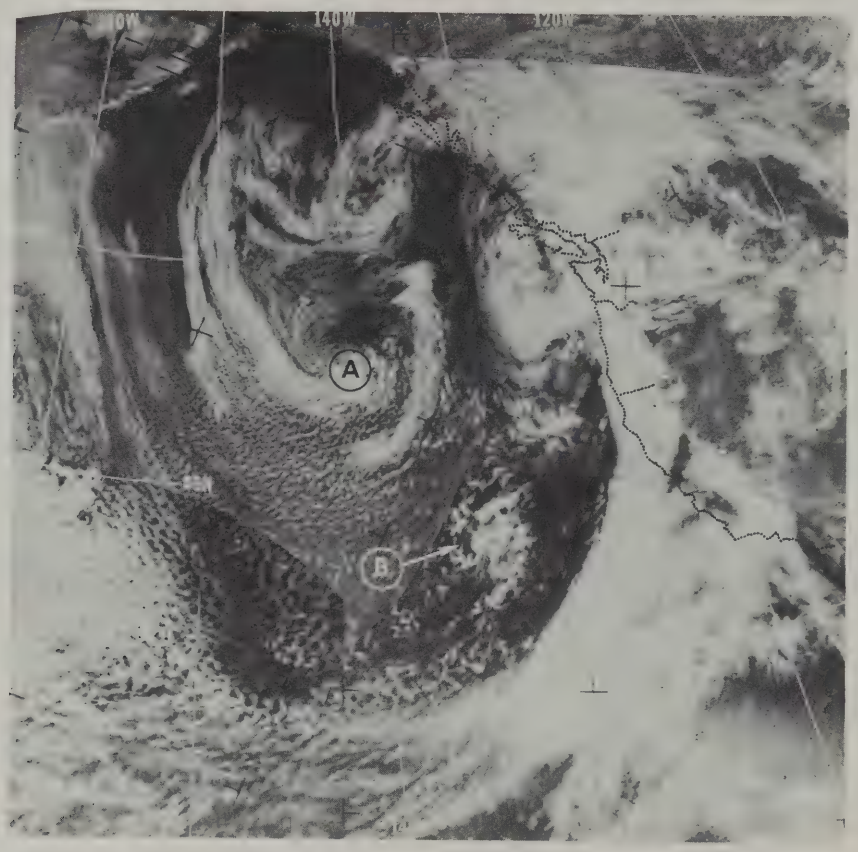

Figure 8-10. Deep cyclone - Gulf of Alaska, 1927 GMT, March 12, 1968, ESSA 6, Pass 1542-1543.

8.2.4 Secondary Centers of Maximum Positive Vorticity

An area of enhanced convective activity in a field of open cellular cumulus clouds to the rear of a cold front usually indicates the presence of a secondary vorticity center. The increase in convection is due to the steep lapse rate and upward vertical motion in advance of a secondary vorticity maximum. The tops of the convective clouds often merge into a continuous band of middle and high clouds to form a comma or crescent-shaped pattern. This cloud mass approximates the area of positive vorticity advection and lies ahead of the vorticity maximum. The amount of cloudiness produced is a function of stability and the speed with which the secondary vorticity center

is moving. The cloud formations at B in figures 8-9 and 8-10 are associated with secondary vorticity maxima. Cloud systems of this type are well defined in cellular cumulus fields over oceans, but are less well defined over land because of the lack of low level moisture. The existence of these cloud patterns was unknown before the era of weather satellites.

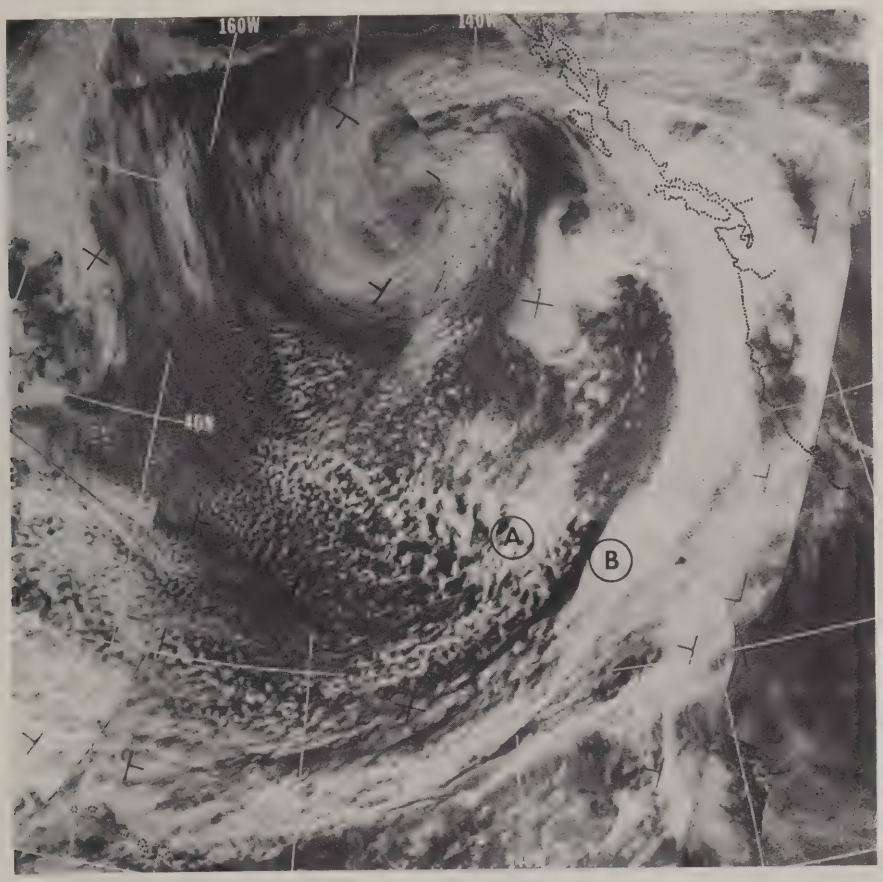

Figure 8-11. Frontal wave development - Eastern Pacific, 1935 GMT, March 11, 1968, ESSA 6, Pass 1530-1531.

8.2.5 Frontal Wave Development

Wave development resulting from the interaction of a secondary vorticity center with a frontal zone is observed frequently in satellite pictures. The cloud bands of most cold fronts bend away from the cold air and are relatively uniform in brightness and width. However, when a vorticity center begins to interact with a front, the cloud band bulges back toward the cold air and becomes wider and brighter indicating wave development. The center of circulation connected with the wave development on the frontal band during early stages of development is not visible in the satellite pictures. The frontal band upstream and downstream from the wave remains essentially the same in appearance while the wave remains open. An example of a developing wave is shown in figure 8-11. The large cloud mass at A is associated with a secondary vorticity center which has moved close to the front. Interaction

between this vorticity center and the front has resulted in the development of an open wave near B. The rear edge of the frontal cloud band in the vicinity of the wave bulges toward the cold air. A wave of this type normally will move northeastward and occlude.

8.2.6 Stages of a Cyclone

Cloud formations associated with vortices, fronts, vorticity maxima, and jet streams have been thoroughly examined and analyzed. Models describing the evolution of cloud systems associated with low level and mid-tropospheric cyclogenesis have been developed.

Figure 8-12 shows the life-cycle of an extratropical cyclone in the eastern Pacific Ocean. This series of satellite photographs was taken on five consecutive days. Three of this series were shown as figures 8-9, 8-10, and 8-11. On the first day, March 8, the comma-shaped cloud at A was associated with a mid-tropospheric vorticity maximum approaching a frontal band. The system intensified on March 9 as indicated by the cirrus outflow along the eastern and northern quadrants of the vortex. Cellular cumulus in the cold air covers much of the area west of the center of circulation. By March 10, the storm (A) had moved northeast and appeared to be fully occluded. A new secondary vorticity maximum was indicated by the increase in convective activity at B. The bulge of the front at C toward the cold air suggests this concentration of positive vorticity was interacting with the baroclinic zone and inducing a wave on the front. On the next day, March 11, the primary vortex at A shows less middle and high clouds than earlier. This implies that the system was no longer deepening. The newly developed low moved northeast and produced a vortical cloud pattern near C. Another vorticity center behind the front at D has initiated the development of another frontal wave at E. On the fifth day, March 12, the first vortex observed in this series is located at A. Clouds around the low continued to decrease in amount. The second and third systems (C and E) moved northward along the coast while still another secondary vorticity maximum appeared at F in the cold air. There was no evidence at this time of interaction between this center (F) and the frontal zone.

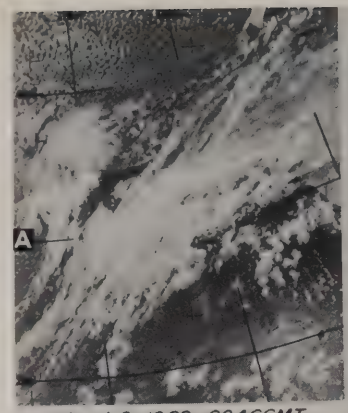

A. March 8, 1968 2046GMT

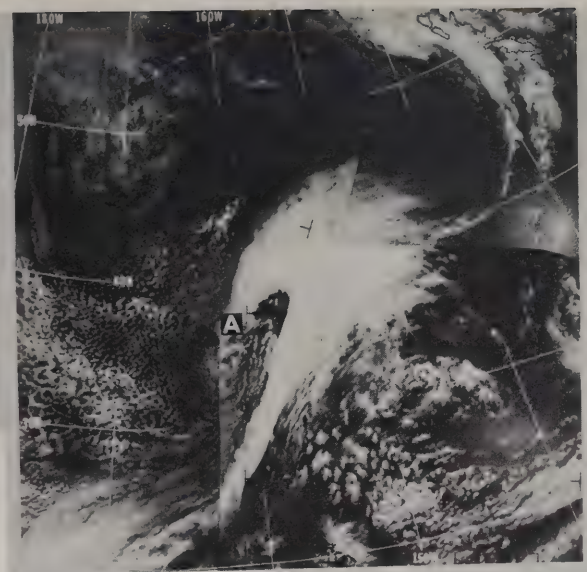

B. March 9, 1968 2037GMT

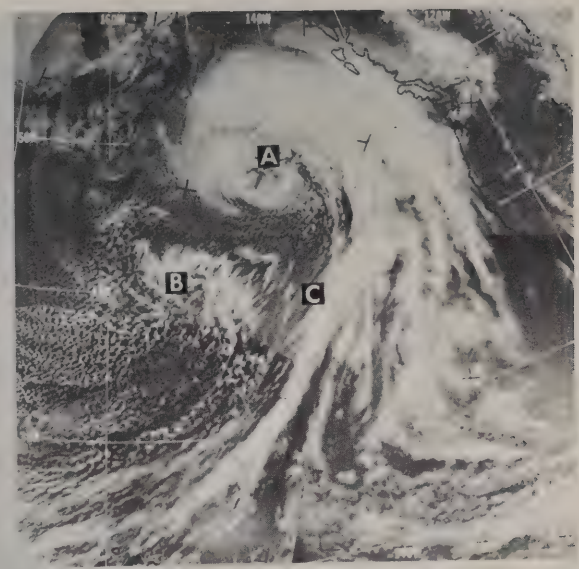

C. March 10, 1968 1935GMT

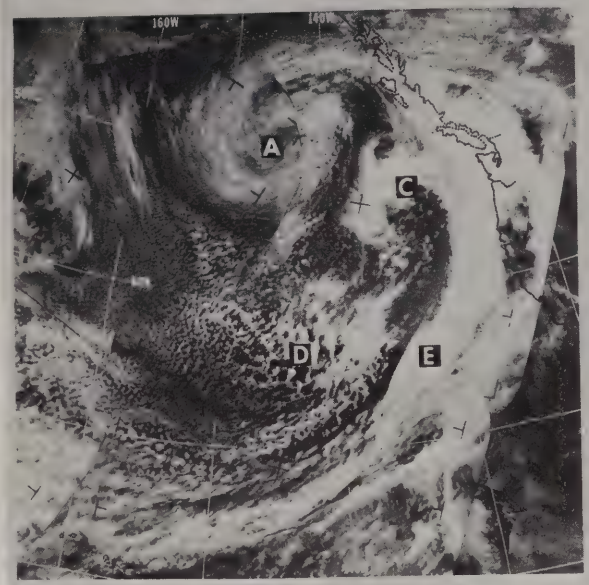

D. March 11, 1968 1935GMT

E. March 12, 1968 1927GMT

A. Initial stage: frontal wave forms
B. Deepening stage
C. Mature stage: with secondary frontal wave
D. Mature stage: with secondary frontal waves
E. Decaying stage

Figure 8-12. Life cycle of a Pacific storm.

8.3 Relationships Between Cloud Distribution and Flow Patterns

8.3.1 Upper Level Trough Lines

Certain changes in the characteristics of frontal cloud bands provide information helpful in locating the position of upper level troughs. Examination of numerous satellite pictures has revealed that the appearance of a frontal band changes abruptly where it is intersected by the 500 millibar trough line. In figure 8-13, the position of the upper level trough line is indicated by a dashed line. The frontal clouds east of the trough appear much brighter and the band is broader due to upward motion in the southwesterly flow aloft. To the west of the trough line in the region of subsiding air, the clouds tend to dissipate, the front appears more ragged, and there are several cloud-free areas within the frontal band.

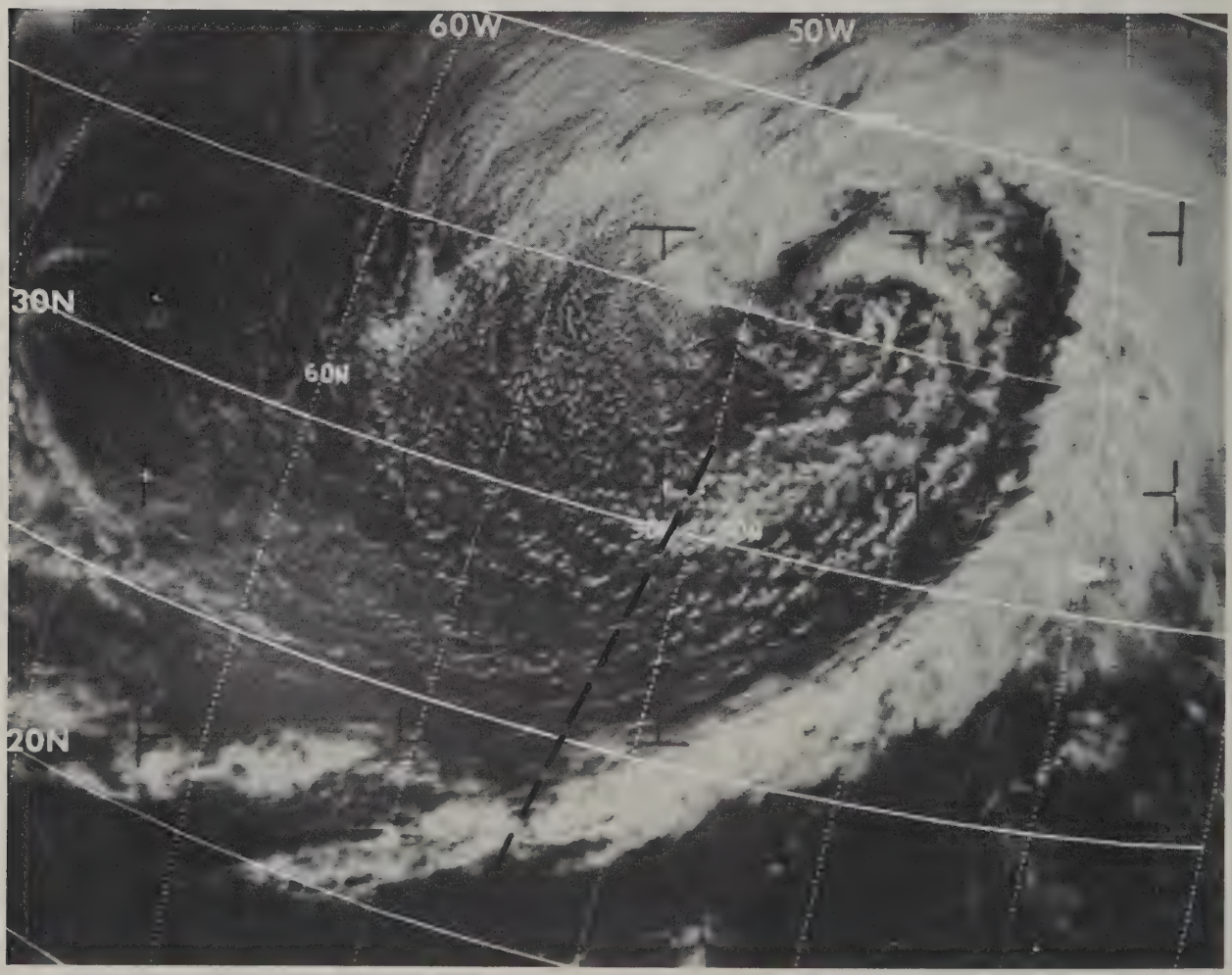

Figure 8-13. Change in frontal clouds where an upper level trough intersects a front - Atlantic, 1752 GMT, March 21, 1969, ESSA 7, Pass 2720.

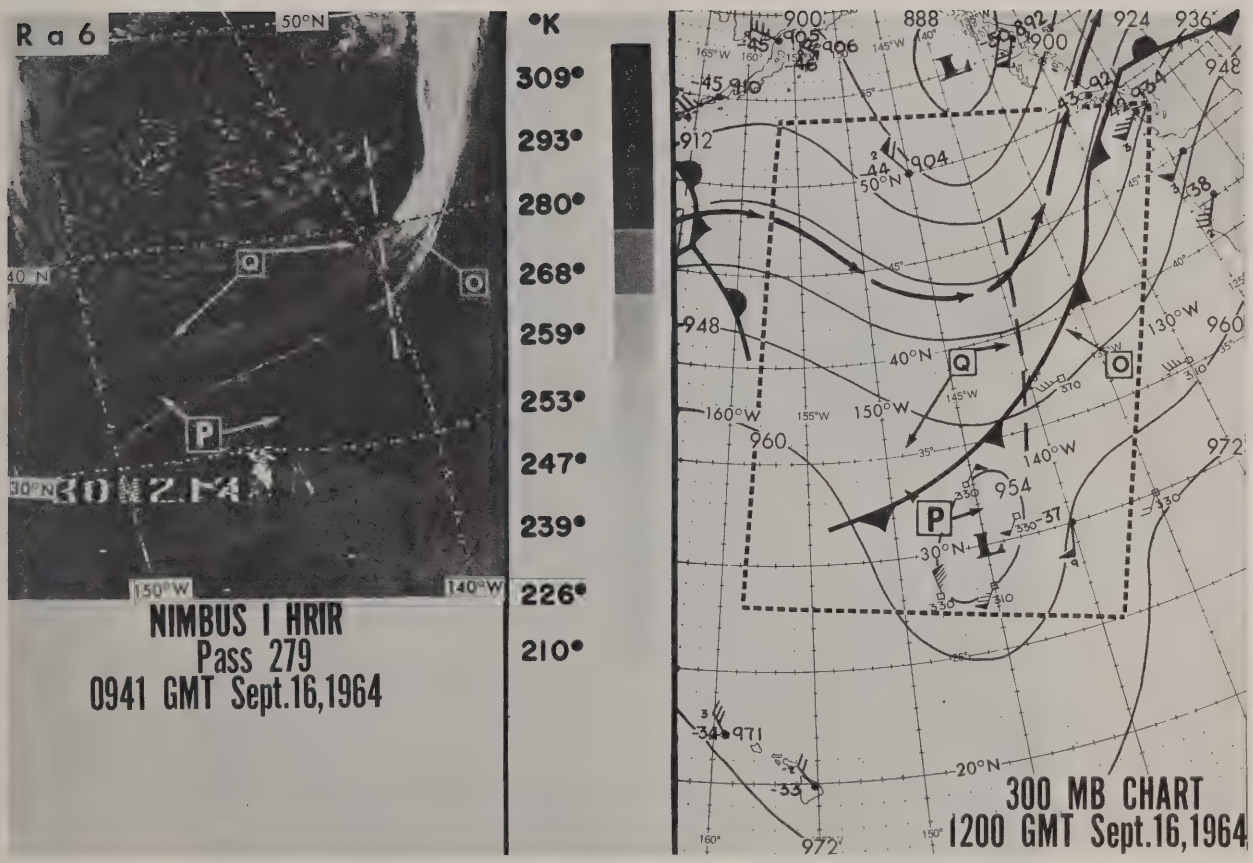

Figure 8-14. Evidence of an upper level trough in HRIR data - Eastern Pacific, 0941 GMT, September 16, 1964, Nimbus I, Pass 279 and accompanying 1200 GMT 300 millibar analysis.

Figure 8-14 is a Nimbus I High Resolution Infrared Radiometer (HRIR) picture of a frontal band in the eastern Pacific. Here, the highest clouds which radiate at the coldest temperature, appear the whitest, and the lower, warmer clouds appear dark gray. In this case, the high bright clouds begin abruptly at O, just east of the point where the 300 millibar trough (dashed line) intersects the frontal band. To the west of the trough line, the frontal band (Q) appears dark gray; here the frontal clouds are warmer and lower than the clouds east of the trough. The darkest areas, (P) correspond to clear sky views of the warm waters of the Pacific Ocean.

8.3.2 Upper Level Ridge Lines

The position of an upper level ridge often can be determined from satellite pictures. The accuracy with which the position of a ridge line can be located is strongly affected by the amplitude of the ridge, and its wind field, which determine the associated cloud structure. If the upper level ridge has sharp anticyclonic curvature, the multi-layered frontal clouds dissipate rapidly in the area of subsidence downstream from the point where the upper level flow has its maximum anticyclonic curvature. In figure 8-15, the eastern edge of the frontal cloudiness ends abruptly at the 500 millibar ridge. The solid lines show the 500 mb flow pattern. If the wind is very strong or the anticyclonic curvature of the upper level ridge is quite gradual, the multi-layered clouds are more diffuse in appearance east of the ridge. Under either of these conditions, the position of the upper level ridge is less clearly defined by the clouds.

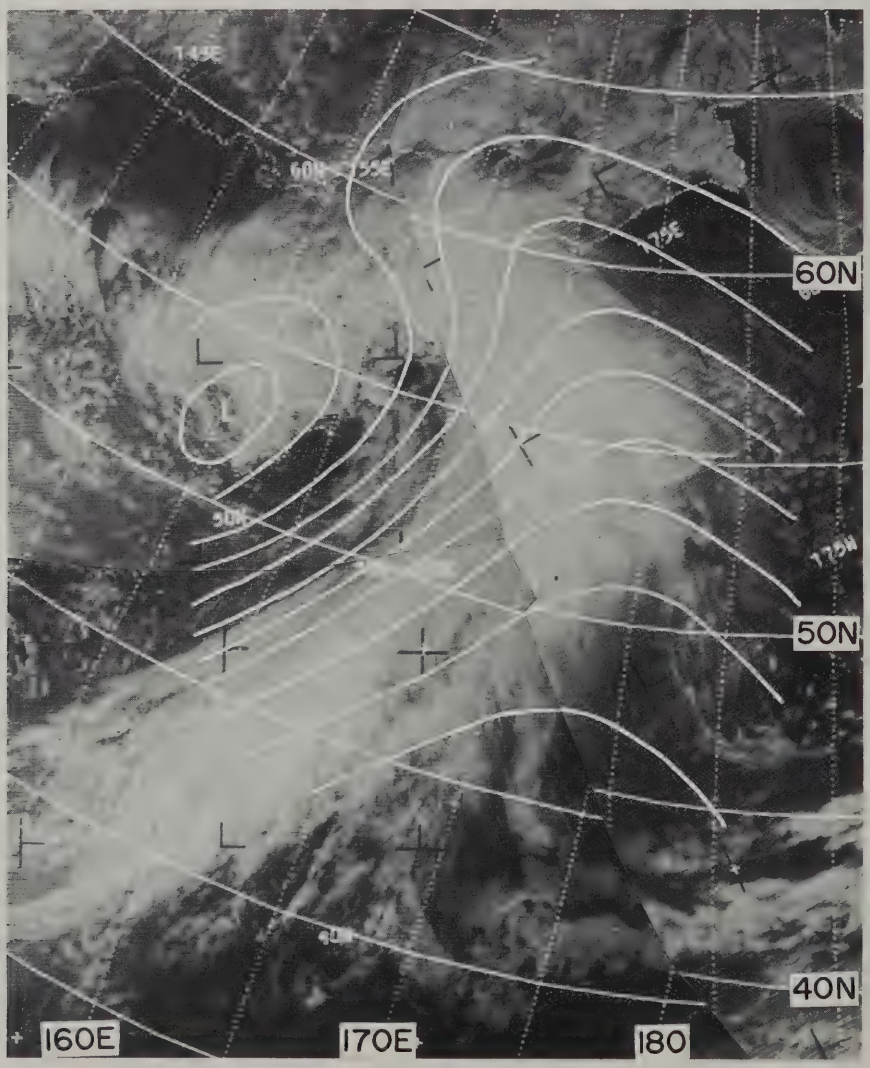

Figure 8-15. Evidence of an upper level ridge - Western Pacific, 0254 GMT, October 7, 1968, ESSA 7, Pass 646.

Figure 8-16 is an HRIR photograph of a large vortex centered south of the British Isles. A long frontal band spirals from A into the storm center at B. Note the bright appearance of the clouds along the northern portion of this band. Using the interpretation techniques described above, an analyst would conclude that the upper level trough line lies along B-C, and the upper level ridge line (D-E) lies along the periphery of the multi-layered cloud band. Note the area of enhanced convection (F) in the cellular cumulus field behind the front. Scotland, Germany, Spain, and North Africa appear in the picture as gray areas.

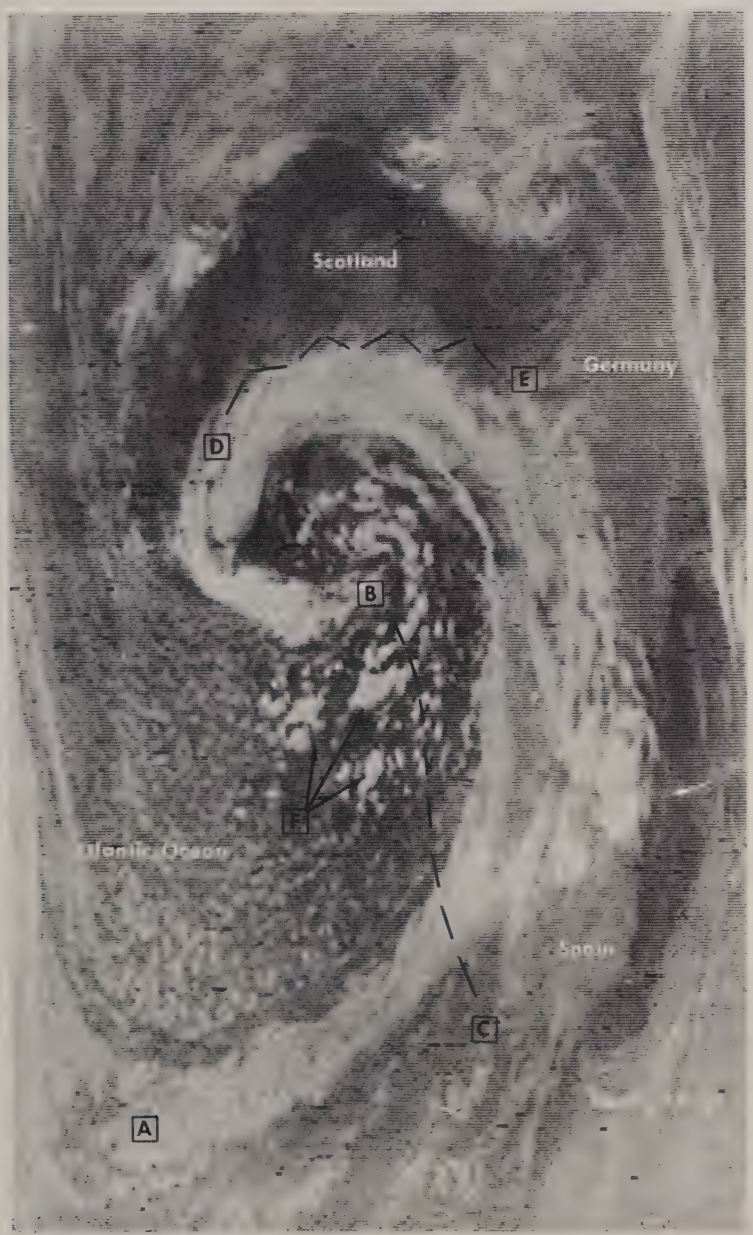

Figure 8-16. Vortex and front, HRIR data - Eastern Atlantic, 0100 GMT, October 18, 1966, Nimbus II, Pass 2073.

8.3.3 Surface Ridges

Certain unique cloud patterns and changes in cloud type can be used to determine the position of surface ridge lines. Three characteristic cloud patterns and rules for placing ridge lines in the Northern Hemisphere are described below.

Type A.

The cloud pattern of type A (figure 8-17) is characterized by long cloud lines or fingers which extend, in a continuous fashion, from a frontal band. These fingers generally are oriented in a more north-south direction than the frontal band. The end of these continuous cloud fingers serve as indicators or points for positioning the surface ridge line on the southwestern side of a subtropical anticyclone.

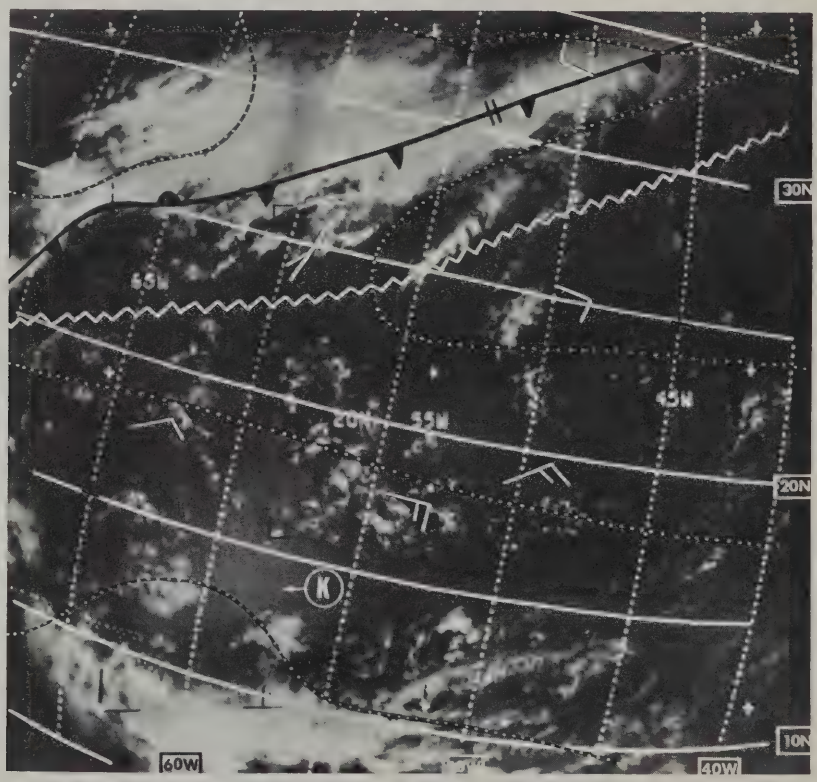

Figure 8-17. Type A surface ridge line (zigzag line). Western Atlantic, 1650 GMT, December 27, 1966, ESSA 3, Pass 1083.

Type B.

The type B surface ridge line generally is found on the western side of a subtropical high where the clouds change in character from cumuliform to stratiform. In figure 8-18, points on the surface ridge lie along the line where the cloud type changes from cumuliform to stratiform. This change in cloud character is generally found where the low level wind changes from a southeasterly to a southwesterly direction. As the air moves poleward more rapidly, stability increases near the surface and produces the observed change in cloud form.

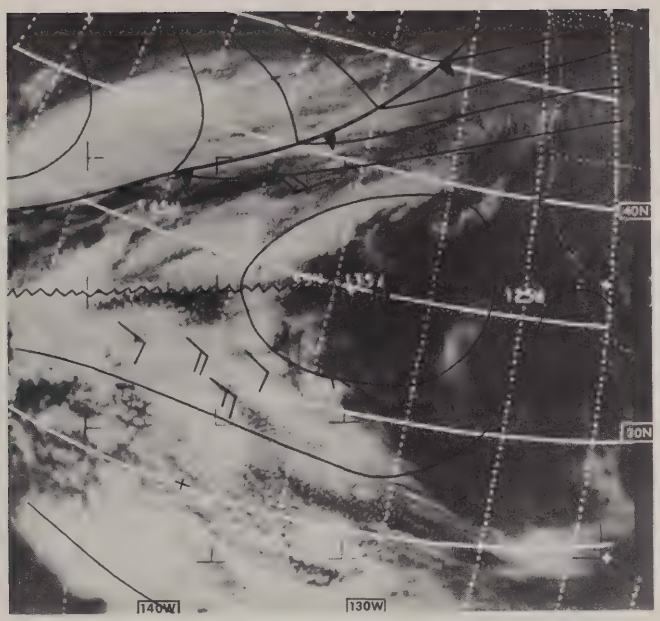

Figure 8-18.
Type B surface ridge line (zig-zag line). Eastern Pacific, 2153 GMT, January 2, 1967, ESSA 3, Pass 1161.

Type C.

The type C pattern (figure 8-19) is associated with a sharp migrating surface ridge that lies between two large cyclones in close proximity to each other. Along this ridge, there is a wind shift from a general southwesterly direction to the northwest. While an air parcel is in the southerly flow, it usually is being cooled from below and thus becomes more stable with time. Air that is in the northerly flow normally is heated from below and becomes unstable. This difference in stability produces two distinctly different cloud patterns that can be recognized in satellite pictures. The clouds in the southerly flow are primarily stratiform, while those in the northerly flow are cumuliform. Hence, the surface ridge is located in the narrow region between the stratiform and cumuliform clouds.

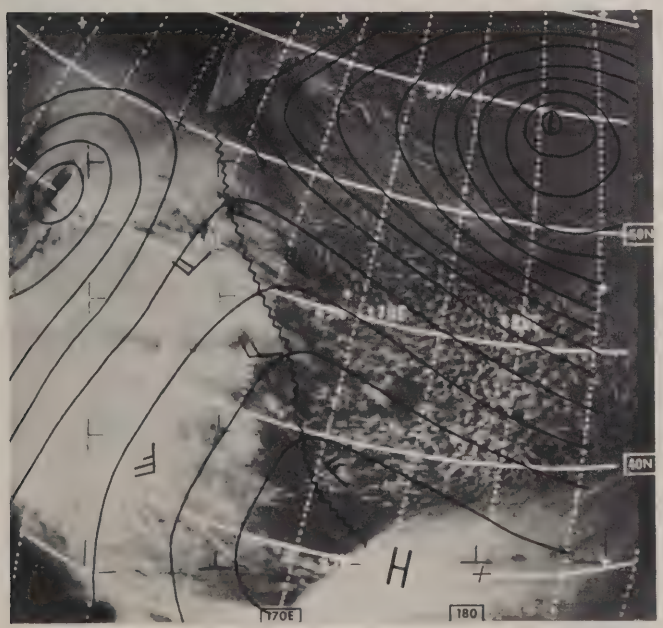

Figure 8-19.
Type C surface ridge line (zig-zag line). Pacific, 0122 GMT, December 20, 1966, ESSA 3, Pass 987.

8.4 Satellite Data Applied to Weather Analysis

The cloud formations produced by fronts, vorticity maxima, and vortices have a definite relationship to the flow patterns appearing on surface and upper air weather charts. Some examples of these relationships are shown on pages 69 and 71. In these two examples, the 1000 mb and the 500 mb analyses for the areas of the satellite pictures have been redrawn to the perspective of the satellite views. The analyses represent the best fit of the surface and 500 mb contours to the satellite cloud formations, and are based on the latest findings regarding these relationships. The analyses are compatible with all conventional data available at the synoptic reporting times nearest to the times of the pictures, and are adjusted slightly toward the times of the satellite pictures.

Example 1.

The relatively broad frontal band in figure 8-20a extends from E northeastward to F. At A, the cloud formation produced by a vorticity maximum appears in the cold air to the rear of the front. A weak 500 mb trough line crosses the frontal zone at G. In the area ahead of the trough, clouds in the frontal band at B appear brighter and thicker. The two bright cloud bands at C and D are orographic clouds on the windward side of the Coast Range and the Rocky Mountains of British Columbia.

Example 1.

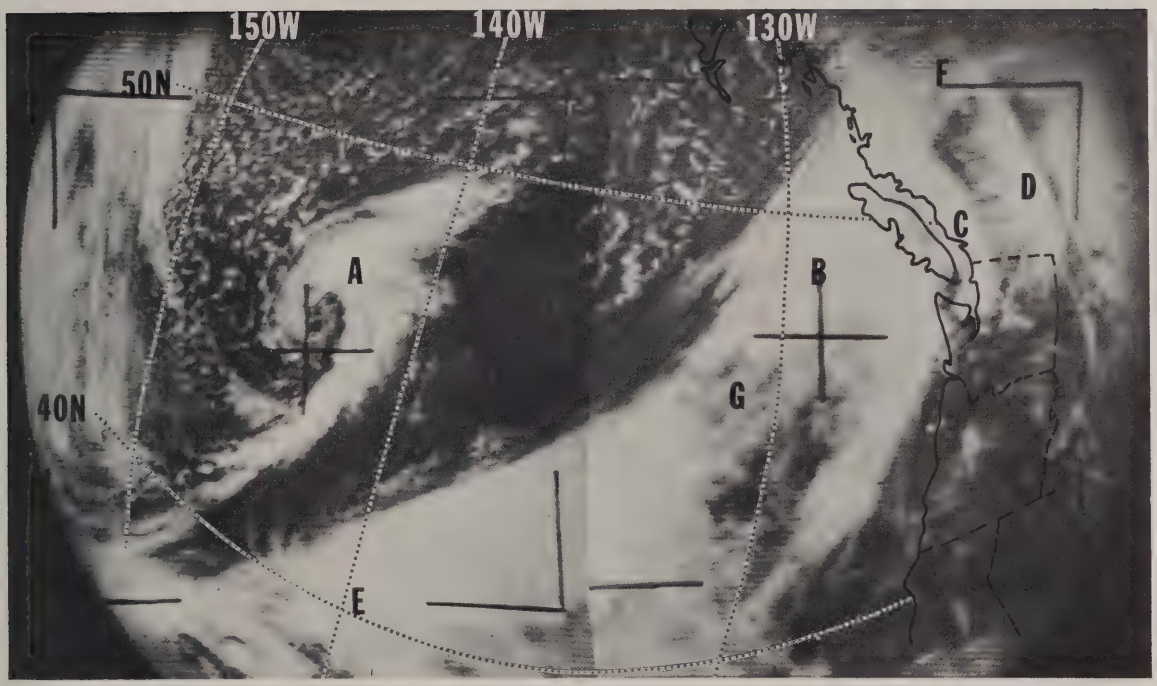

Figure 8-20a.

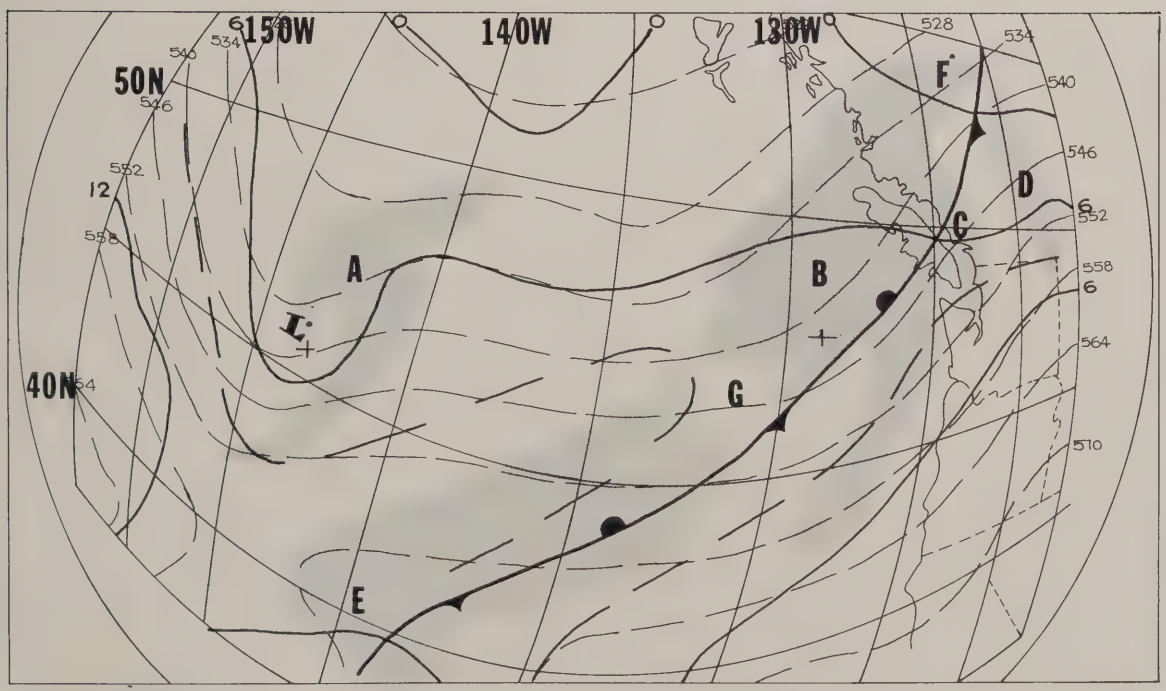

Figure 8-20b.

Example 2.

An occluded storm is shown in figures 8-21a and b. The band of clear air (B, figure 8-21a) spiraling into the vortex center is well defined in this slow moving, cut-off type storm. A change in cloud texture can be seen in figure 8-21a in the area where the jet stream crosses the frontal clouds. On the cold side of the jet (F, figure 8-21a) the clouds have a bumpy appearance. On the warm side, around point G, the clouds appear much smoother.

Example 2.

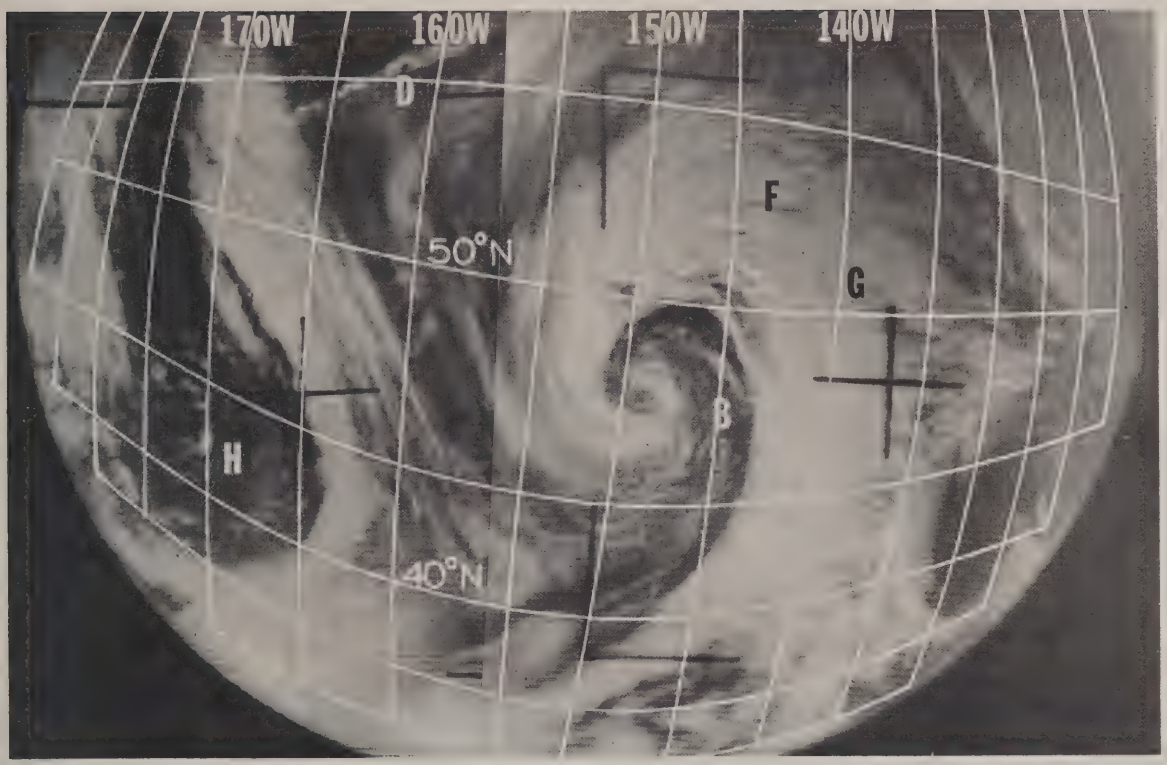

Figure 8-21a.

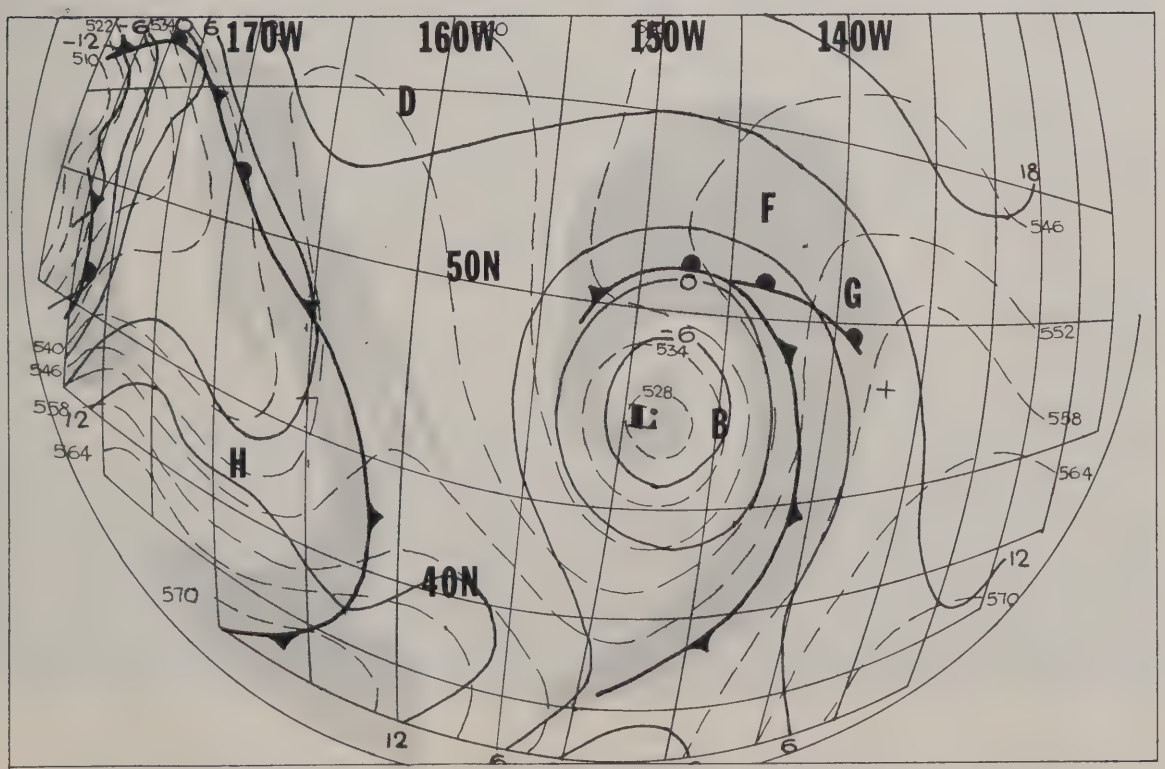

Figure 8-21b.

354-645 O - 69 - 6

8.5 Tropical Cloud Systems

8.5.1 Convective Cloud Systems Near the ITCZ

Near the Intertropical Convergence Zone there generally is a zone of convective activity about five degrees of latitude in width. The cloud zone has sharp north and south boundaries and is easily recognized in satellite pictures. Convective activity varies in intensity along the cloud zone which results in a series of distinct cloud systems interspersed with relatively inactive areas. The width and strength of the cloud zone varies seasonally.

Figure 8-22 shows the appearance of this zone in the equatorial Atlantic in September. Areas of strong convection along this zone can be seen at J and K, while the areas around L and M exhibit a minimum of cumulus activity. There is an absence of convective clouds north and south of the zone. The stratiform clouds at N suggest a marked low level stability in that region. The region south of the zone is relatively free of clouds.

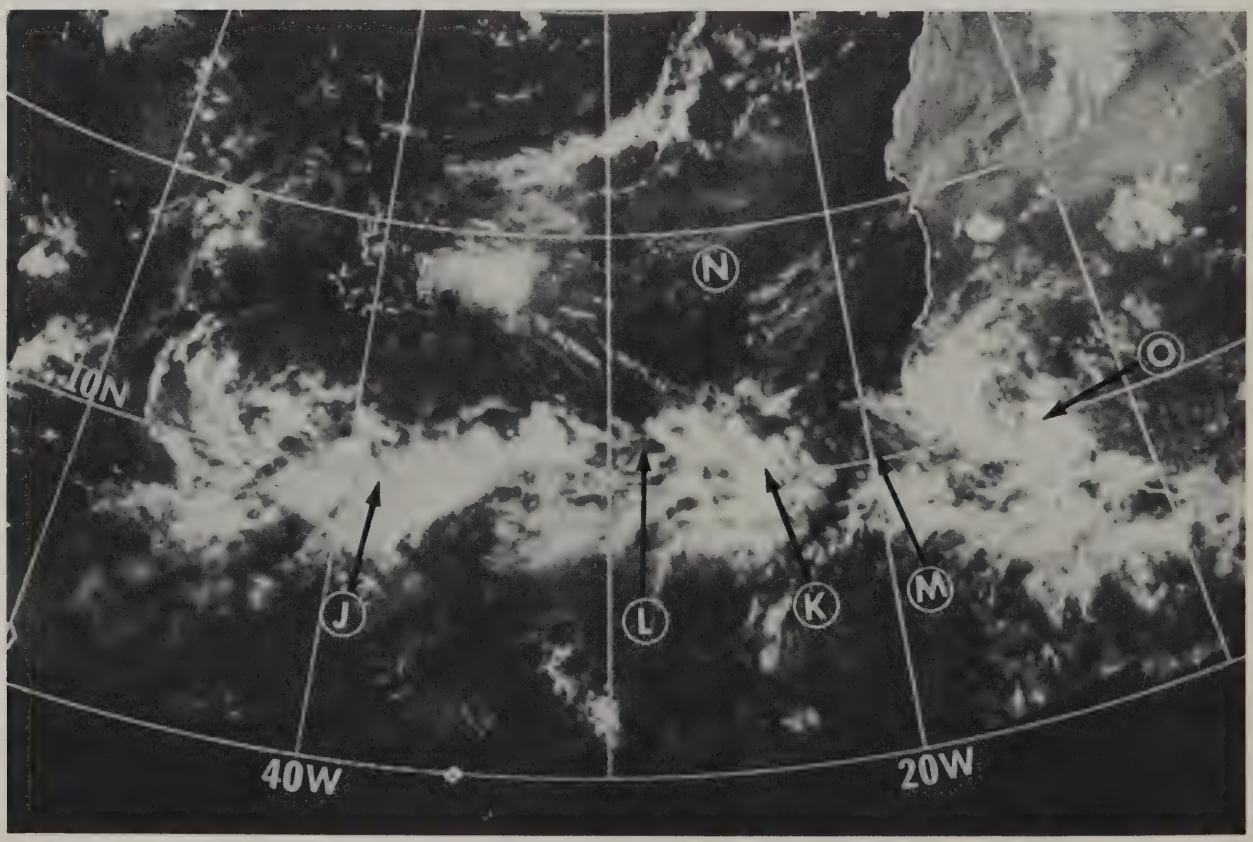

Figure 8-22. Digitized satellite mosaic of the tropical Atlantic, September 22, 1967, ESSA 3.

Satellite pictures of the cloud zone make it possible to identify areas of strongest convection, to observe changes in their intensity and to track their movement. It is common for some disturbances which originate over Africa to move westward into the Atlantic Ocean and then develop into tropical storms. Clouds associated with the early stages of this type of disturbance are similar in appearance to the area of convective activity seen at O in figure 8-22.

8.5.2 Tropical Vortices

Cloud systems produced by tropical storms during their early stages of development take on a variety of forms. The shape and appearance of these cloud systems in satellite pictures depends on the atmospheric conditions in the vicinity of the developing storm. In the initial stages, the appearance of the cloud structure often varies depending on the region of the world. After the storms reach a mature stage, they modify their immediate environment, and look much the same worldwide.

Good estimates of the stage of development and intensity of a storm can be obtained from satellite picture data. A system has been developed to determine the maximum wind speed of a tropical storm from cloud parameters obtained from the satellite pictures. This system classifies tropical cloud patterns into four groups: Stages A, B, C, and X. The basic parameters used in classification are the size and geographical location of the overcast area, the degree of circularity of the spiral band structure, and the location of the center of the spiral band relative to the major cloud mass of the storm. The characteristics of each stage are discussed below and examples of each appear in figures 8-23 through 8-25.

Stage A. This stage represents the least intense tropical disturbance. It is a dense cloud mass which occurs over a region where stronger than normal convection is taking place (see figure 23). When removed and separate from the ITCZ (Intertropical Convergence Zone), a Stage A disturbance must have a cloud system with a minimum average diameter of three degrees of latitude. When within or contiguous to the ITCZ in the Atlantic, Pacific, and South Indian Oceans, the cloud system diameter must be larger than six degrees latitude. In the Arabian Sea and the Bay of Bengal a minimum diameter of eight degrees of latitude is specified. For a disturbance lying within the ITCZ cloud band to be classified as a Stage A it must be separated by breaks on either side from the general cloudiness along the zone.

The clouds associated with a Stage A disturbance are of all types and show no curved lines or bands, so it is impossible to locate a center using these features. Centers for this type of disturbance are estimated by picking the geometrical center of the cloud system. A Stage A disturbance is often, but not necessarily, associated with a wave or perturbation in the low level easterlies. When this is the case, the clouds lie to the east of the perturbation axis. In no case is there a vortex present in the low level wind flow. Wind speeds are generally light but may approach 25-30 knots in the cloudy area where active convection is occurring.

Stage B. At this stage, some curved cumulus cloud lines or bands are observed, but there is no definite center to the pattern (see figure 8-23). These curved cumulus cloud lines are adjacent to, and often immediately west of, a dense cloud mass. Curved bands and breaks sometimes appear in the dense cloud mass. While the curved cloud lines of a Stage B pattern suggest rotation in the wind field, a closed rotation will be detected in the measured winds only when the speed of rotation exceeds the speed of translation of the center of the disturbance. Thus, the curved cloud bands of Stage B do not necessarily imply that a closed circulation exists in the measured wind field at the surface or at any other level. Wind speed near the rotation center of this cloud pattern generally will not exceed twenty knots, although winds of 30-40 knots may be observed in the area of overcast convective cloudiness east of the center.

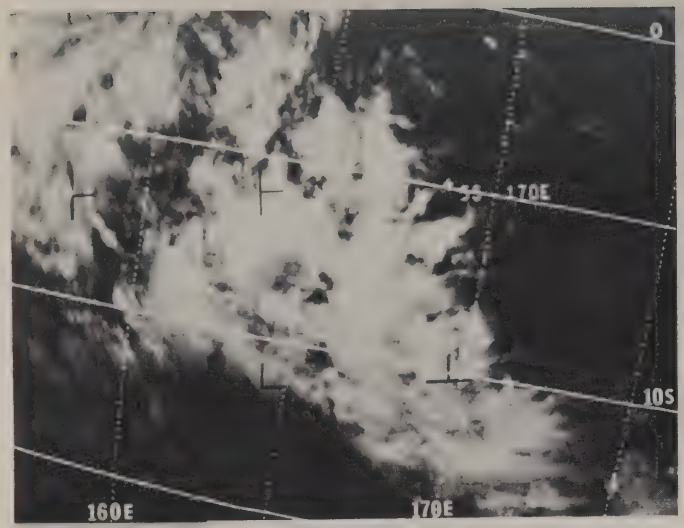

Stage A

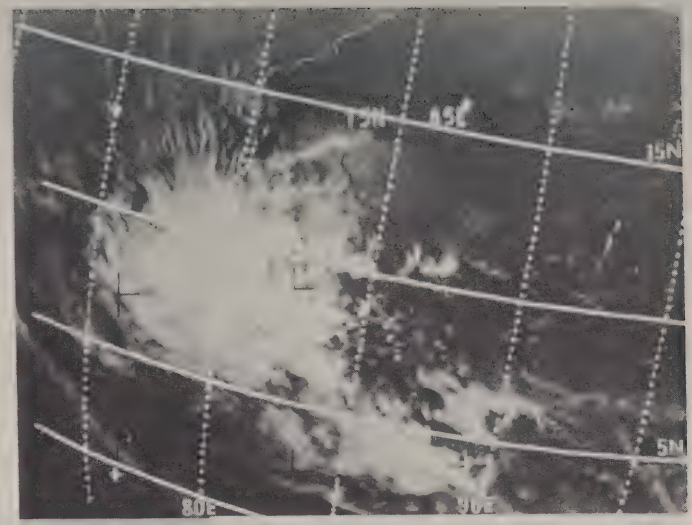

Stage A

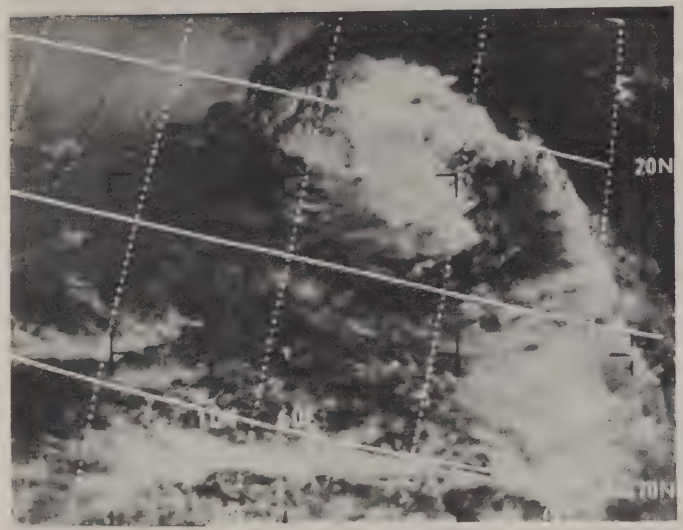

Stage B

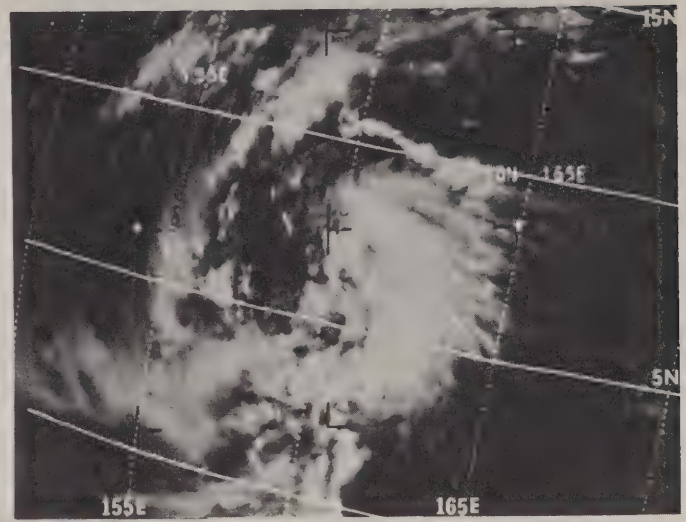

Stage B

Figure 8-23. Tropical Disturbances

Stage C. This stage (see figure 8-24) is divided into three sub-categories: C- (C minus), C, and C+ (C plus). Characteristic of all are the well defined curved cloud lines and bands which define a definite pattern center. The C- stage lacks the large area of convective cloudiness characteristic of Stages A and B. Instead, it is defined by thin cumuliform cloud lines which spiral cyclonically into a center. Stage C is a combination of a large cloud mass and curved cloud lines. Here the dense cloud mass assumes an arc which forms one side of the pattern, and low level cloud lines which spiral towards a center, completing the other side of the pattern. Stage C+ has spiral bands both in the main cloud mass and in the thin cumulus lines. The center of curvature of the cloud lines lies near or is sometimes obscured by the edge of the main cloud mass.

C+ cloud systems are usually indicative of disturbances of tropical storm intensity. At this stage of development, outflow characteristics become exceedingly pronounced. The overcast cloud shield surmounting the storm center may range from one to three degrees in diameter, becoming larger as intensity increases. However, the center of circulation, as defined by the curved cloud bands, remains near the edge of the overcast; it is never imbedded more than one-half degree inside of the cloud pattern.

In Stages C and C-, maximum wind speeds near the center of curvature range from 20 to 40 knots. It is not uncommon to find wind speeds of over 50 knots in the area of overcast convective cloudiness of Stage C. In Stage C+, typical wind speeds range from 30-65 knots. However, speeds up to 75 knots occasionally have been observed.

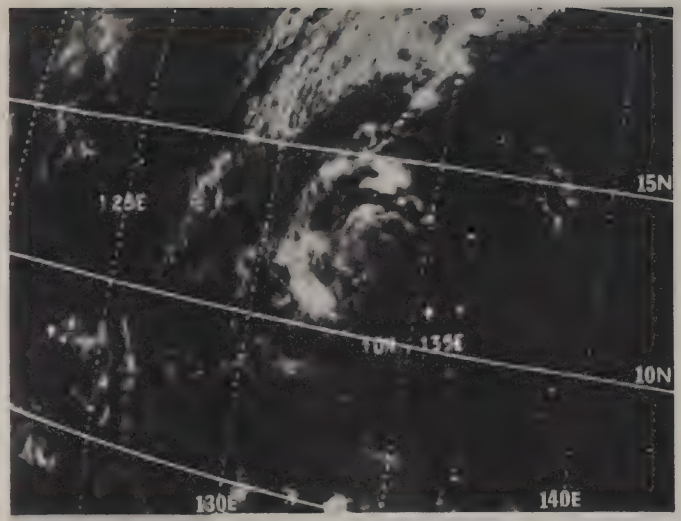

Stage C-

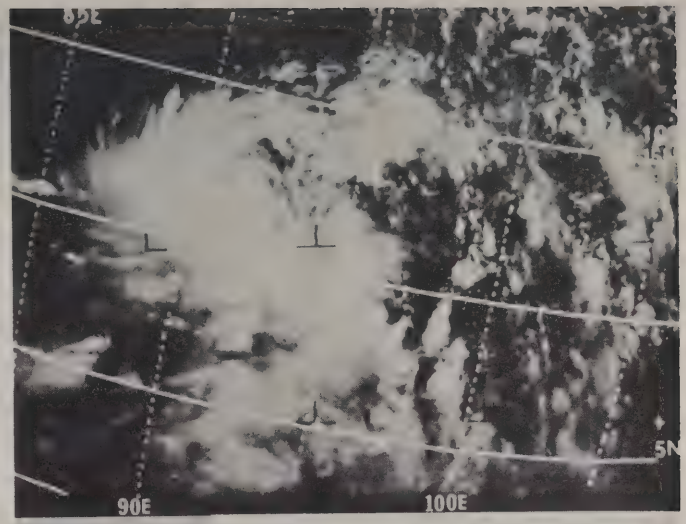

Stage C

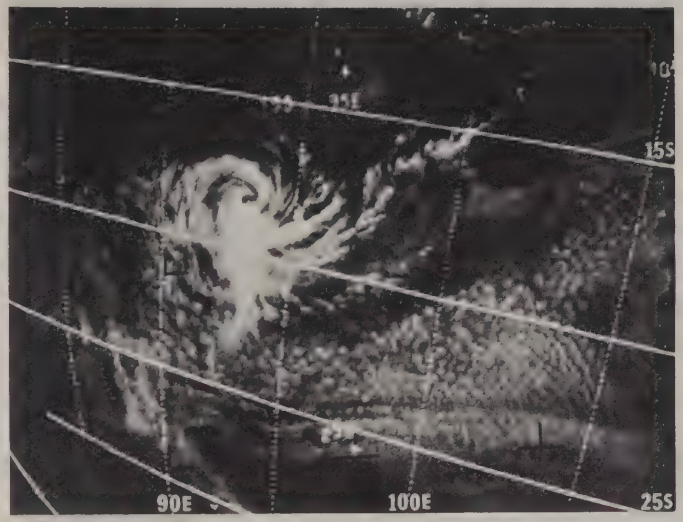

Stage C

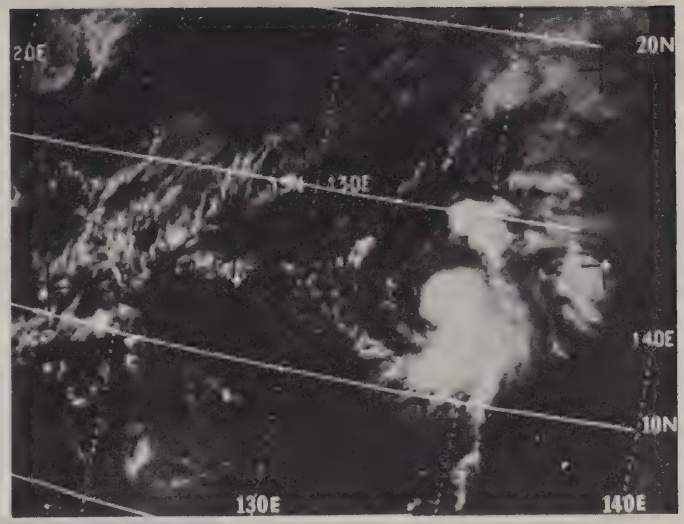

Stage C+

Figure 8-24. Tropical Disturbances

Stage X. The major characteristic of storms in this class is that the center of curvature lies within the major cloud mass (see figure 8-25). The degree of organization (circularity) in the curved and spiral clouds has a wide range. Four subdivisions or categories are used to describe this variation. Table 8 shows, schematically, the typical appearance of the cloud pattern associated with each category and defines the criteria used in assigning categories to Stage X storms. Using these measures of storm organization in conjunction with the diameter of the storm's overcast area, it is possible to estimate the maximum wind speeds in Stage X storms. Research shows that these two parameters, category and diameter, when used together, yield the wind speed estimates accurate to ± 20 knots (see figure 8-26).

Table 8. Stage X Tropical Storms

TROPICAL AND SUBTROPICAL DISTURBANCE CLASSIFICATION FROM SATELLITE DATA

STAGE X

X CAT. 1 POORLY ORGANIZED SPIRAL BANDS ILL-DEFINED CENTER OF ORGANIZATION WITHIN CENTRAL CLOUD MASS		Category 1 has a bright generally circular central overcast which is cirriform in appearance. Curved cirrus outflow is often restricted to one quadrant. Poorly organized, slightly curved cumuliform cloud bands appear near the periphery of the central overcast and cross into it at a large angle. This banding remains close to the overcast edge; away from the overcast, organized curved bands are usually absent. An eye is not visible. The center of the spiral pattern can be located approximately by extrapolating inward along the curved peripheral bands. This estimated center must be more than one-half degree latitude within the central cloud mass.
X CAT. 2 WELL ORGANIZED BANDS SPIRAL BANDS DEFINE CENTER WITHIN CENTRAL CLOUD MASS		Category 2 has a bright, often asymmetrical central overcast. Cirrus outflow is curved and more extensive. At least one long, major, well organized band spirals at a large angle into the central cloud mass. A linear curved break accompanies this band. Within the central cloud mass, the break is covered by thin cirrus but is readily detectable. Minor peripheral bands outside the overcast are poorly organized. An eye is not visible. The central tip of the major spiral band defines the center. This center must be more than one-half degree latitude within the central cloud mass.
X CAT. 3 MODERATE DEGREE OF CONCENTRICITY TO CLOUD BANDS IRREGULARLY SHAPED EYE WITHIN CENTRAL CLOUD MASS		Category 3 has a bright central overcast that is compact and tends to be circular. There is considerable curved cirrus outflow visible at the edge of the central overcast. Curved striations within the central cloud mass define spiral cloud bands which are moderately concentric about a visible eye. Well organized peripheral bands, some with well developed cirrus, are present. A ragged and irregularly shaped eye is normally visible. This defines the storm center.
X CAT. 4 HIGH DEGREE OF CONCENTRICITY TO CLOUD BANDS ROUND EYE NEAR CENTER OF CENTRAL CLOUD MASS		Category 4 has a very circular bright central overcast. The edge is often sharp and smooth over one or two quadrants, otherwise, it is striated cirrus. Highly concentric striations appear within the central overcast. Banding outside the central overcast is very well organized and circular. The entire cloud system is very symmetrical in appearance. A well defined eye appears as a small dark circular area surrounded by a bright ring. This defines the storm center.

Table 8 NESC JUNE 1968

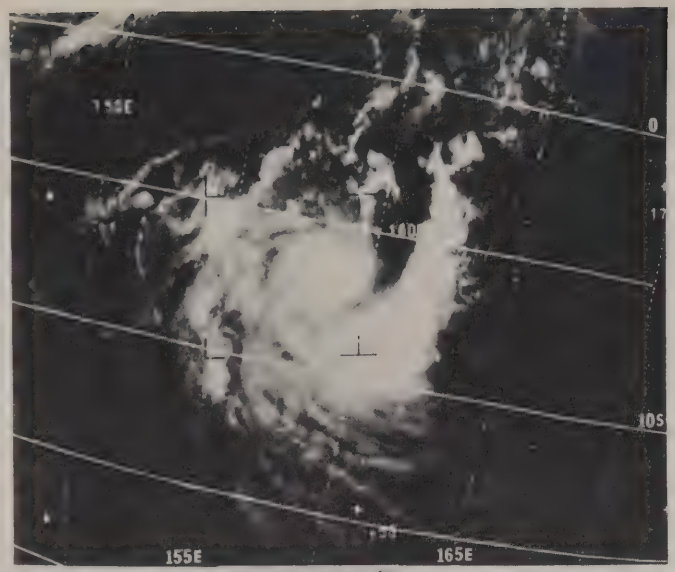

Category 1

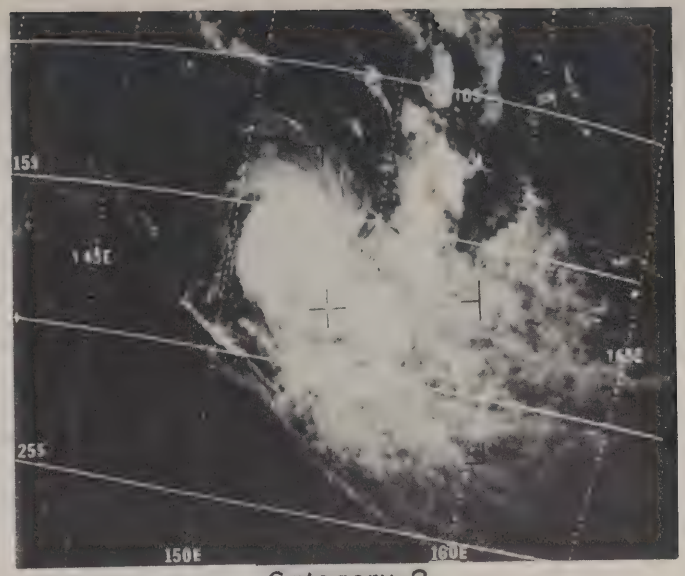

Category 2

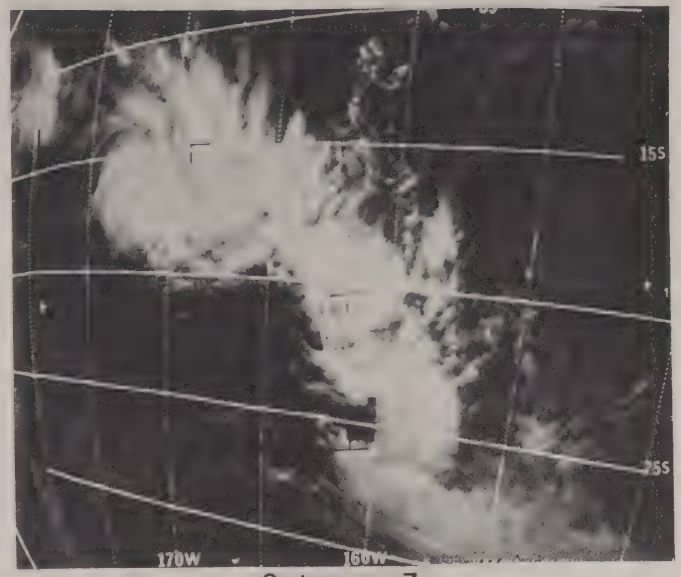

Category 3

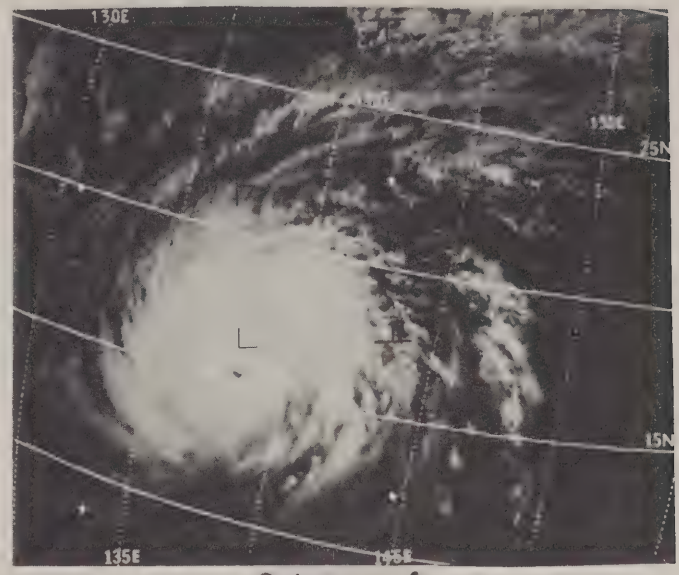

Category 4

Figure 8-25. Tropical Disturbances Categories

Certain guidelines have been established for determining the diameter of the storm's overcast. The measured cloud area must be either completely overcast, or be overcast with only minor breaks which satisfy all of the following conditions:

A. Breaks must be less than 60 nautical miles wide and covered with a thin overcast;

B. Breaks must be parallel to the spiral cloud bands;

C. Obvious spiral banding or striations must be present in the overcast area included outside the breaks.

The diameter, measured in degrees of latitude, of the largest circle that can be inscribed within the above described cloud area is the diameter used to determine the wind speed of the storm. If the diameter is determined to be less than one degree, the disturbance is classified as Stage A, B, C, or C+, depending of course on the cloud configuration.

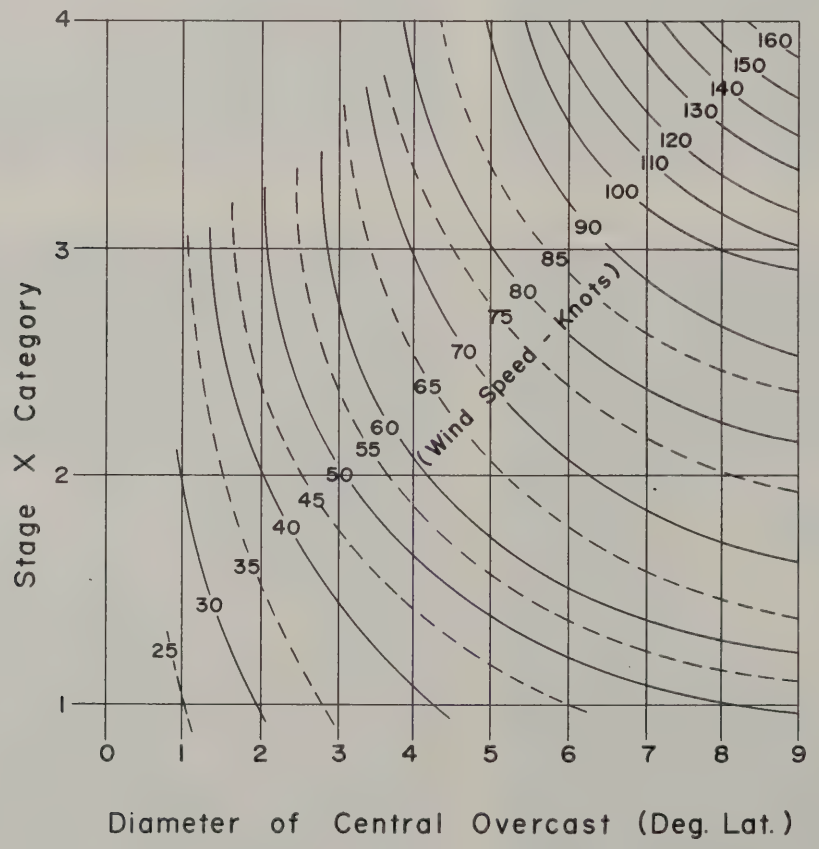

NESC 1965 ____

Figure 8-26. Nomogram for obtaining maximum winds of Stage X tropical disturbances.

8.5.3 Appearance of a Hurricane in Infrared Data

A photo-facsimile presentation of the High Resolution Infrared (HRIR) data over Hurricane GLADYS appears in figure 8-27. Below the picture is an analog trace of a single scan of the sensor through the center of the storm. The observed radiation intensity scale, converted to equivalent blackbody temperature in degrees K, is shown at right, with heights at which these temperatures occur in tropical atmospheres. Note the cold temperature (210-230° K) of the heavy overcast, and the much warmer temperatures (280-300° K) recorded over the eye and over the breaks to the east and west of the hurricane. The classification scheme developed for APT data does not apply exactly to DRIR data. As more IR data become available for study, rules and guidelines will be established for estimating the maximum wind speed of tropical storms on the basis of DRIR data.

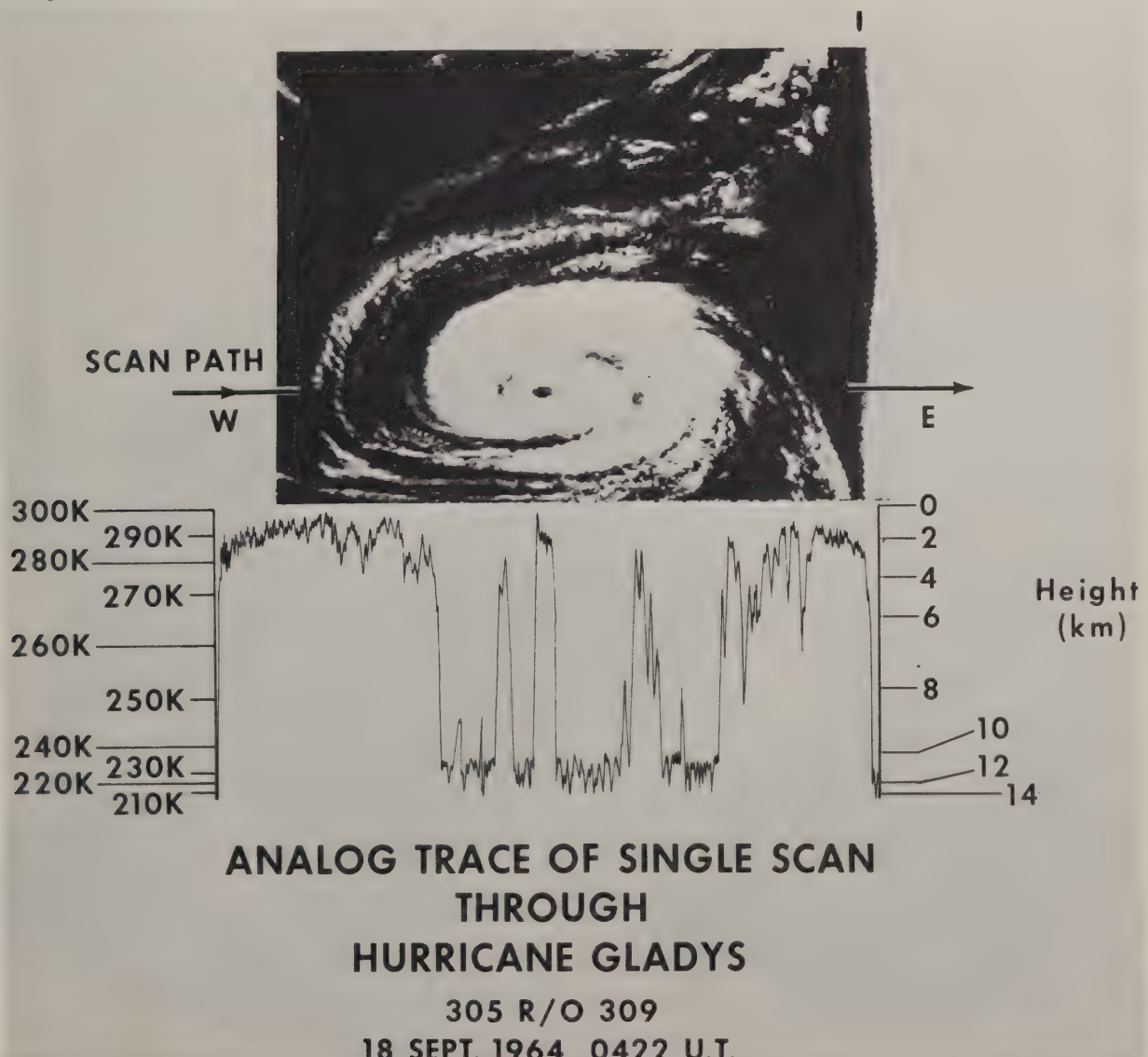

Figure 8-27. Hurricane GLADYS - HRIR data, 0422 GMT, September 18, 1964, Nimbus I, Pass 305-309.

8.5.4 Estimating Upper Level Winds from Tropical Cumulonimbus Plumes

Cirrus plumes from cumulonimbi are usually aligned with the shear through the layer from cloud base to cloud top. Cirrus plumes, emanating from convective formations in the tropics are relatively thin and generally occur near the 200 millibar level. Over large areas of the tropics, the speed of the upper level winds, where the plume forms, is several times greater than the mean speed of the layer where the lower or generating portion of the cloud is located. This results in the shear and the anvils being nearly parallel to the upper level flow.

Both cirrus plumes and jet-associated cirrus, when used with climatology and continuity, (see Jager, et al) have proven useful in estimating the upper level wind direction and speed in data sparse regions of the tropics and subtropics. An example of this analysis appears in figure 8-28. Here the 200 mb wind direction and speed, determined from the appearance and orientation of the cirriform clouds, are superimposed on the satellite data.

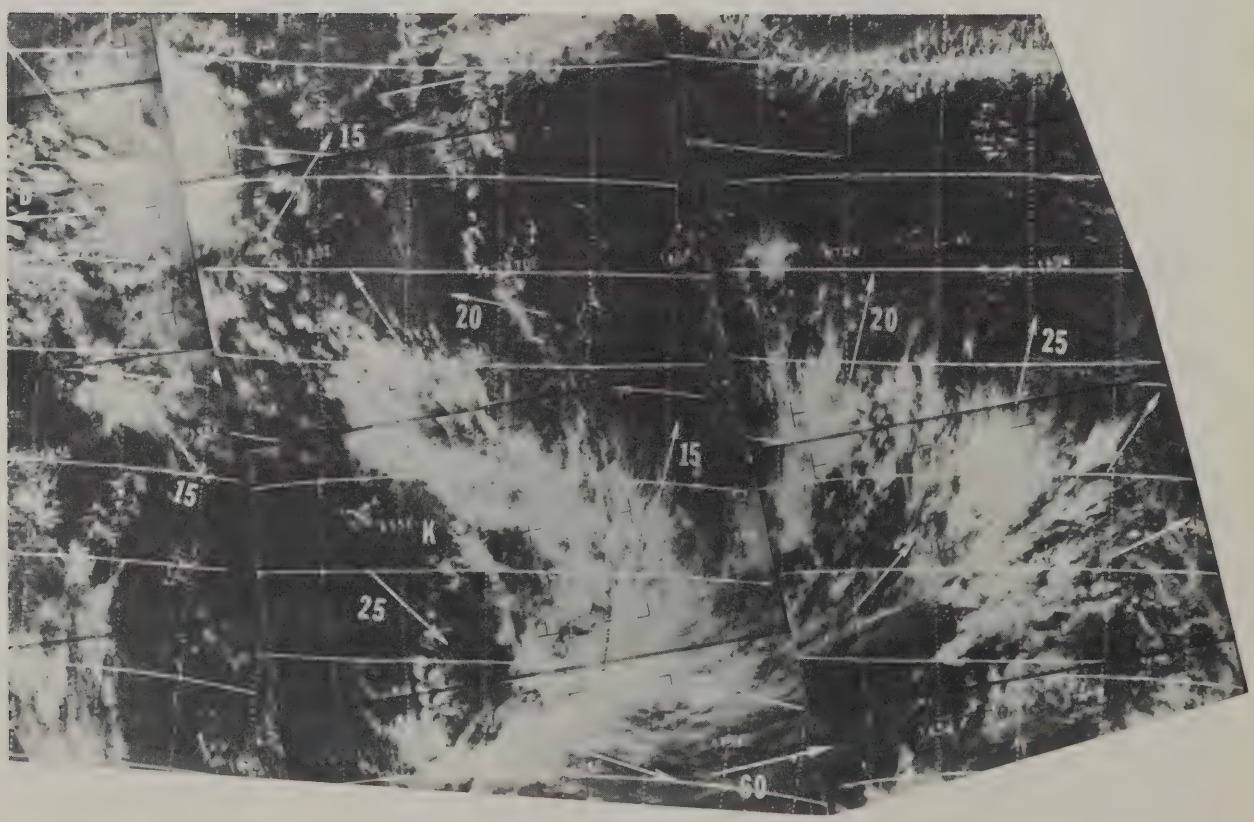

Figure 8-28. Estimated 200 millibar winds from satellite data - West Pacific, February 25, 1967, ESSA 3.

8.6 Terrain Effects and Mesoscale Cloud Systems

8.6.1 Wave Clouds

Analyses of the small details of cloud patterns seen in satellite pictures can provide information on the field of flow and the stability of the atmosphere. One feature from which this type information can be deduced is the wave cloud phenomena that forms to the lee of mountain barriers. This pattern, which consists of small cloud bands aligned parallel to the mountain barrier, and perpendicular to the wind flow, is common to all major mountain chains throughout the world. It is known that the following criteria must be met for wave clouds to form:

(a) The wind direction must be approximately perpendicular to the mountains through a deep layer of the atmosphere;

(b) winds at the mountain-top level should be blowing with a minimum speed of about 20 knots;

(c) the wind speed should increase rapidly with height; and

(d) the atmosphere should be stable.

The wavelength or distance between the cloud bands of these patterns varies directly with the speed of the mean wind through the layer in which the waves form. Preliminary studies of the turbulence associated with this pattern of wave clouds indicate that the turbulent layer is confined to the region within and below the clouds.

Figure 8-29 shows some of the effects of terrain features on the cloud distribution in the western United States. An example of the appearance of wave clouds is included in this satellite picture. At the time of this picture, strong southwesterly flow prevailed in the upper levels over western North America. The wave cloud pattern (E) over Nevada and Utah formed as a result of this flow passing over the Sierra Nevada and the Snake and Shell Creek Ranges. The cloud mass at D is due to the upslope conditions along the windward side of the Sierra Nevada, while the relatively clear area at B is in a region of strong downslope motion on the leeward side of the mountain barrier. East of C, fog and stratus fills the bays and inlets along the southern California coast and clearly defines these coastal features. Other items of interest in this picture include the vortical cloud pattern (S) and accompanying frontal band (F) just off the west coast of North America.

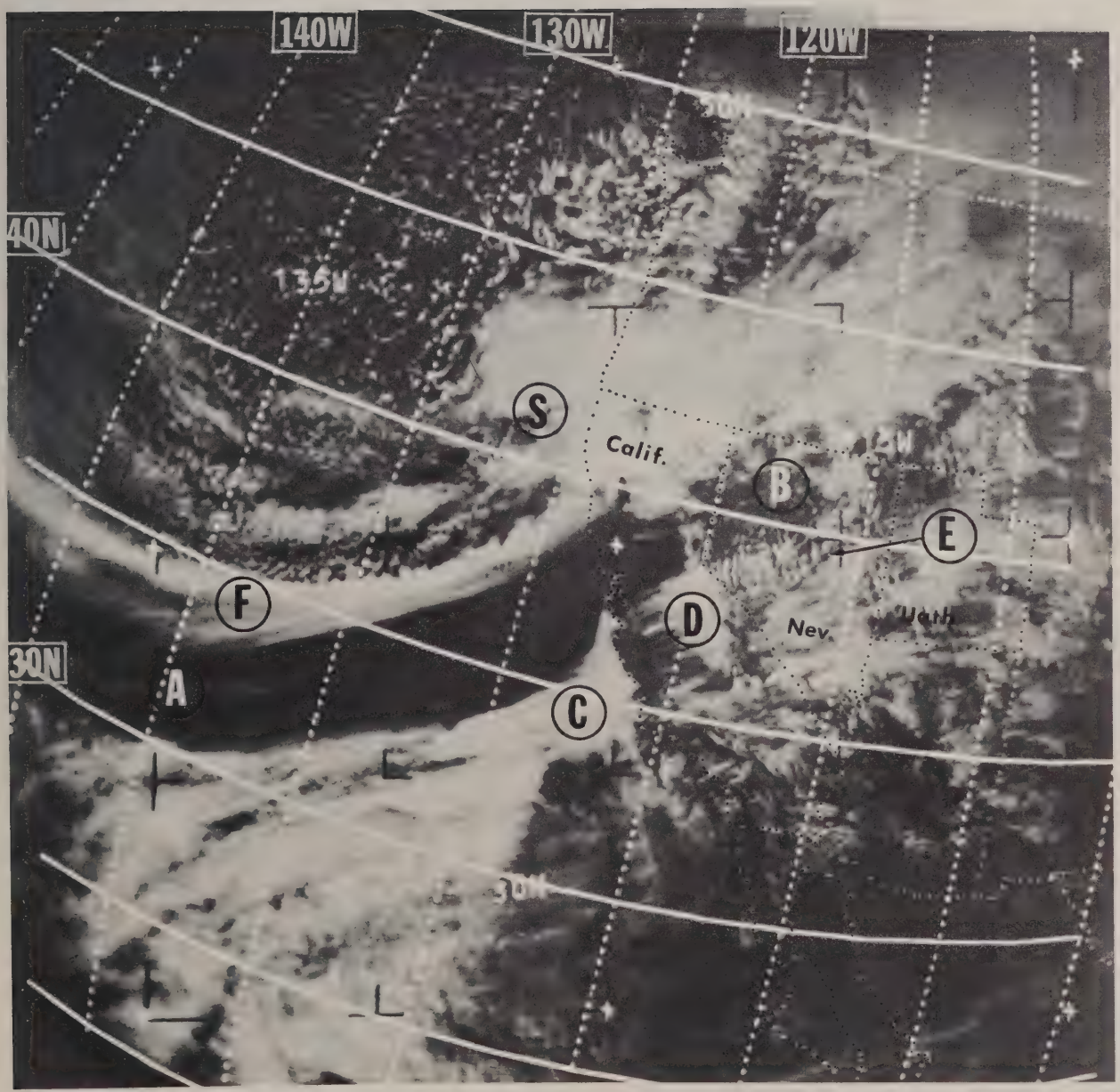

Figure 8-29. Terrain effects on cloud distribution - Western United States, 2132 GMT, February 13, 1967, ESSA 3, Pass 1688.

8.6.2 Fair Weather Cumulus

Although individual cloud elements in a field of fair weather cumulus are usually too small to be resolved by the satellite camera system, mesoscale variations in the amount of this cumulus cloudiness are detectable. These variations are caused by terrain and surface differences of the area over which the cumulus are observed.

Figure 8-30 shows an example of these effects over the Florida Peninsula. Most of the clouds in the interior of the peninsula are too small to be resolved by the camera, thus giving the area a mottled gray appearance. The effects of coastlines and interior lakes on the cumulus cloud distribution can be seen in this picture. Over Lake Okeechobee (A) and the lakes in northern Florida (B), where land induced convection is absent, the skies appear relatively cloud-free. Tampa Bay, east of point C, and Charlotte Harbor, east of point D, are also free of cloud. Local convergence has caused a concentration of cloudiness along the coastlines near points E and F. On the St. Petersburg Peninsula (G), to the west of Tampa Bay, convergence has produced a single cloud which appears larger than the rest. The clouds over the Atlantic and south of the Florida Keys, at points H and I, are cumulonimbus. The effects of local terrain on the development and distribution of cumulus cloud are often evident in satellite pictures such as this one.

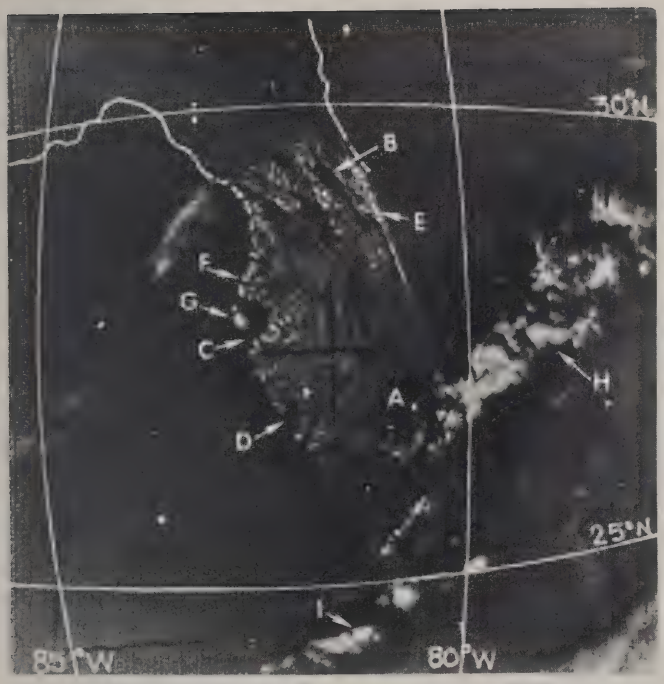

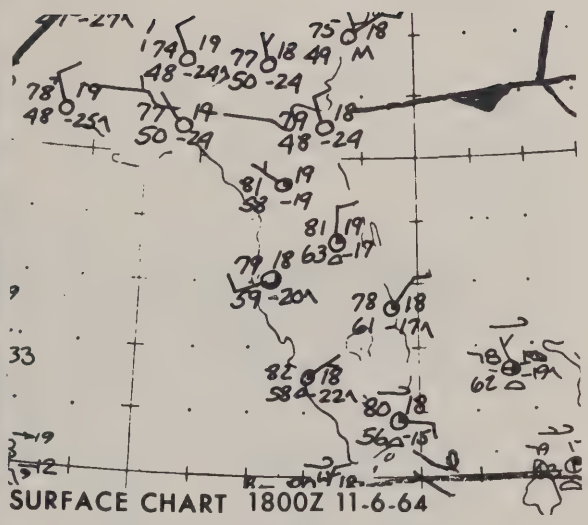

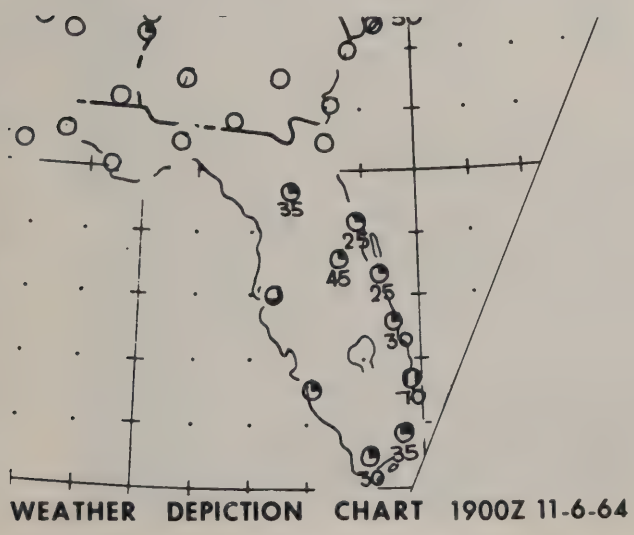

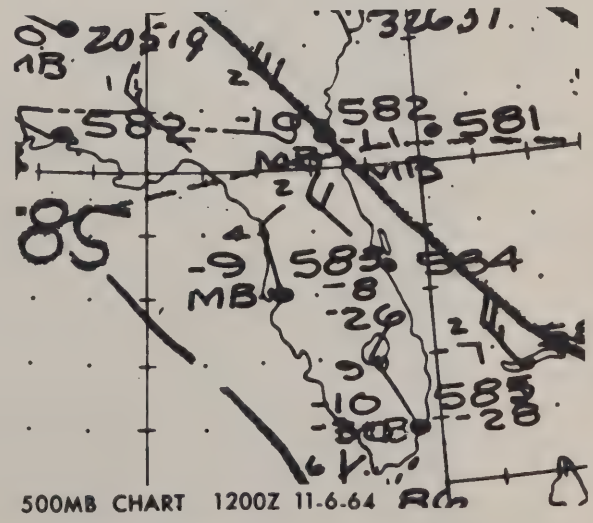

Figure 8-30. Fair weather cumulus - Florida Peninsula, United States, 1747 GMT, November 6, 1964, TIROS 8, Pass 4659T.

354-645 O - 69 - 7

8.6.3 Cumulonimbus Clouds

Cumulonimbus clouds are often the brightest clouds observed in satellite photographs. Individual cumulonimbus clouds associated with a mature thunderstorm have an average diameter of 10 to 20 miles, and are large enough to be seen in satellite pictures. Often these individual clouds combine to form large cumulonimbus clusters under whose anvil canopy severe local storms are often observed. In figure 8-31, a broken band of cumulonimbus clusters extends from Texas north-northeastward to Minnesota. These clouds lie along and to the east of an advancing cold front. Radar reports indicated the tops of the highest convective cells were at 50,000 feet. The bright, smooth appearance of these clusters, and those to the east at A, are typical of cirrus canopies produced by the merging of the anvil tops of the individual thunderstorms. These canopies characteristically have a sharp edge on the upwind side of the anvil. The cirrus canopy thins out as it moves away from its source, resulting in an indistinct or fuzzy edge to the cloud on the downwind side. More than 50 tornadoes were reported on this day -- one of the most active of the 1968 severe storm season.

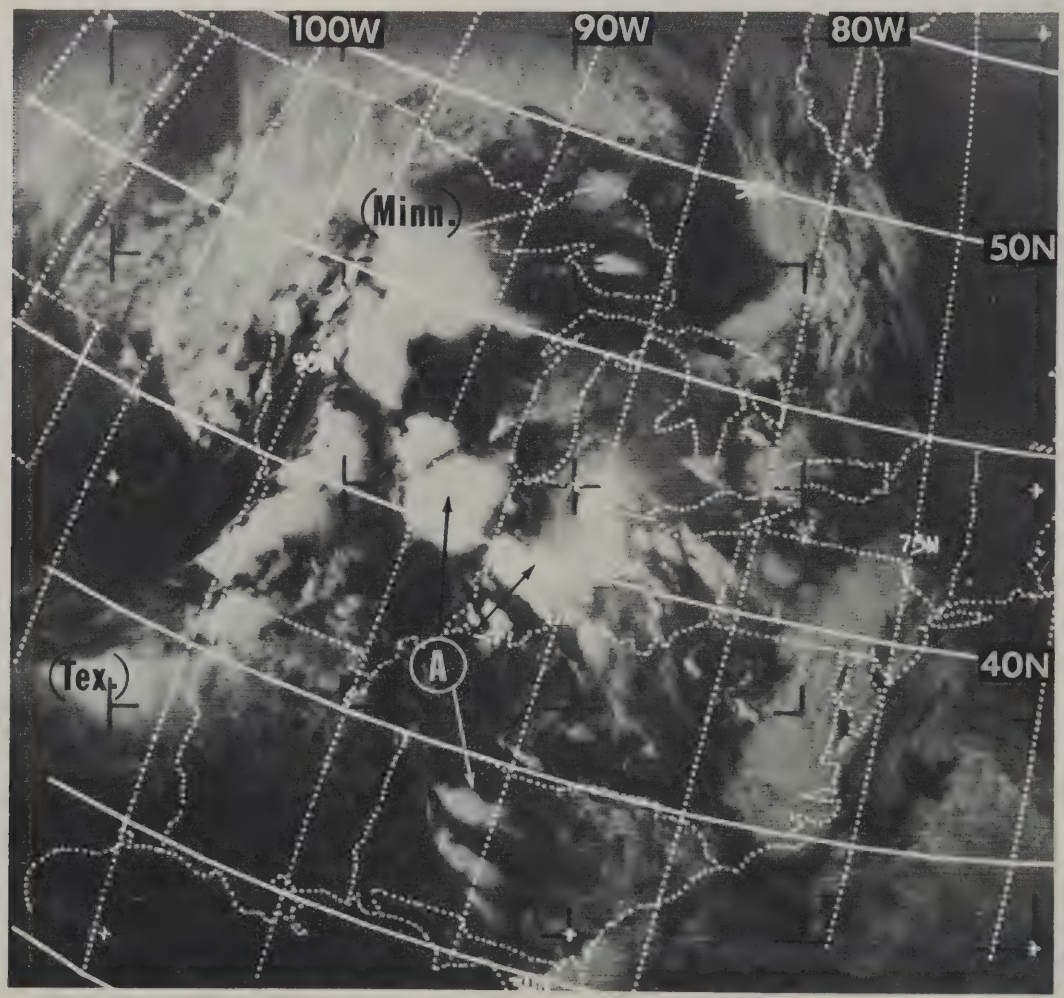

Figure 8-31. Cumulonimbus clusters - Central United States, 2119 GMT, May 15, 1968, ESSA 5, Pass 4961.

Cumulonimbus often occurs in an area where extensive low cloud is also present, so that it becomes impossible to observe cumulonimbus from the ground except by radar. In the satellite picture of figure 8-32, a cold front lies through north central Texas with an extensive area of clouds to the north of the front. The winds aloft are from the southwest and strong warm air overrunning is taking place.

The radar summary chart of figure 8-32 outlines the area of scattered radar echoes observed one hour before the satellite picture. The areas of cumulonimbus in the satellite picture (B, C, figure 8-32) can be separated from the lower clouds by their brighter appearance toward the southeast and by the shadows which they cast on the tops of the lower clouds toward the northwest. The larger well defined shadow at point D indicates that the convective tower which cast the shadow extends highest above the general cloud level at that point. The cloud layer around A is stratiform; the top of the layer is smooth in appearance. In contrast, the upper cloud surface to the east and northeast where cumulonimbus are present exhibits the typical "bumpy" appearance of cumuliform clouds.

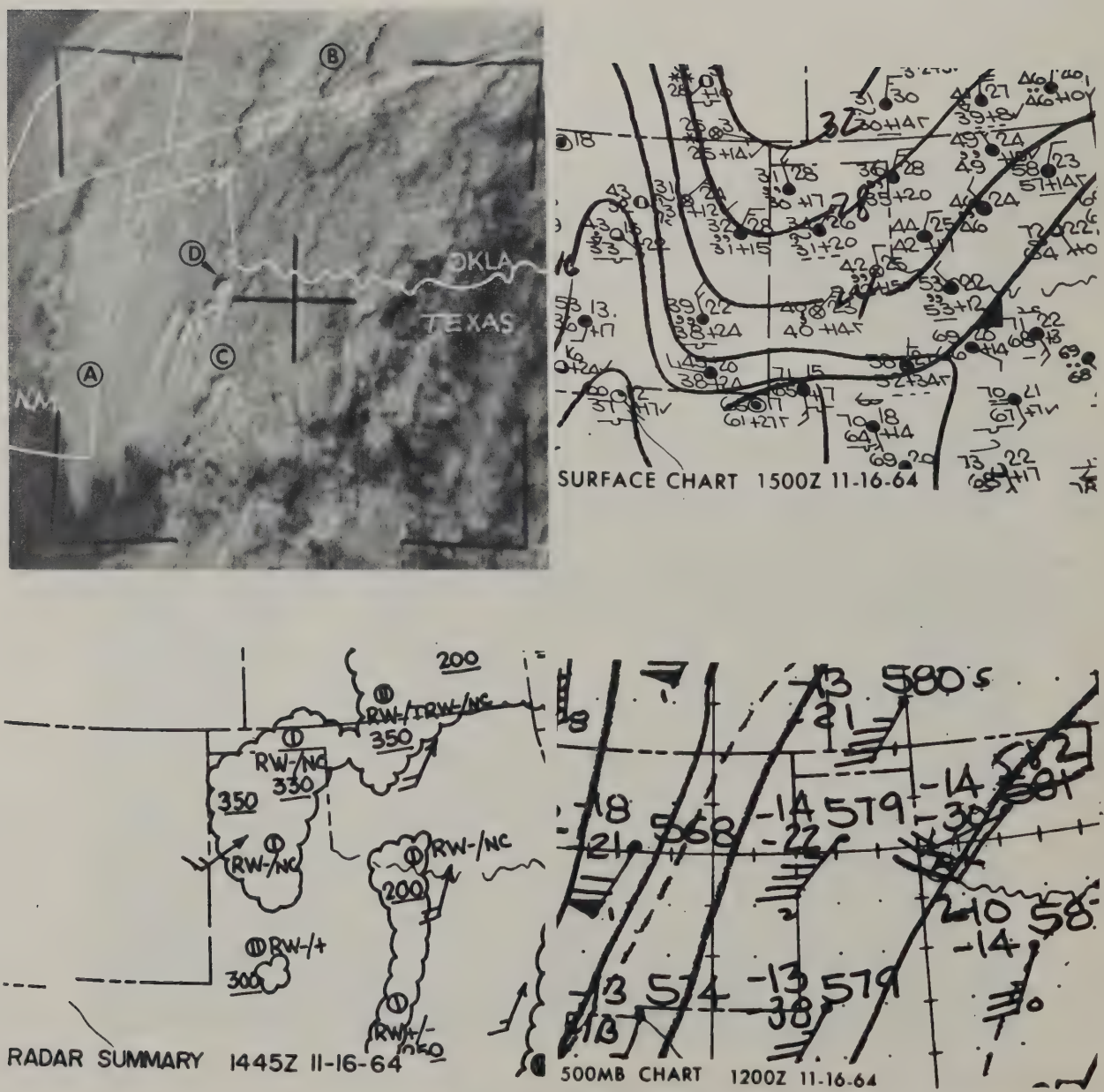

Figure 8-32. Cumulonimbus and stratiform cloud - Central United States, 1555 GMT, November 16, 1964, TIROS 7, Pass 7633T.

Cirrus spissatus often has the appearance of cumulus in satellite pictures. The globular clouds over Africa shown in figure 8-33 are cirrus spissatus. The shadows which are visible to the north of each cloud element identify these clouds as high clouds rather than low cumulus. While the cloud shadows suggest cumulonimbus, the appearance of the cloud area is not typical of cumulonimbus. The tops of cumulonimbi cloud masses extend to various altitudes, not all of which are high enough to cast shadows. In figure 8-33, all of the cloud elements are observed to have shadows, suggesting a formation of high altitude clouds such as cirrus spissatus rather than cumulonimbus.

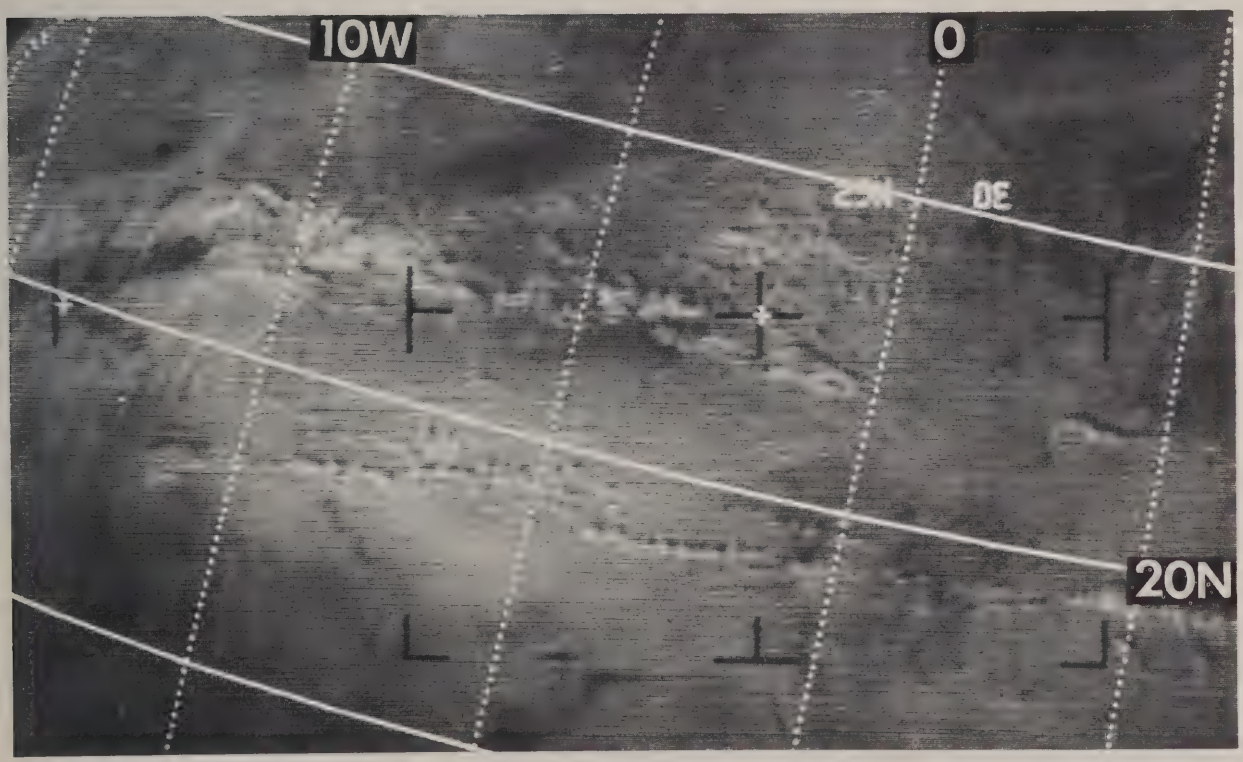

Figure 8-33. Cirrus spissatus over Africa, 1443 GMT, December 3, 1968, ESSA 7, Pass 366.

8.6.4 Fog and Stratus

Thick ground fog or low stratus over land has a distinct appearance. The top of a fog or stratus area appears very smooth and flat as at point A in figure 8-34. In northern Illinois south of point A, the fog area has a relatively smooth edge; this is typical of an area of fog over flat terrain. The cumuliform clouds in Missouri (B) are much more irregular and ragged in appearance. High cirrus spissatus are visible above the top of the fog and stratus layer in eastern Iowa (C). These upper clouds can be detected by the shadows they cast on the cloud surface beneath them.

Figure 8-34. Fog, stratus and cumuliform clouds - Central United States, 1746 GMT, November 6, 1964, TIROS 8, Pass 4659T.

Satellite pictures can be an aid in determining the exact boundary of an area of fog or low stratus. Figure 8-35 shows Puget Sound (A), and the Willamette River Valley (E) covered with fog and stratus. The Coast Range between points B and C and the Cascade Range between points D and F are cloud-free. Low clouds cover the Columbia Plateau (G). Most of the weather stations reporting fog and stratus on the Weather Depiction Chart are located in the lowlands. The continuous smooth line shown in the Weather Depiction Analysis attempts to enclose the areas where cloud bases are less than 1000 feet. The analysis, based on available surface reports only, has erroneously included the cloud-free Cascades in the cloud-covered area. The satellite pictures show at a glance those areas where the terrain is free of low clouds.

Snow-covered mountain peaks can also be seen in the picture. Immediately south of point D, Mount Rainier (14,410 feet) shows as a small bright area. Also visible are Mount St. Helens (9,671 feet) and Mount Adams (12,307 feet).

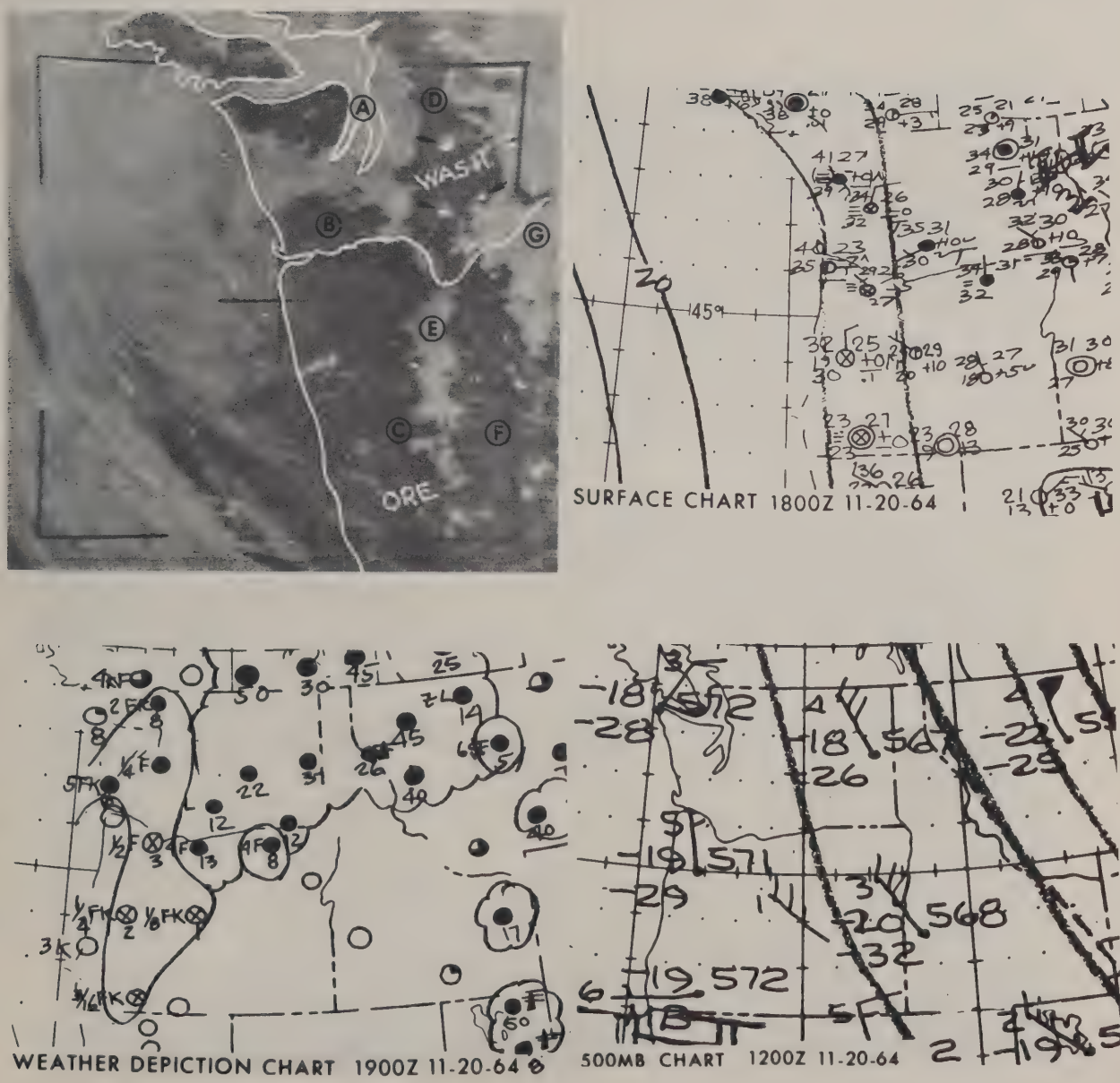

Figure 8-35. Fog and coastal stratus - Northwestern United States, 1725 GMT, November 20, 1964, TIROS 7, Pass 7692D.

During the summer, much sea fog and stratus occurs at high latitudes over the ocean areas. This extensive cloudiness can make the identification of other cloud formations, such as frontal bands, quite difficult. Areas of oceanic fog and stratus are characteristically gray and mottled, with long alternating bands of thin and thicker stratus (L and M in figure 8-36). In this satellite view of the northern Pacific, a frontal band lies across the bottom part of the picture (N to O). The thicker clouds of the frontal band appear brighter than the surrounding area of fog. Since fog and stratus form close to the surface and are often shallow in depth, orographic barriers can exert a visible effect on the cloud pattern. When low level winds are blowing against an island barrier, the fog and stratus thicken along the windward portion of the island, while a clear area forms to the leeward side. An example of this is shown around St. Lawrence Island at P in figure 8-36.

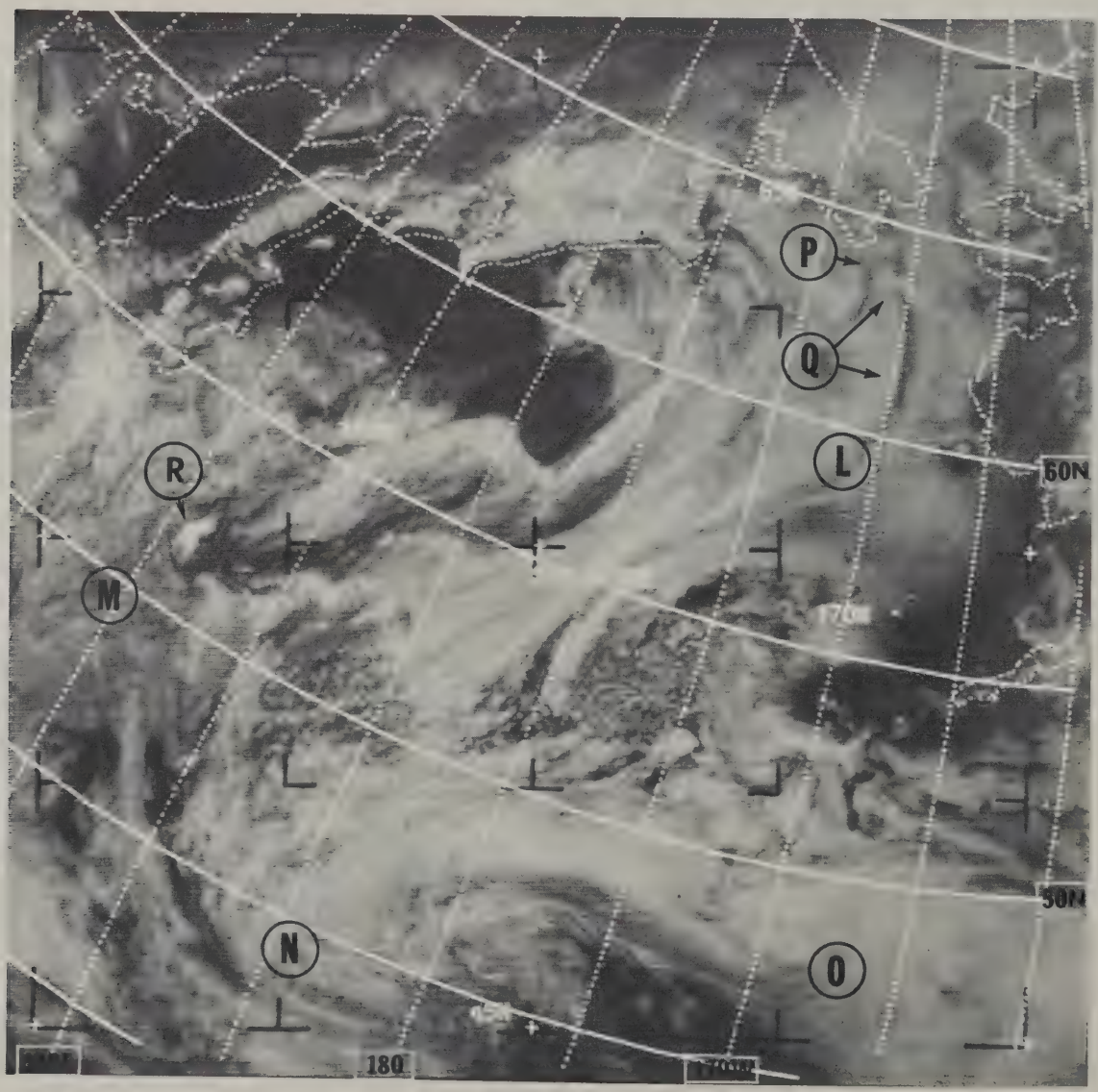

Figure 8-36. Oceanic fog and stratus - North Pacific, 0321 GMT, June 4, 1968, ESSA 5, Pass 5205.

8.7 Snow and Ice

8.7.1 Snow-Covered Land

Water resource management requires the collection and analysis of data on snow cover and ice formations. It is not possible to gather information on these parameters by standard techniques in remote, inaccessible, or sparsely populated areas. However, daily satellite observations allow hydrologists to chart the changes of snow fields. River and lake ice coverage can also be mapped.

To do this, the hydrologist must be able to discriminate between areas of snow and clouds. Both snow and clouds can appear equally white in satellite pictures. This similarity in appearance presents a problem in interpretation when both snow-covered ground and bright clouds appear together. Another problem is that small isolated snow areas such as snow-covered mountain tops, and cumuliform clouds appear much the same when viewed from above. In spite of these difficulties, it is possible to separate snow from clouds by learning to recognize orographic features visible in snow-covered terrain, and to identify cloud shadows over the snow.

Topography and vegetation determine the appearance of snow-covered terrain. Every snow-covered region of the world has a unique appearance which forms a background to the ever-changing cloud cover. While snow patterns may appear the same from one day to the next, cloud patterns seldom appear the same on successive days.

The snow cover on mountain ranges forms distinct dendritic patterns which can be distinguished easily in satellite pictures. The cloud-free view of western Canada (figure 8-37), shows dendritic snow patterns on the Coastal and Rocky Mountain Ranges. The edge of the snow field (A) appears along the western slope of the Coastal Range. A weekly analysis of the snow fields in the Northern Hemisphere is prepared from data such as this. Variations in brightness over snow-covered areas are due to differences in vegetation and the age of the snow. Such variations appear in the area of coniferous forests (B) between the Coastal and Rocky Mountains, and in the area further east. Ice and snow-covered Lake Athabasca and Great Slave Lake can be seen along the right-hand edge of the picture.

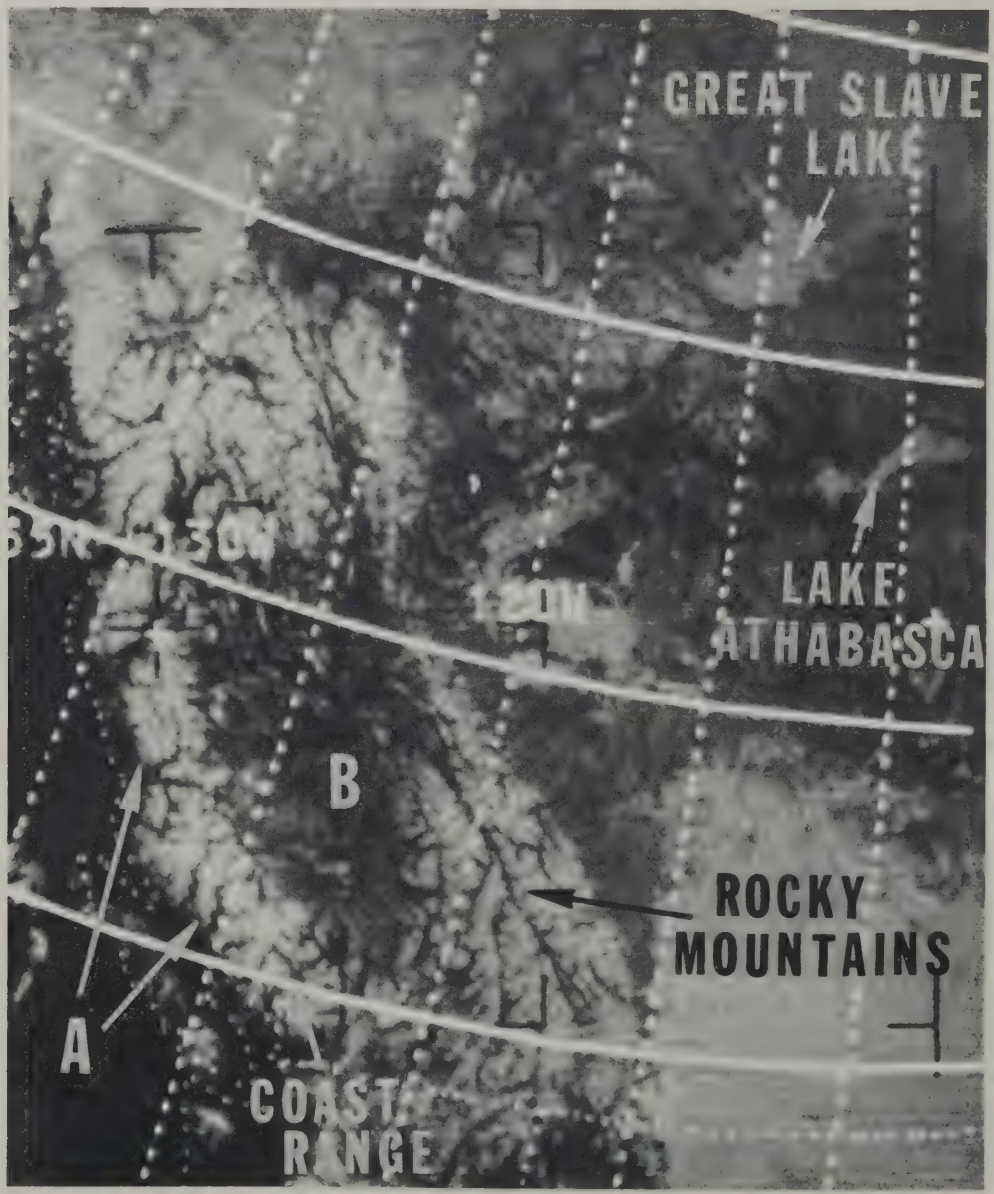

Figure 8-37. Snow cover on mountain ranges - Western Canada, 2123 GMT, March 12, 1967, ESSA 3, Pass 2027.

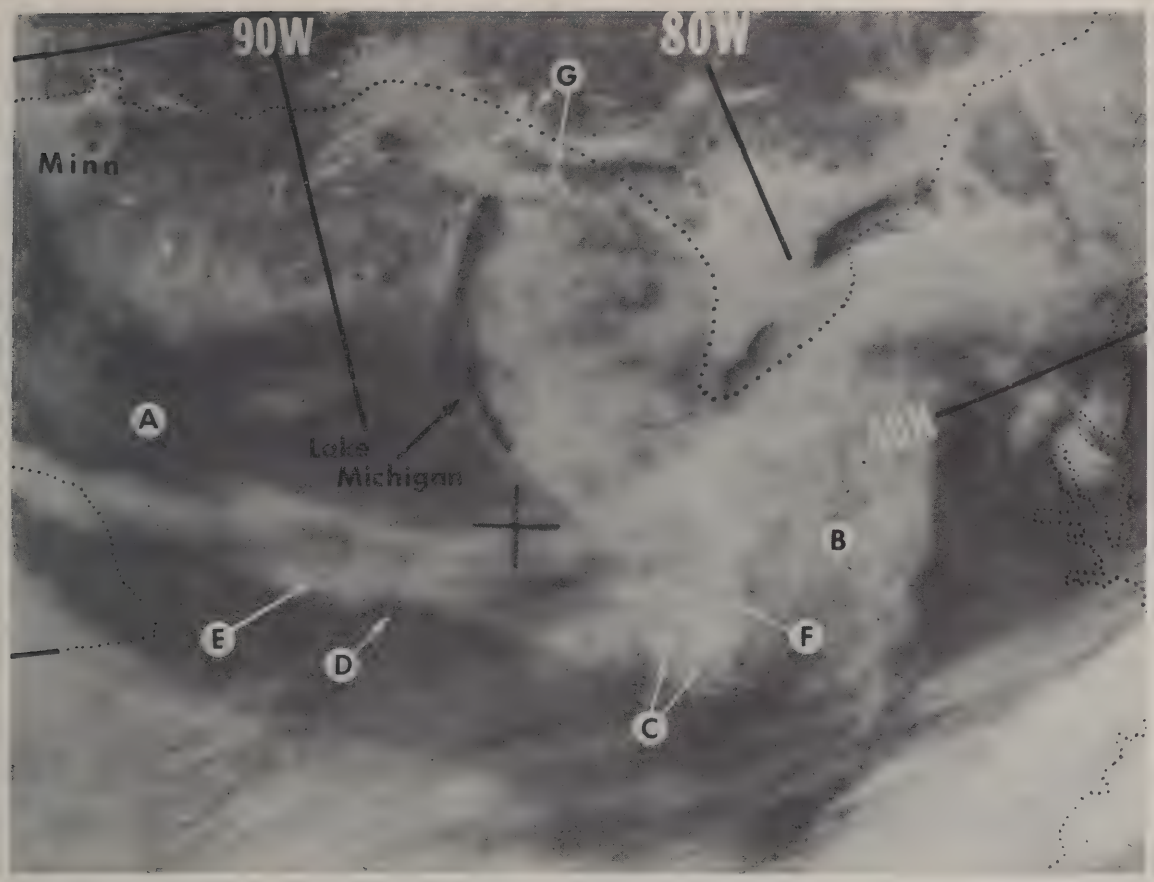

Figure 8-38. Snow cover on relatively flat terrain - United States, 1602 GMT, February 21, 1968, ESSA 6, Pass 1290.

The appearance of snow cover over relatively flat topography is shown in figure 8-38. An area of fresh snow lies to the south of a line extending from A to B. This snow-covered area is nearly all open farmland with some deciduous forestation, and has the typical mottled appearance caused by differences in vegetation. The brightest areas within this snow field occur in the Bluegrass region of Kentucky (C). The Illinois (D), Missouri (E), and Ohio (F) Rivers appear as thin dark lines caused by the presence of trees obscuring the snow along their banks. Snow and ice can also be seen along the western shore of Lake Michigan and through northern Minnesota into Canada. The bright areas at G are snow-covered and frozen areas of Whitefish Bay and the Strait of Mackinac. Details of ice conditions such as these in the Great Lakes region are analyzed and mapped weekly during the winter and spring seasons.

8.7.2 Sea Ice

One of the first applications of satellite data to oceanography was the mapping of sea ice boundaries. The Arctic and Antarctic ice packs, ice floes and sea ice fragments, can be seen quite easily in satellite pictures. The southern edge of the Arctic ice pack in the Davis Strait appears at Q in figure 8-39. This southern boundary of the Arctic ice pack is mapped for the Northern Hemisphere from satellite pictures throughout the year. Another area of pack ice extends southward from R to S along the Labrador coast. As cold air from the snow-covered land and ice moves over the warmer waters of the Strait, numerous low level cumuliform cloud lines (T) begin to form. Southern Greenland appears as a huge mass of ice and snow in the top portion of the picture.

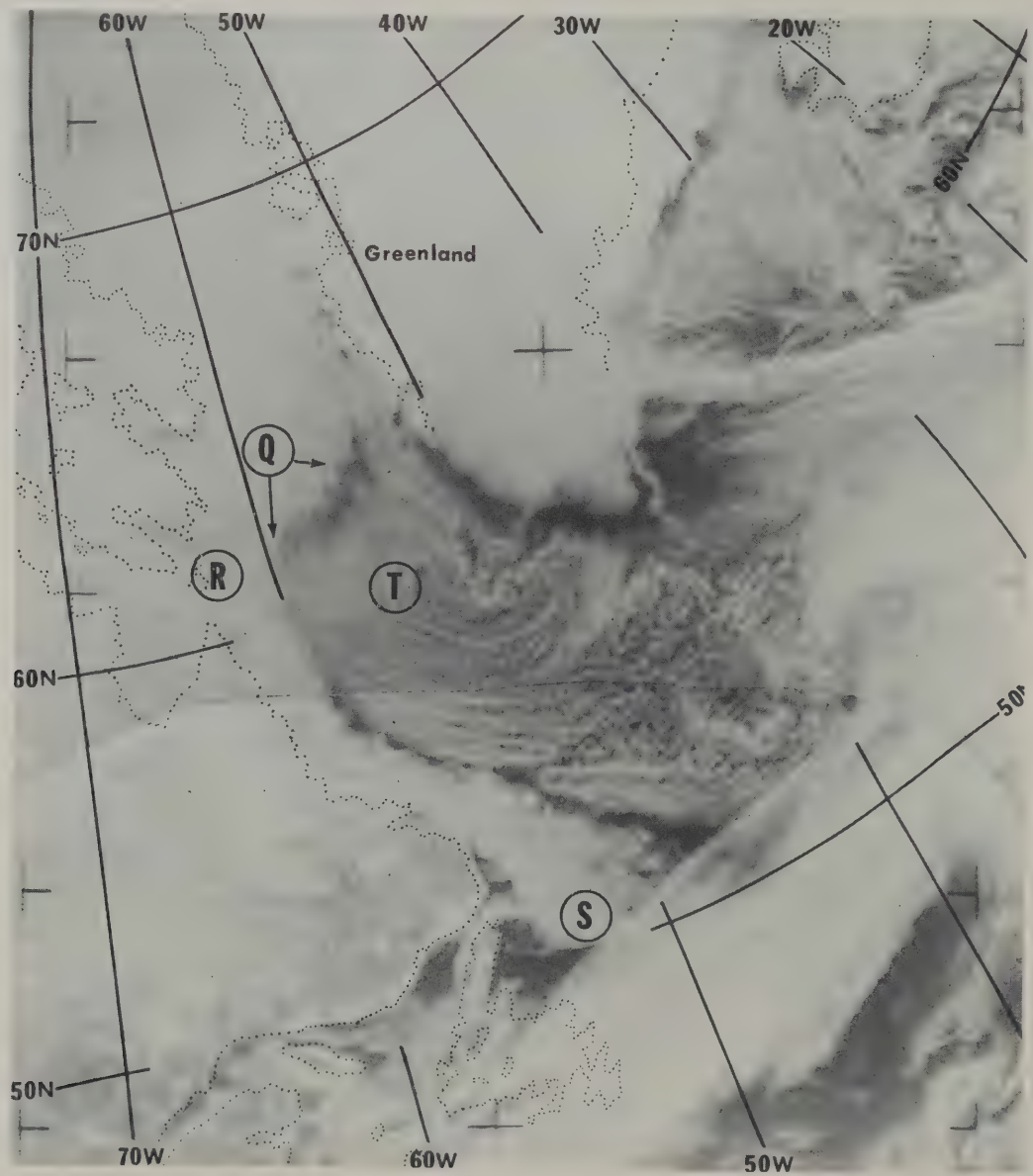

Figure 8-39. Pack ice - Labrador Sea, 1413 GMT, March 18, 1968, ESSA 6, Pass 1615.

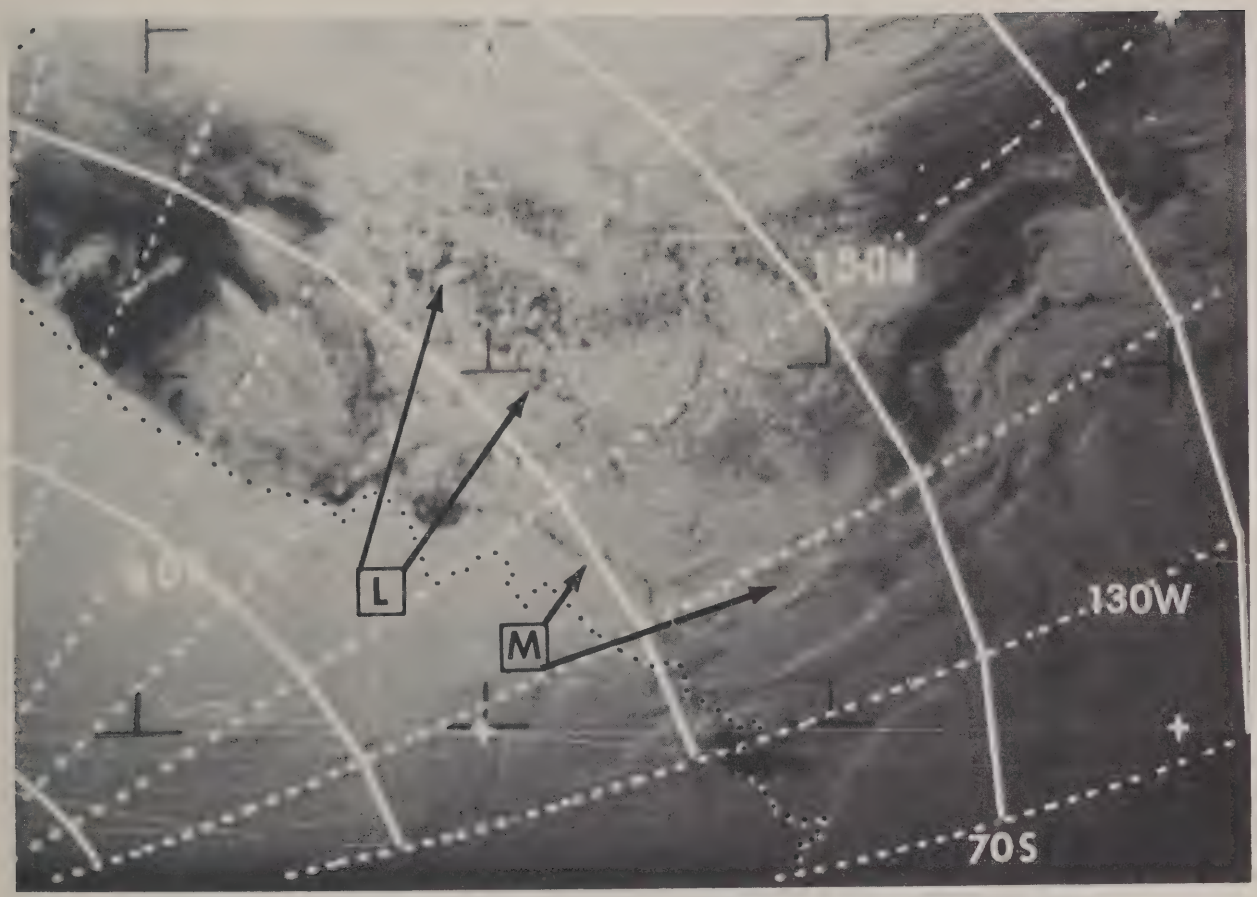

Figure 8-40. Sea ice - Antarctica, 0336 GMT, January 12, 1967, ESSA 3, Pass 1277.

In figure 8-40, a large area of ice floes and windbroken sea ice fragments can be seen at L in the area off the Ruppert Coast of Antarctica. Further east, shelf and solid pack ice are visible at M. Ice forecasters, especially those concerned with polar missions, are particularly concerned with the stage of ice formation or breakup. Information on impending storms and high winds is also important in forecasting the duration of navigable leads. Here satellite data is useful both for ice surveillance and for forecasting.

8.8 Sunglint

Variations in the sea surface reflectivity are presently being studied from satellite photographs. We find the extent and brightness of reflecting areas on satellite pictures are a function of the roughness of the water surface. Because the roughness of an ocean surface depends largely on the strength of the low level wind flow, information on the surface wind speed can be derived from the appearance of a sunglint area. Under calm conditions, the smooth sea surface acts as a mirror and produces a small, bright reflection (A, figure 8-41), but with moderate or strong wind conditions, the rough sea surface produces a diffuse reflection, hence, a less bright and larger sunglint area (an example is shown at K in figure 8-17). Small-scale variations in surface roughness of 20-40 miles wide are also detectable within a sunglint area.

A small, bright sunglint area over an ocean (as at R in figure 8-36) can be confused with clouds; just as sunglint on a small lake or bay can be misinterpreted as an isolated cumulonimbus. Since sunglint appears in a different position on the earth in each successive satellite picture, it can correctly be interpreted by comparing the same areas in the overlap region of adjacent pictures.

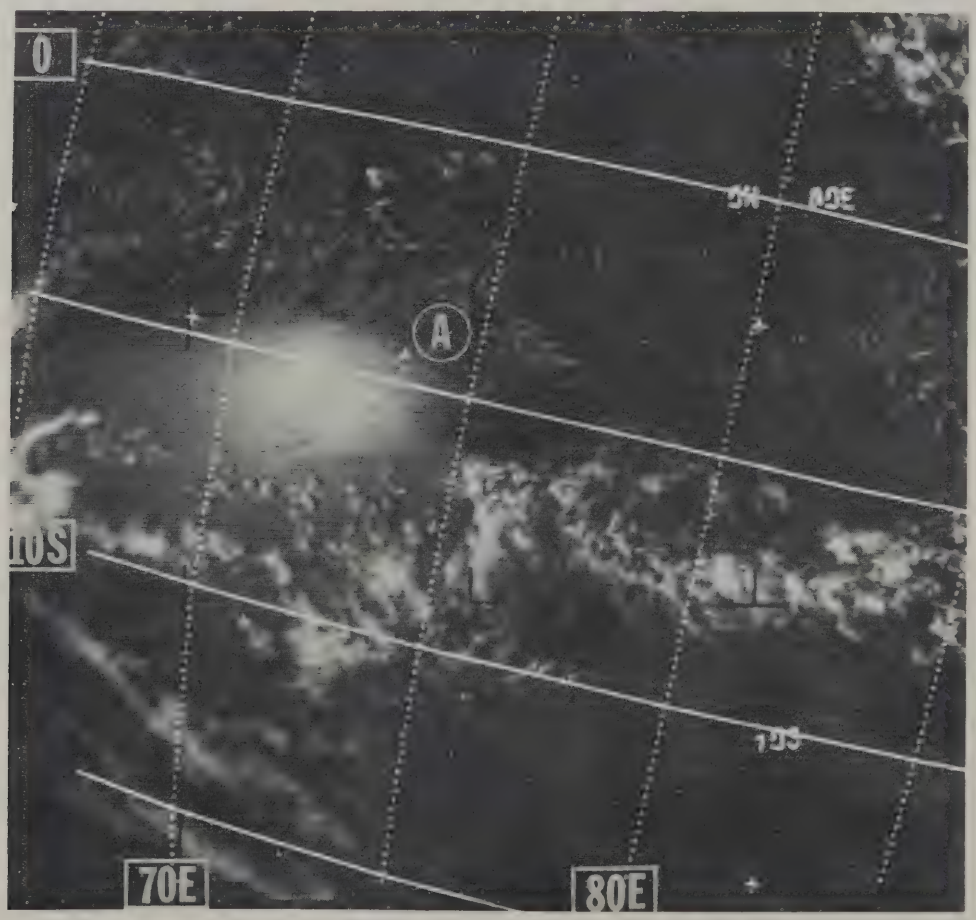

Figure 8-41. Sunglint - Indian Ocean, 0936 GMT, November 15, 1968, ESSA 7, Pass 1138.

BIBLIOGRAPHY

Adem, Julian, "On the Relation Between Outgoing Long-Wave Radiation, Albedo, and Cloudiness", Monthly Weather Review, Vol. 95, No. 5, May 1967, pp 257-260.

Allison, Lewis J., Nicholas, George W., and Kennedy, James S., "Examples of the Meteorological Capability of the High Resolution Infrared Radiometer on the Nimbus I Satellite", Journal of Applied Meteorology, Vol. 5, No. 3, June 1966, pp 314-333.

Anderson, R. K., Ferguson, E. W. and Oliver, V. J., "The Use of Satellite Pictures in Weather Analysis and Forecasting", World Meteorological Organization Technical Note No. 75, World Meteorological Organization, Geneva, Switzerland, 1966, 186 pp.

Barr, Sumner, Lawrence, Miles B., and Sanders, Fredrick, "TIROS Vortices and Large-Scale Vertical Motion", Monthly Weather Review, Vol. 94, No. 12, December 1966, pp 675-696.

Boucher, Roland J., "Relationships Between the Size of Satellite-Observed Cirrus Shields and the Severity of Thunderstorm Complexes", Journal of Applied Meteorology, Vol. 6, No. 3, June 1967, pp 564-572.

Bristor, C. L., Callicott, W. M., and Bradford, R. E., "Operational Processing of Satellite Cloud Pictures by Computer", Monthly Weather Review, Vol. 94, No. 8, August 1966, pp 515-527.

Conover, John H., "Anomalous Cloud Lines", Journal of Atmospheric Sciences, Vol. 23, No. 6, November 1966, pp 778-785.

Conover, John H., "Cloud and Terrestrial Albedo Determination from TIROS Satellite Pictures", Journal of Applied Meteorology, Vol. 4, No. 3, June 1966, pp 378-386.

Conover, John H., "Note on the Flora and Snow Cover Distribution Affecting the Appearance of Northeastern U. S. as Photographed by TIROS Satellites", Monthly Weather Review, Vol. 93, No. 10, October 1965, pp 644-646.

Erickson, Carl O., "Some Aspects of the Development of Hurricane Dorothy", Monthly Weather Review, Vol. 95, No. 3, March 1967, pp 121-130.

Fett, Robert W., "Life Cycle of Tropical Cyclone Judy as Revealed by ESSA II and Nimbus II", Monthly Weather Review, Vol. 94, No. 10, October 1966, pp 605-610.

Fett, Robert W., "Some Unusual Aspects Concerning the Development and Structure of Typhoon Billie--July 1967", Monthly Weather Review, Vol. 96, No. 9, September 1968, pp. 637-648.

354-645 O - 69 - 8

Fett, Robert W., "Typhoon Formation Within the Zone of Intertropical Convergence", Monthly Weather Review, Vol. 96, No. 2, February 1968, pp 106-117.

Fett, Robert W., "Upper Level Structure of the Formative Tropical Cyclone", Monthly Weather Review, Vol. 94, No. 1, January 1966, pp 9-18.

Fritz, Sigmund, "The Significance of Mountain Lee Waves as Seen from Satellite Pictures", Journal of Applied Meteorology, Vol. 4, No. 1, February 1965, pp 31-37.

Fritz, S., and Rao, P. Krishna, "On the Infrared Transmission through Cirrus Clouds and the Estimation of Relative Humidity from Satellites", Journal of Applied Meteorology, Vol. 6, No. 6, December 1967, pp 1088-1096.

Fritz, S., Hubert, L. F., and Timchalk, A., "Some Inferences from Satellite Pictures of Tropical Disturbances", Monthly Weather Review, Vol. 94, No. 4, April 1966, pp 231-236.

Fujita, Tetsuya, Bandeen, William, "Resolution of the Nimbus High Resolution Infrared Radiometer", Journal of Applied Meteorology, Vol. 4, No. 4, August 1966, pp 492-503.

Glahn, Harry R., "On the Usefulness of Satellite Infrared Measurements in the Determination of Cloud Top Heights and Areal Coverage", Journal of Applied Meteorology, Vol. 5, No. 2, April 1966, pp 189-197.

Huang, Chin-Hua, Panofsky, H. A., and Schwalb, A., "Some Relationships Between Synoptic Variables and Satellite Radiation Data", Monthly Weather Review, Vol. 95, No. 7, July 1967, pp 483-486.

Jager, Gilbert, Follansbee, Walton A., and Oliver, Vincent J., "Operational Utilization of Upper Tropospheric Wind Estimates Based on Meteorological Satellite Photographs", (submitted to), Monthly Weather Review.

Lyons, Walter A., and Fujita, Tetsuya, "Meso-Scale Motions in Oceanic Stratus as Revealed by Satellite Data", Monthly Weather Review, Vol. 96, No. 5, May 1968, pp 304-314.

McClain, E. Paul, "On the Relation of Satellite-Viewed Cloud Conditions to Vertically Integrated Moisture Fields", Monthly Weather Review, Vol. 94, No. 8, August 1966, pp 509-514.

McClain, E. Paul, Ruzecki, Mary Ann, and Brodrick, Harold J., "Experimental Use of Satellite Pictures in Numerical Prediction", Monthly Weather Review, Vol. 93, No. 7, July 1965, pp 445-452.

Merritt, Earl S., and Wexler, Raymond, "Cirrus Canopies in Tropical Storms", Monthly Weather Review, Vol. 95, No. 3, March 1967, pp 111-120.

Smith, Arthur H., "Statistical Test of Rules for Determining Points in Surface Ridge Lines from Weather Satellite Photographs", Monthly Weather Review, Vol. 96, No. 5, May 1968, pp 315-318.

Smith, William L., "An Improved Method for Calculating Tropospheric Temperature and Moisture from Satellite Radiometric Measurements", Monthly Weather Review, Vol. 96, No. 6, June 1968, pp 387-396.

Snider, C. R., "Great Lakes Ice Season 1967", Monthly Weather Review, Vol. 95, No. 10, October 1967, pp 685-696.

Streten, N. A., "Some Aspects of High Latitude Southern Hemisphere Circulation as Viewed by ESSA 3", Journal of Applied Meteorology, Vol. 7, No. 3, June 1968, pp 324-332.

Thompson, Aylmer H., and West, Philip W., "Use of Satellite Cloud Pictures to Estimate Average Relative Humidity below 500-Millibar, with Application to the Gulf of Mexico", Monthly Weather Review, Vol. 95, No. 11, November 1967, pp 791-798.

Viezee, W., Endlich, R. M. and Serebreny, S. M., "Satellite-Viewed Jet Stream Clouds in Relation to the Observed Wind Field", Journal of Applied Meteorology, Vol. 6, No. 5, October 1967, pp 929-935.

Wexler, Raymond, "TIROS and Radar Observations of a Thunderstorm Complex over Florida", Monthly Weather Review, Vol. 93, No. 8, August 1965, pp 523-527.

Whitney, L. F., Timchalk, A., and Gray, T. I. Jr., "On Locating Jet Streams from TIROS Photographs", Monthly Weather Review, Vol. 94, No. 3, March 1966, pp 127-138.

Young, Murray J., "Variability on Estimating Total Cloud Cover from Satellite Pictures", Journal of Applied Meteorology, Vol. 6, No. 3, June 1967, pp 573-579.

APPENDIX A

APT DAILY PREDICT MESSAGE

The APT Daily Predict Message contains basic orbital data for the real-time transmission spacecraft in a minimum length teletype transmission. The message, composed of four parts, as explained in 3.3.4, is transmitted over worldwide meteorological communications circuits under the communications heading TBUS-1 or TBUS-2. The TBUS-1 heading is reserved for orbits where the spacecraft is moving from north to south during the daylight portion of the orbit. TBUS-2 is reserved for those orbits where the spacecraft is moving from south to north during the daylight portion of the orbit. Data provided in either TBUS-1 or TBUS-2 will pertain only to that portion of the orbit where real-time data may be transmitted. For example, if an APT camera is the only working real-time transmission sensor on the spacecraft, data for only the daylight portion of the orbit will be provided. Conversely, if a sensor (or two separate sensors) is used for full orbit data transmission, spacecraft spatial data for the full orbit (day and night) will be provided.

For the convenience of the user, daylight and night portions of the message have been separated. Thus, there will be two Part II and two Part III segments, one providing day data, the other night data. The user can use the portion of the message with which he is concerned and ignore the remainder.

Subpoint data is provided at 2-minute intervals throughout the portions of the orbit where data may be expected. All times are referenced to the ascending node (northbound equator crossing) and are given as minutes after or before this time as shown in Figure #A1.

The TBUS-2 Bulletin is encoded in exactly the same manner as the TBUS-1 Bulletin with the exception that night and day segments of the orbit are reversed as may be seen in the schematic form.

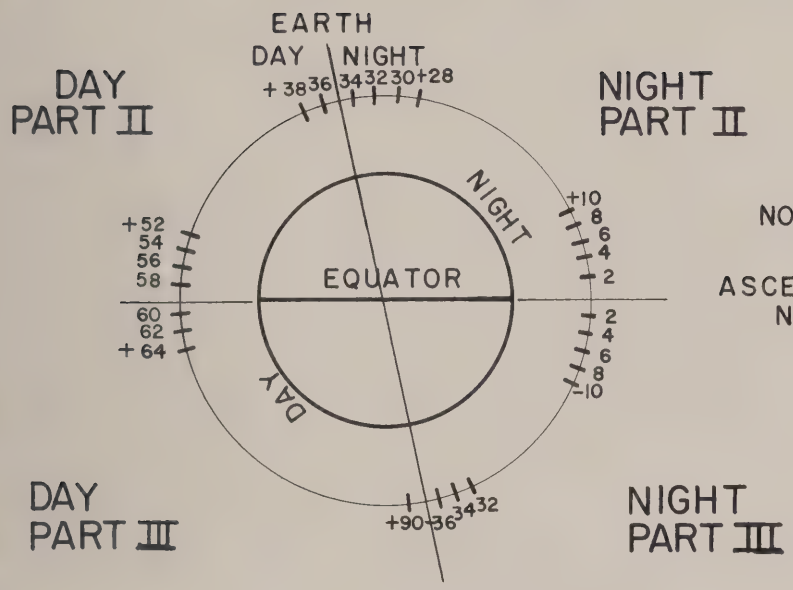

TBUS-1

NORTH TO SOUTH DAYLIGHT ORBIT

ASCENDING NODE

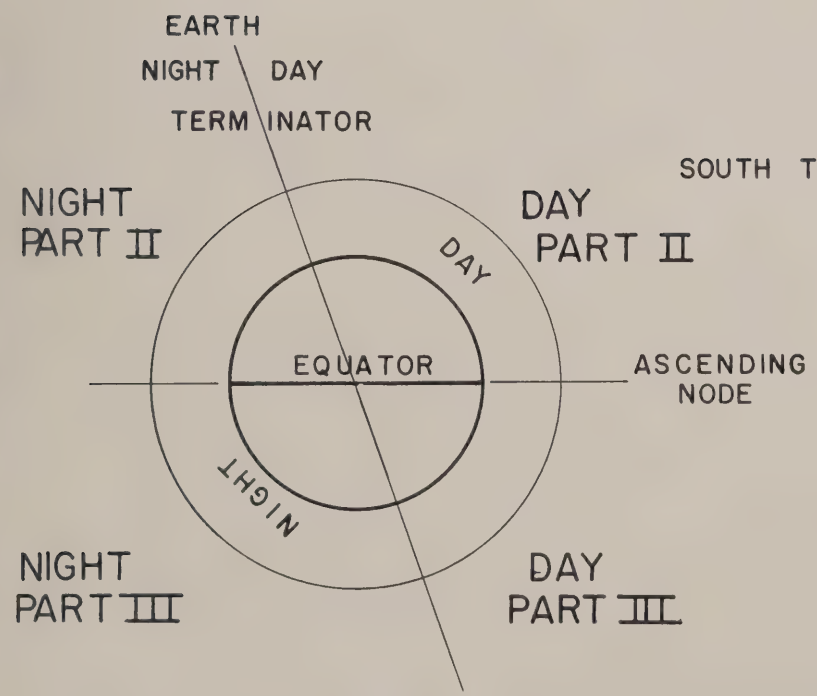

TBUS-2

SOUTH TO NORTH DAYLIGHT ORBIT

FIGURE A-1

SCHEMATIC MESSAGE FORMAT FOR EPHEMERIS PREDICT MESSAGE

TBUS 2 KWBC
APT PREDICT
MMYYSS

PART I

$ON_rN_rN_rN_r$ $OY_rY_rG_rG_r$ $Og_rg_rs_rs_r$ $Q_rL_oL_ol_ol_o$ Tggss $LL_oL_ol_ol_o$

$N_4N_4N_4N_4G_4$ $G_4g_4g_4s_4s_4$ $Q_4L_oL_ol_ol_o$

$N_8N_8N_8N_8G_8$ $G_8g_8g_8s_8s_8$ $Q_8L_oL_ol_ol_o$

$N_{12}N_{12}N_{12}N_{12}G_{12}$ $G_{12}g_{12}g_{12}s_{12}s_{12}$ $Q_{12}L_oL_ol_ol_o$

PART II (DAY)

$02Z_{02}Z_{02}Q_{02}$ $L_aL_al_aL_oL_ol_o$ $04Z_{04}Z_{04}Q_{04}$ $L_aL_al_aL_oL_ol_o$

$06Z_{06}Z_{06}Q_{06}$ $L_aL_al_aL_oL_ol_o$ $08Z_{08}Z_{08}Q_{08}$ $L_aL_al_aL_oL_ol_o$

$10Z_{10}Z_{10}Q_{10}$ $L_aL_al_aL_oL_ol_o$ ..... to terminator (Near N. Pole)

PART III (DAY)

$02Z_{02}Z_{02}Q_{02}$ $L_aL_al_aL_oL_ol_o$ $04Z_{04}Z_{04}Q_{04}$ $L_aL_al_aL_oL_ol_o$

$06Z_{06}Z_{06}Q_{06}$ $L_aL_al_aL_oL_ol_o$ $08Z_{08}Z_{08}Q_{08}$ $L_aL_al_aL_oL_ol_o$

$10Z_{10}Z_{10}Q_{10}$ $L_aL_al_aL_oL_ol_o$ ..... to terminator (Near S. Pole)

PART II (NIGHT)

$28Z_{28}Z_{28}Q_{28}$ $L_aL_al_aL_oL_ol_o$ $30Z_{30}Z_{30}Q_{30}$ $L_aL_al_aL_oL_ol_o$

$32Z_{32}Z_{32}Q_{32}$ $L_aL_al_aL_oL_ol_o$ .... to last point north of equator.

PART III (NIGHT)

$56Z_{56}Z_{56}Q_{56}$ $L_aL_al_aL_oL_ol_o$ $58Z_{58}Z_{58}Q_{58}$ $L_aL_al_aL_oL_ol_o$

$60Z_{60}Z_{60}Q_{60}$ $L_aL_al_aL_oL_ol_o$ ... to terminator (Near S. Pole)

PART IV

TRANSMISSION FREQUENCY XXX.XX MHZ

(NOTE: Day PART III is given in minutes before the reference orbit equator crossing. All other times are minutes after the equator crossing. Times given in this schematic are examples only. Actual times will be determined by orbital parameters and season of the year.

SCHEMATIC MESSAGE FORMAT FOR EPHEMERIS PREDICT MESSAGE

TBUS 1 KWBC
APT PREDICT
MMYYSS

PART I

$ON_rN_rN_rN_r$ $OY_rY_rG_rG_r$ $Og_rg_rs_rs_r$ $Q_rL_oL_ol_ol_o$ Tggss $LL_oL_ol_ol_o$

$N_4N_4N_4N_4G_4$ $G_4g_4g_4s_4s_4$ $Q_4L_oL_ol_ol_o$

$N_8N_8N_8N_8G_8$ $G_8g_8g_8s_8s_8$ $Q_8L_oL_ol_ol_o$

$N_{12}N_{12}N_{12}N_{12}G_{12}$ $G_{12}g_{12}g_{12}s_{12}s_{12}$ $Q_{12}L_oL_ol_ol_o$

PART II (DAY)

$28Z_{28}Z_{28}Q_{28}$ $L_aL_al_aL_oL_ol_o$ $30Z_{30}Z_{30}Q_{30}$ $L_aL_al_aL_oL_ol_o$

$32Z_{32}Z_{32}Q_{32}$ $L_aL_al_aL_oL_ol_o$ .... to last point north of equator.

PART III (DAY)

$56Z_{56}Z_{56}Q_{56}$ $L_aL_al_aL_oL_ol_o$ $58Z_{58}Z_{58}Q_{58}$ $L_aL_al_aL_oL_ol_o$

$60Z_{60}Z_{60}Q_{60}$ $L_aL_al_aL_oL_ol_o$ .... to terminator (Near So. Pole)

PART II (NIGHT)

$02Z_{02}Z_{02}Q_{02}$ $L_aL_al_aL_oL_ol_o$ $04Z_{04}Z_{04}Q_{04}$ $L_aL_al_aL_oL_ol_o$

$06Z_{06}Z_{06}Q_{06}$ $L_aL_al_aL_oL_ol_o$ $08Z_{08}Z_{08}Q_{08}$ $L_aL_al_aL_oL_ol_o$

$10Z_{10}Z_{10}Q_{10}$ $L_aL_al_aL_oL_ol_o$ ..... to terminator (Near No. Pole)

PART III (NIGHT)

$02Z_{02}Z_{02}Q_{02}$ $L_aL_al_aL_oL_ol_o$ $04Z_{04}Z_{04}Q_{04}$ $L_aL_al_aL_oL_ol_o$

$06Z_{06}Z_{06}Q_{06}$ $L_aL_al_aL_oL_ol_o$ $08Z_{08}Z_{08}Q_{08}$ $L_aL_al_aL_oL_ol_o$

$10Z_{10}Z_{10}Q_{10}$ $L_aL_al_aL_oL_ol_o$ ..... to terminator (Near So. Pole)

PART IV
TRANSMISSION FREQUENCY XXX.XX MHZ

(Note: NIGHT PART III is given in minutes before the reference orbit equator crossing. All other times are minutes after the equator crossing. Times given in this schematic are examples only. Actual times will be determined by orbital parameters and season of the year.

EXPLANATION OF CODE SYMBOLS

TBUS 1	- APT Bulletin originating in the United States: North to South picture taking orbit.
KWBC	- Traffic entered at Washington, D.C.
APT PREDICT	- Identifies message content.
MMYYSS	- Message serial number MM - Month of year YY - day of month SS - number of spacecraft to which predict applies.
PART I	- Equator crossing predicts follow.
$ON_rN_rN_rN_r$ $OY_rY_rG_rG_r$ $Og_rg_rs_rs_r$	
O	- Indicator, reference orbit equator crossing information follows. (NOTE: Information in Parts II and III applies directly to this reference orbit).
$N_rN_rN_rN_r$	- Number of reference orbit.
$Y_rY_rG_rG_rg_rg_rs_rs_r$	- Day (YY), hour (GG), minute (gg), and second (ss) - GMT - on which satellite crosses the equator <u>northbound</u> on the reference orbit $N_rN_rN_rN_r$° (In TBUS 1 equator crossing takes place on <u>night</u> side of orbit).
$Q_rL_oL_ol_ol_o$	- Octant and longitude in degrees and hundredths at which satellite crosses the equator northbound on reference orbit $N_rN_rN_rN_r$° (Octant at equator will be that into which the satellite is moving).
T	- Indicator, nodal period follows.
ggss	- Nodal period, minutes and seconds between consecutive equator crossings. (Hundreds group will not be included: ex 100 minutes 13 seconds will be coded as 0013).
L	- Indicator, nodal longitude increment follows.

$L_oL_ol_ol_o$	- Degrees and hundredths of longitude degrees between consecutive equator crossings.
$N_4N_4N_4N_4$	- Number of the fourth orbit following the reference orbit.
$G_4G_4g_4g_4s_4s_4$	- Hour (GG), minute (gg), and second (ss), at which satellite crosses the equator northbound on orbit $N_4N_4N_4N_4$.
$Q_4L_oL_ol_ol_o$	- Octant and longitude in degrees and hundredths at which satellite crosses equator northbound on orbit $N_4N_4N_4N_4$.
$N_8N_8N_8N_8$	- 8th and 12th orbits following reference orbit.
$N_{12}N_{12}N_{12}N_{12}$	
PART II	- Satellite altitude and subpoint coordinates at 2-minute intervals -- after time of equator crossing follows.
$28Z_{28}Z_{28}Q_{28}$ 28	- Information pertinent to 28 minutes after equator crossing follows.
$Z_{28}Z_{28}$	- Satellite altitude in tens of kilometers. At 28 minutes after equator crossing. (Thousands figure understood hence 1440km is encoded as 44).
Q_{28}	- Octant of globe at 28 minutes after equator crossing.
$L_aL_al_aL_ol_ol_o$	
$L_aL_al_a$	- Latitude of satellite subpoint in degrees and tenths of degrees at 28 minutes after equator crossing.
$L_oL_ol_o$	- Longitude of satellite subpoint in degrees and tenths of degrees at 28 minutes after equator crossing.

(This information is repeated at 2-minute intervals over the sunlit portion of the orbit north of the equator.)

PART III (DAY) - Satellite altitude and subpoint coordinates at 2-minute intervals south of the equator. This will be a continuation of Part II with the same format.

(This information is repeated at 2-minute intervals over the sunlit portion of the orbit south of the equator).

NOTE: Should the time after ascending node become greater than 99, the hundreds will be assumed (example, minute 102 will be encoded as 02).

PART II (NIGHT) - Satellite altitude and subpoint coordinates at 2-minute intervals -- after time of equator crossing follows.

$02Z_{02}Z_{02}Q_{02}$ - Information pertinent to 2 minutes after equator crossing follows.

$Z_{02}Z_{02}$ - Satellite altitude in tens of kilometers. At 2 minutes after equator crossing (Thousands figure understood hence 1440km is encoded 44).

Q_{02} - Octant of globe at 2 minutes after equator crossing.

$L_aL_la_aL_oL_lo$

$L_aL_la_a$ - Latitude of satellite subpoint in degrees and tenths of degrees at 2 minutes after equator crossing.

L_oL_lo - Longitude of satellite subpoint in degrees and tenths of degrees at 2 minutes after equator crossing.

(This information is repeated at 2 minute intervals over the NIGHT portion of the orbit north of the equator).

PART III (NIGHT) - Satellite altitude and subpoint coordinates at 2 minute intervals prior to time of equator crossing follows.

$02Z_{02}Z_{02}Q_{02}$

02 - Information pertinent to minute 2 <u>before</u> equator crossing follows.

$Z_{02}Z_{02}$ - Satellite altitude in tens of kilometers at 2 minutes before equator crossing. (Thousands figure understood hence 1440km is encoded as 44).

Q_{02} - Octant of globe at 2 minutes before equator crossing.

$L_aL_aL_aL_oL_oL_o$

$L_aL_aL_a$ - Latitude of satellite subpoint in degrees and tenths of degrees at 2 minutes before equator crossing.

$L_oL_oL_o$ - Longitude of satellite subpoint in degrees and tenths of degrees at 2 minutes before equator crossing.

(This information is repeated at 2 minute intervals over the NIGHT portion of the orbit south of the equator.

NOTE: Should the time after ascending node become greater than 99, the hundreds will be assumed (example, minute 102 will be encoded as 02).

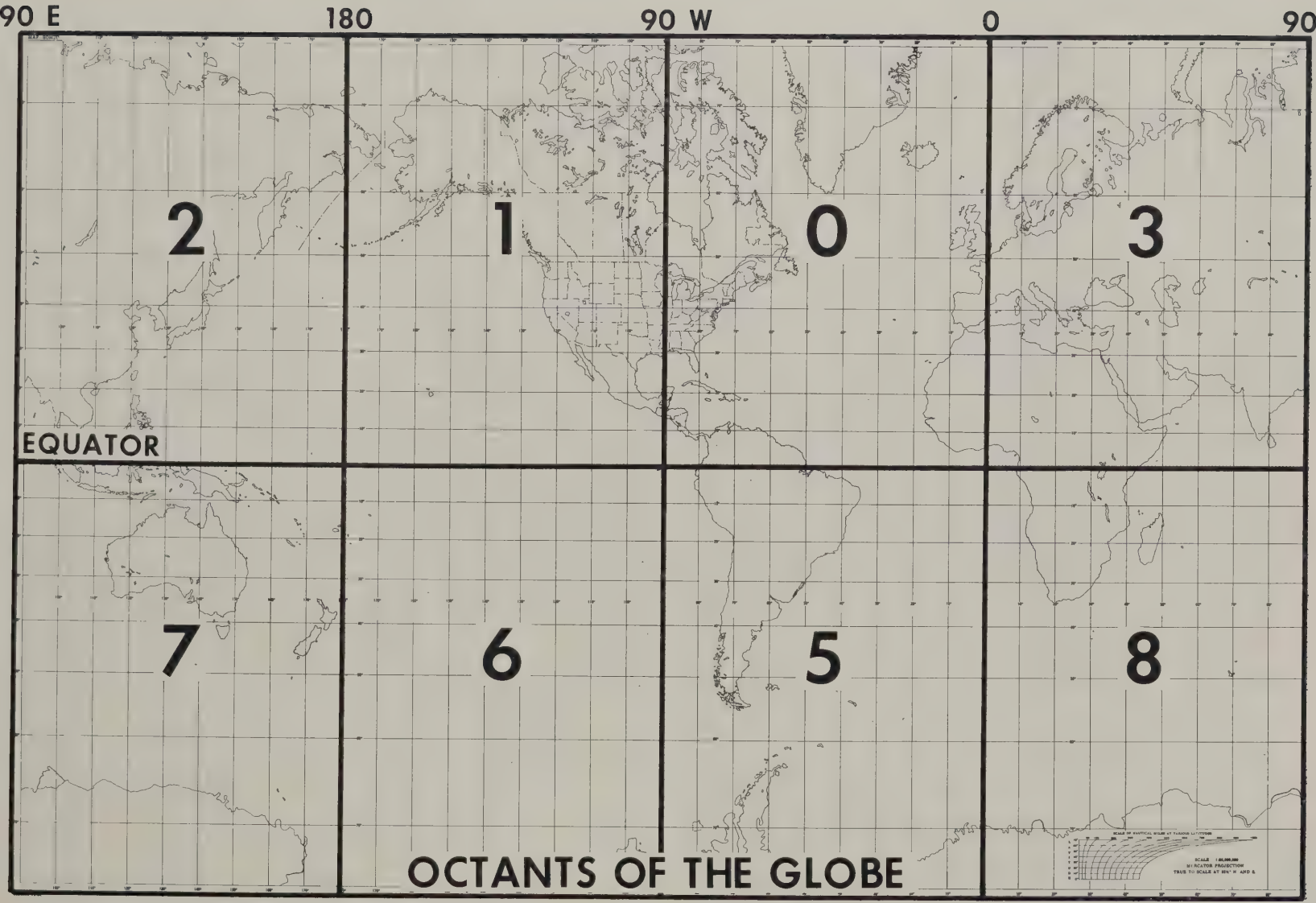

FIGURE A-2

The following encoded APT Predict Message example is referred to throughout the remaining appendices. This particular message, originally valid for ESSA 6 on April 25, 1968, was expanded to provide data for the night portion of the orbit on this day. The major features of the message are decoded on the following pages.

```
TBUS 1 KWBC N 221900
APT PREDICT
042506
PART I
02091 02513 00142 22944 T1453 L2871
20952 04115 31457
20990 42048 10030
21031 20020 24482

PART II (DAY)
22442 659954 24443 710850 26433 753684
28433 777427 30433 772129 32420 741099
34420 694242 36420 641333 38410 584396
40410 526443 42410 466479 44410 405510
46410 343536 48410 282559 50410 220580
52410 158600 54410 096619 56420 034638

PART III (DAY)
58425 027656 60425 089674 62435 151693
64435 213713 66445 274734 68455 335756
70455 396782 72465 456811 74475 515846
76475 573890 78486 629948

PART II (NIGHT)
02482 061277 04472 123253 06472 183239
08462 244219 10462 305198 12462 366173
14452 426146 16452 486114 18452 545075
20442 603024

PART III (NIGHT)
02487 061313 04497 122331 06497 183350
08497 244370 10507 305392 12507 365416
14507 425443 16517 484474 18517 542512
20517 598561 22517 654628 24517 705727
26516 747718 28506 775477 30506 774184
32506 748948 34495 705793 36495 654693
PART IV TRANSMISSION FREQUENCY 137.50 MHZ
```

DECODED MESSAGE

PART I
02091 02513 00142 22944 T 1453 L2871

2091	REFERENCE ORBIT NUMBER
25	DAY OF MONTH
130142	ASCENDING NODE TIME (13:01:42Z) FOR ORBIT 2091
2	OCTANT 2 (90° E to 180°)
2944	129.44 DEGREES EAST (EQUATOR CROSSING FOR ORBIT 2091 IN OCTANT 2)
T	INDICATOR LETTER
1453	ORBITAL PERIOD 114 MINUTES 53 SECONDS
L	INDICATOR LETTER
2871	NODAL LONGITUDINAL INCREMENT 28.71 DEGREES

20952 04115 31457

2095	ORBIT NUMBER 2095 (4TH AFTER REFERENCE)
204115	TIME (20:41:15Z) OF ASCENDING NODE FOR ORBIT 2095
3	OCTANT 3 (0 TO 90°E)
1457	14.57 DEGREES EAST (EQUATOR CROSSING FOR ORBIT 2095)

20990 42048 10030 DECODED IN SAME MANNER AS PREVIOUS LINE OF DATA
21031 20020 24482

PART II (DAY)
22442 659954 24433 710850 ETC.

22	MINUTE 22 AFTER EQUATOR CROSSING
44	SPACECRAFT HEIGHT 1440 KM
2	OCTANT 2 (90°E TO 180°)
659	LATITUDE 65.9°N
954	95.4°E
24	MINUTE 24 AFTER EQUATOR CROSSING
43	SPACECRAFT HEIGHT 1430KM
3	OCTANT 3 (0° TO 90°E)
710	LATITUDE 71.0°N
850	LONGITUDE 85.0°E

REMAINDER OF DAY PART II & DAY PART III DECODED IN SAME MANNER. DATA CONTINUOUS AT 2 MINUTE INTERVALS TO SOUTHERN TERMINATOR.

PART II (NIGHT)

02482 061277 04472 123253 ETC.

02	MINUTE 02 AFTER EQUATOR CROSSING
48	SPACECRAFT HEIGHT 1480KM
2	OCTANT 2 (90°E TO 180°)
061	LATITUDE 06.1°N
277	LONGITUDE 127.7°E
04	MINUTE 04 AFTER EQUATOR CROSSING
47	SPACECRAFT HEIGHT 1470KM
2	OCTANT 2 (90°E TO 180°)
123	LATITUDE 12.3°N
253	LONGITUDE 125.3°E

REMAINDER OF NIGHT PART II DECODED IN SAME MANNER. DATA CONTINUOUS AT 2 MINUTE INTERVALS.

PART III (NIGHT)

02487 061313 04497 122331... ETC.

02	MINUTE 02 BEFORE EQUATOR CROSSING
48	SPACECRAFT HEIGHT 1480KM
7	OCTANT 7 (90°E TO 180°)
061	LATITUDE 06.1°S
313	LONGITUDE 131.3°E
04	MINUTE 04 BEFORE EQUATOR CROSSING
49	SPACECRAFT HEIGHT 1490KM
7	OCTANT 7 (90°E TO 180°)
122	LATITUDE 12.2°S
331	LONGITUDE 113.1°E

REMAINDER DECODED IN SAME MANNER. DATA CONTINUOUS AT 2 MINUTE INTERVALS TO SOUTHERN TERMINATOR.

APPENDIX B

PLOTTING BOARD PREPARATION*

I Orbital Overlay

a. Figure B1 shows the APT Plotting Board with the Reference Orbit plotted from the APT Predict Message in Appendix A.

b. The equatorial line has been subdivided into increments of 28.71 degrees of longitude (nodal longitudinal increment) with orbits +4, (2095) +8 (2099) and +12 (2103) plotted directly from data in Part I of the predict message. Note that orbits -1, -2 and -3 are also indicated on the overlay.

II Equator Line on Plotting Board

Figures B2 a, b, c and d show the method used in determining the zones of equatorial crossing (ascending nodes) which will bring the spacecraft above the zero degree elevation circle at the antenna site (Section 3.4.2.2).

a. Maximum Spacecraft Height during one full orbit: 1510 KM. (from Daily Message-Night PART III, Minutes Minus 16 to 26).

b. Zero degree elevation with spacecraft height of 1510 KM: 36 degrees of great circle arc (Table 4, Page 21), the outer circle (elipse) on the Tracking Diagram.

Figure B2 a: The plotted subpoint track just touches the zero degree elevation circle east of the station (southbound portion of the orbit). Equator crossing (ascending node) 152.5°E.

Figure B2 b: The plotted subpoint track just touches the zero degree elevation circle west of the station (southbound portion of the orbit). Equator crossing (ascending node) 46°E.

The spacecraft is above the zero degree elevation circle (moving generally from north to south) whenever the equator crossing (ascending node) lies between 46°E and 152.5°E. The area is indicated by a heavy line on the Plotting Board (Figure B2 b).

---

* This example is for an orbit southbound during daylight (northbound during darkness). Procedures are similar for northbound daylight orbits. Station Location 38.0°N
75.2°W

The procedure is repeated for the northbound portion of the orbit (Figure B2 c & d).

The zone of equator crossings which will bring the spacecraft above zero degrees of elevation while the spacecraft is moving from south to north is 3°W to 109°W. This zone is also indicated on the Plotting Board (Figure B2 d).

354-645 O - 69 - 9

APT SYSTEM

METEOROLOGICAL SATELLITE

PLOTTING BOARD

AND

TRACKING DIAGRAM

APT STATION: Wallops

LOCATION

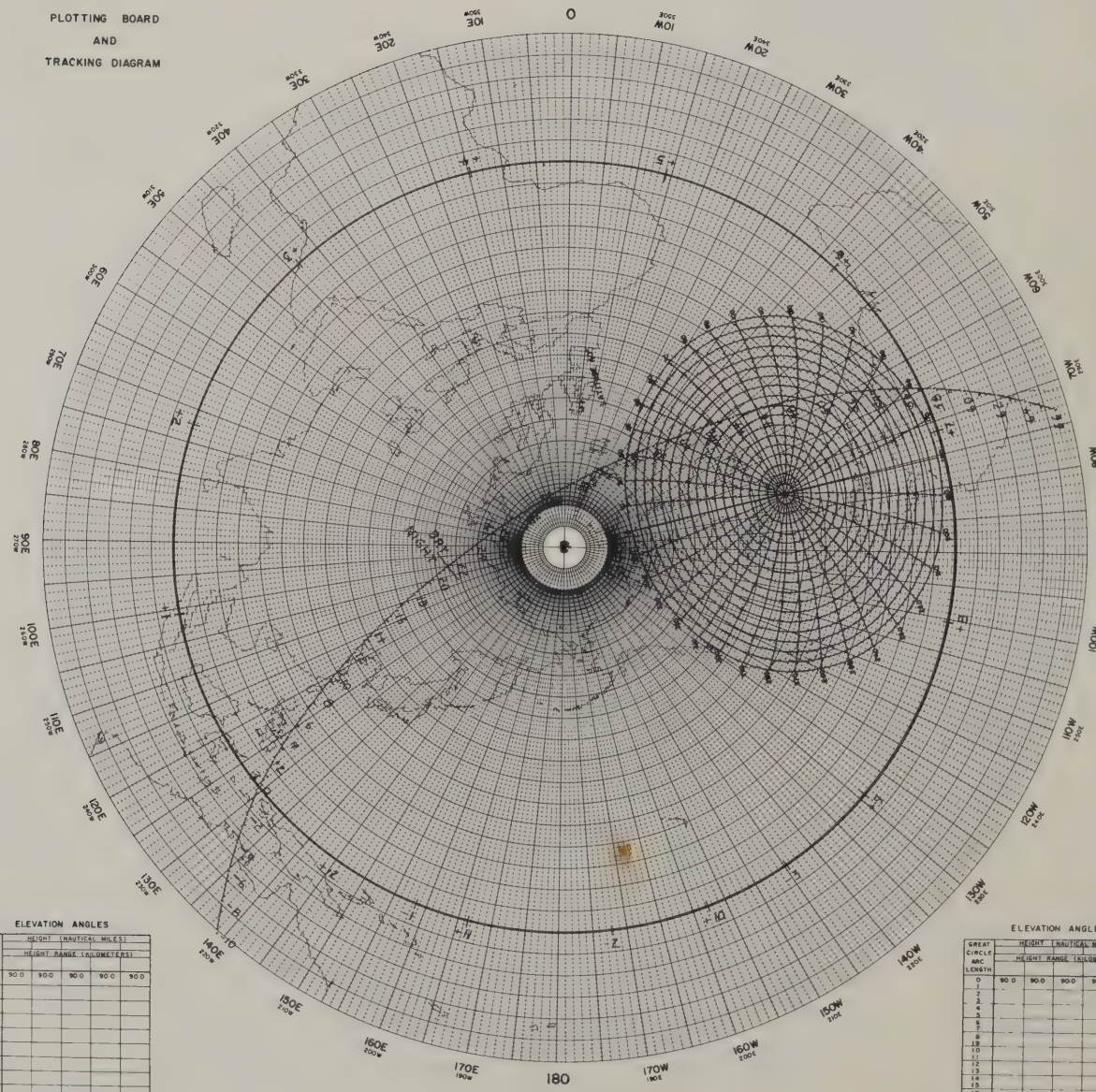

ELEVATION ANGLES

GREAT CIRCLE ARC LENGTH	HEIGHT (NAUTICAL MILES) / HEIGHT RANGE (KILOMETERS)				
0	90.0	90.0	90.0	90.0	90.0
1					
2					
3					
4					
5					
6					
7					
8					
9					
10					
11					
12					
13					
14					
15					
16					
17					
18					
19					
20					
21					
22					
23					
24					
25					
26					
27					
28					
29					
30					
31					
32					
33					
34					
35					

ELEVATION ANGLES

GREAT CIRCLE ARC LENGTH	HEIGHT (NAUTICAL MILES) / HEIGHT RANGE (KILOMETERS)				
0	90.0	90.0	90.0	90.0	90.0
1					
2					
3					
4					
5					
6					
7					
8					
9					
10					
11					
12					
13					
14					
15					
16					
17					
18					
19					
20					
21					
22					
23					
24					
25					
26					
27					
28					
29					
30					
31					
32					
33					
34					
35					

FIGURE B-1

PLOTTED ORBIT FROM DAILY MESSAGE

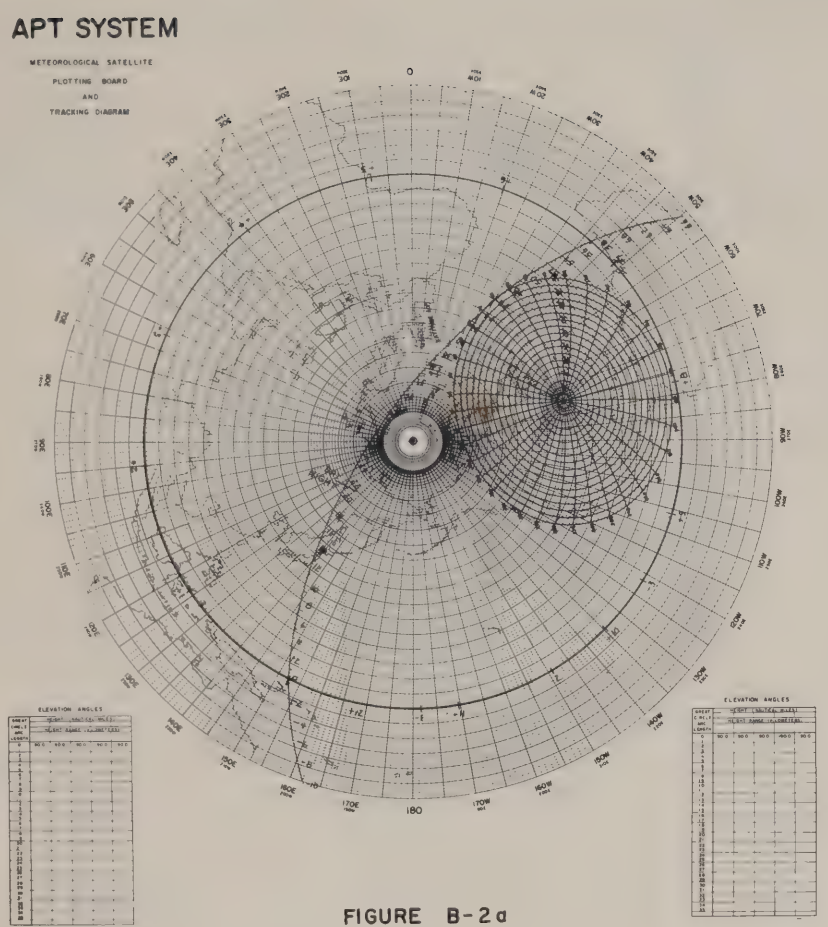

FIGURE B-2a

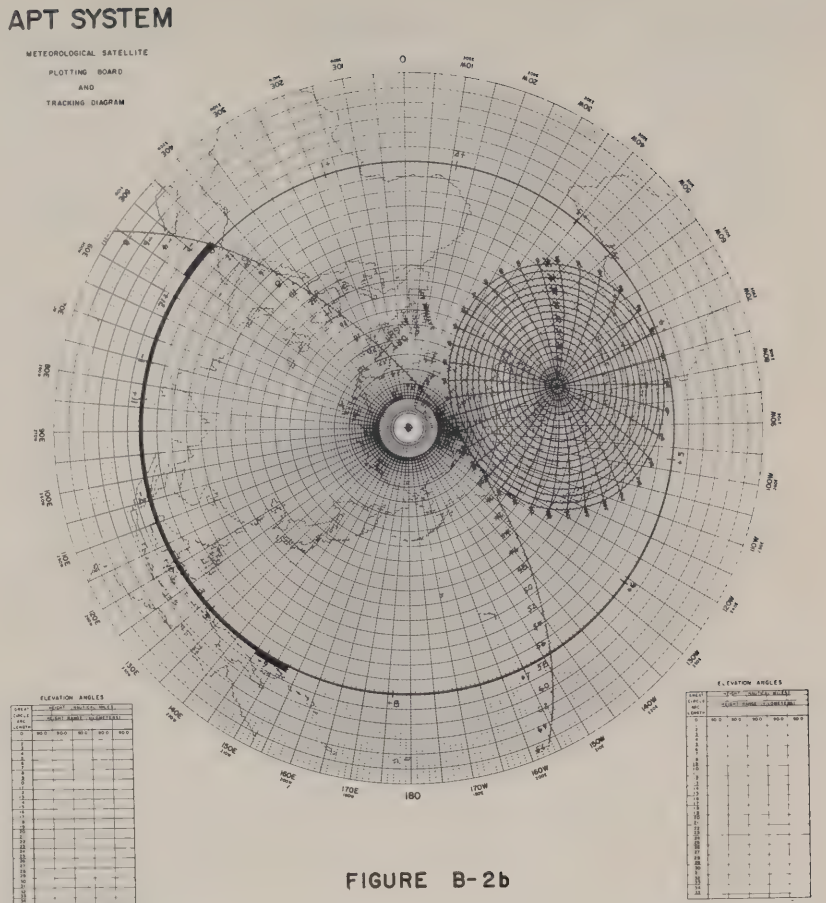

FIGURE B-2b

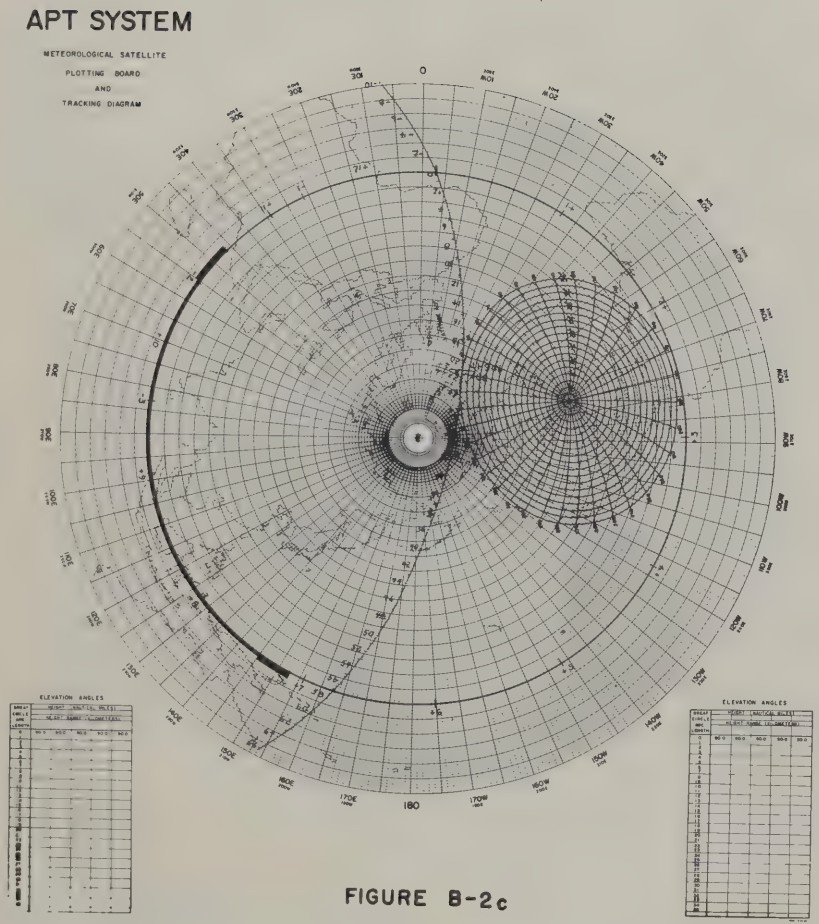

FIGURE B-2c

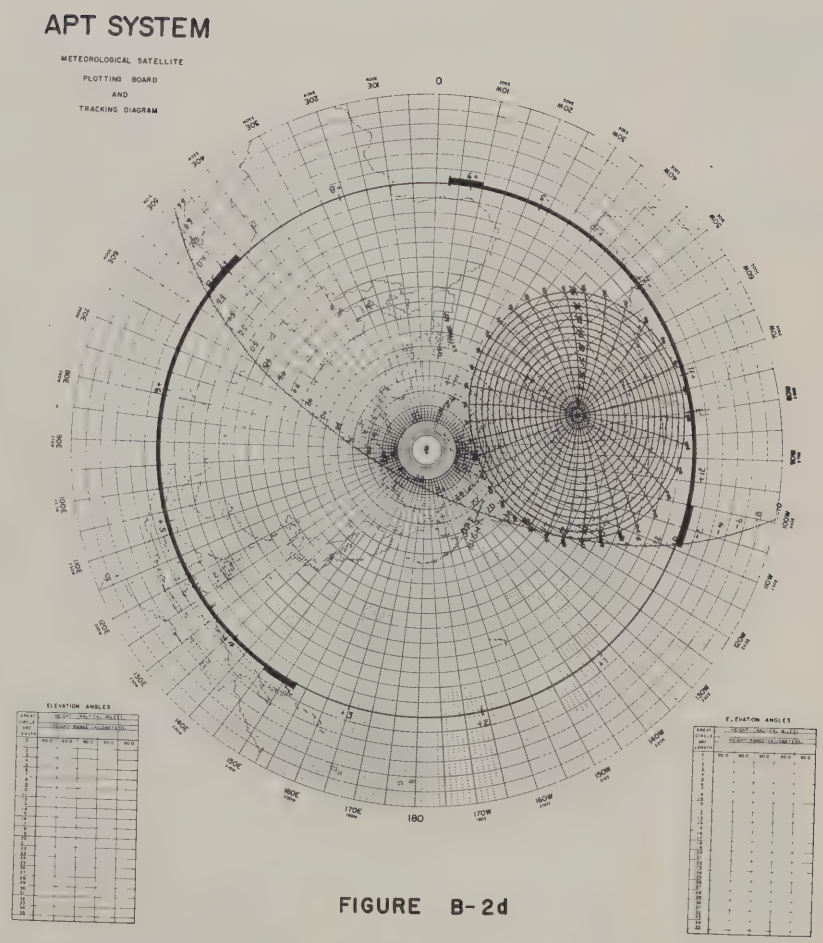

FIGURE B-2d

APPENDIX C

TRACKING EXERCISE

Refer to APT Predict Message Appendix A.

Figure C1 shows the Plotting Board with the orbital track set at the equator crossing (ascending node) of the reference orbit. Note that the reference orbit (2091) and the following two orbits (+1 and +2) southbound during daylight, are within the "above zero degree elevation" area (ascending node zone) previously determined. Additionally, orbits plus 5, 6, 7 and 8 are within the zero degree elevation circle for acquisition while northbound (in this example, at night).

For this exercise, tracking data will be computed for orbits plus 1 (2092, ascending node 100.7 degrees east) and plus 6 (2097, ascending node 42.8 degrees west) as determined directly from the Plotting Board and later computed mathematically in Appendix D.

Worksheets on the following pages show the computation of the tracking data using information read directly from the Plotting Board.

APT SYSTEM

METEOROLOGICAL SATELLITE

PLOTTING BOARD

AND

TRACKING DIAGRAM

APT STATION: Wallops

LOCATION.

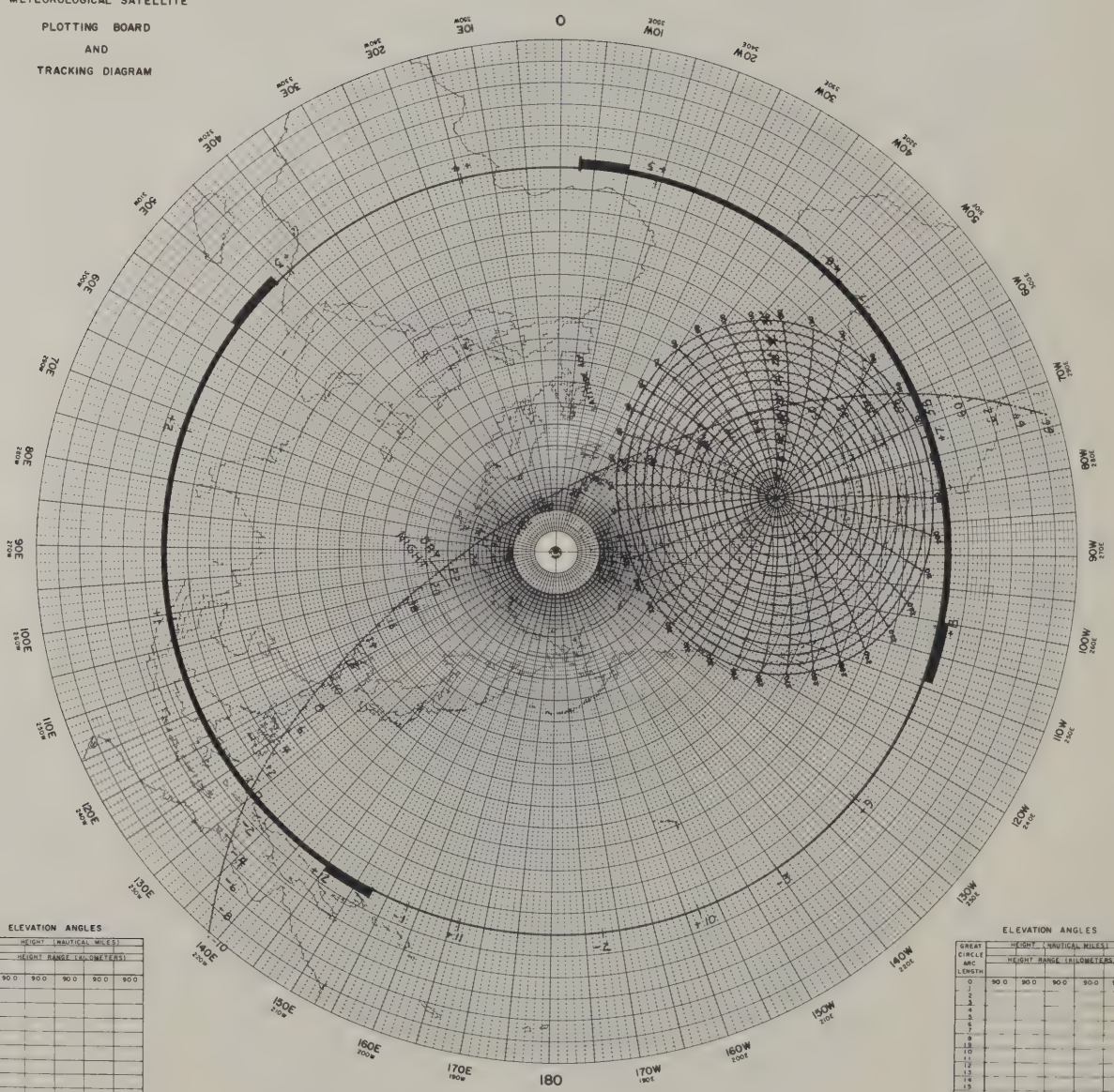

ELEVATION ANGLES

GREAT CIRCLE ARC LENGTH	HEIGHT (NAUTICAL MILES) / HEIGHT RANGE (KILOMETERS)				
0	90.0	90.0	90.0	90.0	90.0
1					
2					
3					
4					
5					
6					
7					
8					
9					
10					
11					
12					
13					
14					
15					
16					
17					
18					
19					
20					
21					
22					
23					
24					
25					
26					
27					
28					
29					
30					
31					
32					
33					
34					
35					

ELEVATION ANGLES

GREAT CIRCLE ARC LENGTH	HEIGHT (NAUTICAL MILES) / HEIGHT RANGE (KILOMETERS)				
0	90.0	90.0	90.0	90.0	90.0
1					
2					
3					
4					
5					
6					
7					
8					
9					
10					
11					
12					
13					
14					
15					
16					
17					
18					
19					
20					
21					
22					
23					
24					
25					
26					
27					
28					
29					
30					
31					
32					
33					
34					
35					

FIGURE C-1

PLOTTING BOARD SET FOR REFERENCE ORBIT

APT SYSTEM

METEOROLOGICAL SATELLITE
PLOTTING BOARD
AND
TRACKING DIAGRAM

APT STATION: Wallops

LOCATION:

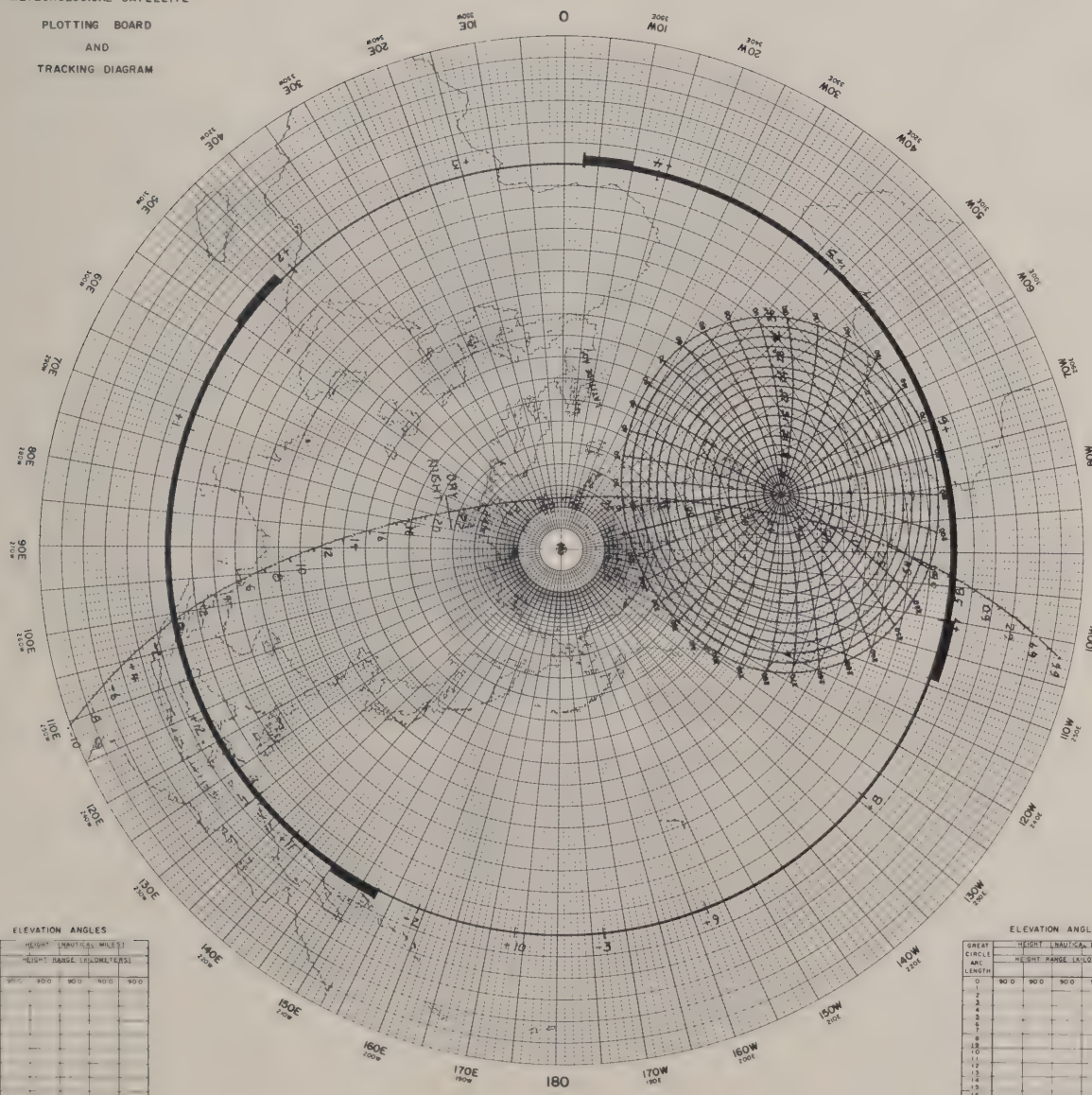

ELEVATION ANGLES

GREAT CIRCLE ARC LENGTH	HEIGHT (NAUTICAL MILES)				
	HEIGHT RANGE (KILOMETERS)				
	900	900	900	900	900
0					
1					
2					
3					
4					
5					
6					
7					
8					
9					
10					
11					
12					
13					
14					
15					
16					
17					
18					
19					
20					
21					
22					
23					
24					
25					
26					
27					
28					
29					
30					
31					
32					
33					
34					
35					

ELEVATION ANGLES

GREAT CIRCLE ARC LENGTH	HEIGHT (NAUTICAL MILES)				
	HEIGHT RANGE (KILOMETERS)				
	900	900	900	900	900
0					
1					
2					
3					
4					
5					
6					
7					
8					
9					
10					
11					
12					
13					
14					
15					
16					
17					
18					
19					
20					
21					
22					
23					
24					
25					
26					
27					
28					
29					
30					
31					
32					
33					
34					
35					

FIGURE C-2
PLOTTING BOARD SET FOR ORBIT 2092

APT TRACKING WORKSHEET

STATION WALLOPS

SPACECRAFT ESSA

ORBIT 2092 DATE 4/25

CAMERA SHUTTER TIME = TONE CHANGE + 2 1/2 SEC. EQ XING LONG. 100.73E

TIME 14:56:35Z

TIME AAN.	TIME (Z)	AZIMUTH	ELEV.†	GREAT CIRCLE DIST.	HEIGHT
32	15:28:35	--	--	--	1420
33	29:35	014	0	--	1420
34	30:35	013	1.3	34.0	1420
35	31:35	012	5.1	30.5	1420
36	32:35	012	9.4	27.0	1420
37	33:35	011	13.5	24.0	1420
38	34:35	010	17.4	21.0	1410
39	35:35	008	22.8	18.0	1410
40	36:35	005	31.0	14.5	1410
41	15:37:35	360	38.6	11.5	1410
42	38:35	353	48.9	8.5	1410
43	39:35	337	59.1	6.0	1410
44	40:35	310	68.6	4.0	1410
45	41:35	265	68.6	4.0	1410
46	15:42:35	238	58.3	6.2	1410
47	43:35	225	46.9	9.0	1410
48	44:35	220	37.1	12.0	1410
49	45:35	215	28.9	15.2	1410
50	15:46:35	213	21.9	18.5	1410
51	47:35	212	15.8	22.0	1410
52	48:35	211	11.4	25.0	1410
53	49:35	210	7.5	28.0	1410
54	15:50:35	210	4.0	31.0	1410
55	51:35	209	0	34.5	1410

MAX. ELEV. MINUTE 44 1/2

PICTURE TIMES

1. TONE CHANGE 15:34:55Z
   PLUS 2 1/2 SEC.
   PICTURE TIME 15:34:58Z
   MINUS: EQ CROSSING TIME
   14:56:35Z
   PICTURE TIME 38:23 AAN*

2. TONE CHANGE 15:40:47Z
   PLUS 2 1/2 SEC.
   PICTURE TIME 15:40:50Z
   MINUS: EQ CROSSING TIME
   14:56:35Z
   PICTURE TIME 44:15 AAN*

3. TONE CHANGE 15:46:39Z
   PLUS 2 1/2 SEC.
   PICTURE TIME 15:46:42Z
   MINUS EQ CROSSING TIME:
   14:56:35Z
   PICTURE TIME 50:07 AAN*

* EQUATOR CROSSING TIME REFERS TO ASCENDING NODE.

AAN -- AFTER ASCENDING NODE

† FROM THE TABLE ON P. 24

APT SYSTEM

METEOROLOGICAL SATELLITE

PLOTTING BOARD

AND

TRACKING DIAGRAM

APT STATION: Wallops

LOCATION:

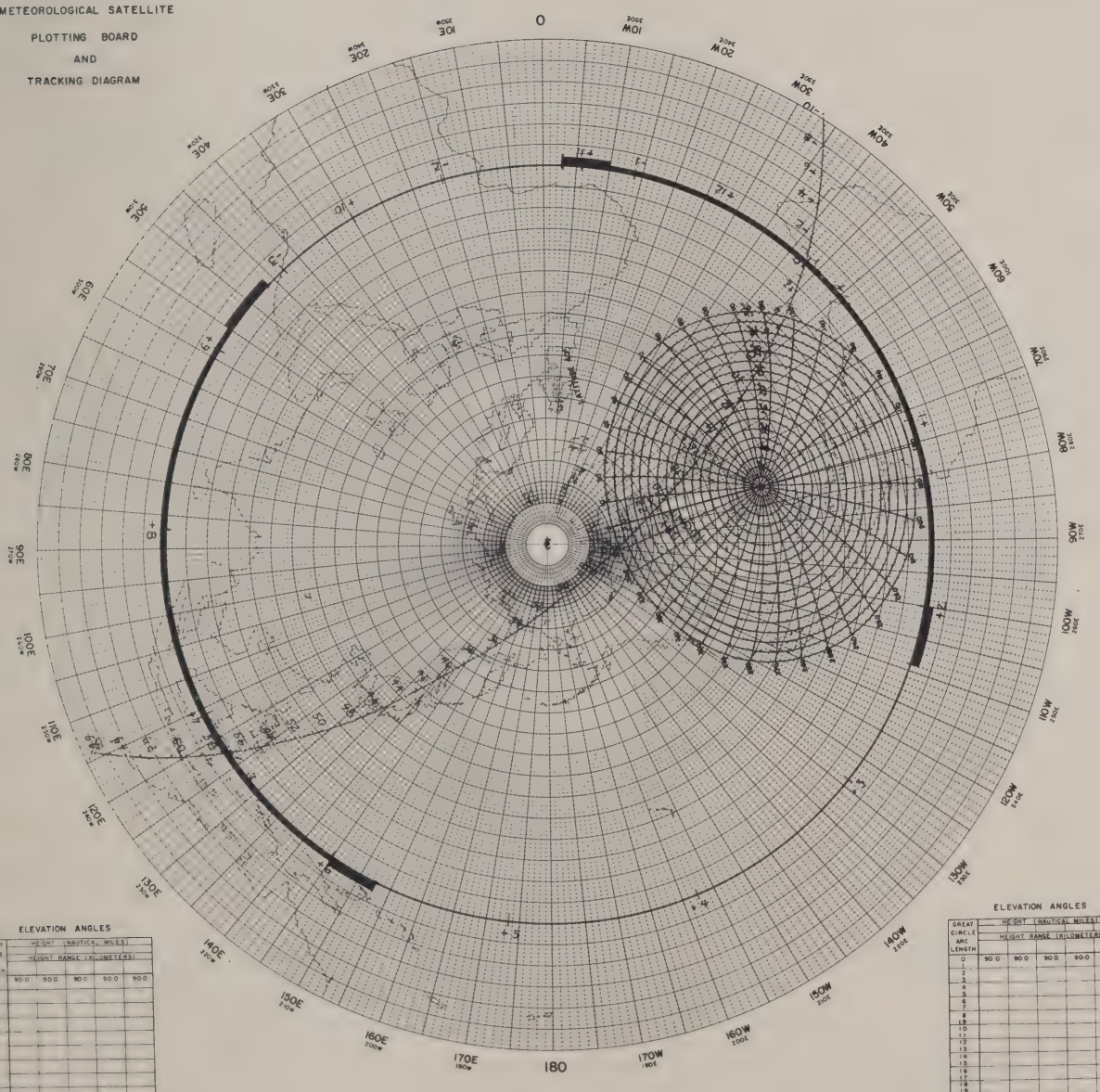

ELEVATION ANGLES

GREAT CIRCLE ARC LENGTH	HEIGHT (NAUTICAL MILES)				
	HEIGHT RANGE (KILOMETERS)				
0	90.0	90.0	90.0	90.0	90.0
1					
2					
3					
4					
5					
6					
7					
8					
9					
10					
11					
12					
13					
14					
15					
16					
17					
18					
19					
20					
21					
22					
23					
24					
25					
26					
27					
28					
29					
30					
31					
32					
33					
34					
35					

ELEVATION ANGLES

GREAT CIRCLE ARC LENGTH	HEIGHT (NAUTICAL MILES)				
	HEIGHT RANGE (KILOMETERS)				
0	90.0	90.0	90.0	90.0	90.0
1					
2					
3					
4					
5					
6					
7					
8					
9					
10					
11					
12					
13					
14					
15					
16					
17					
18					
19					
20					
21					
22					
23					
24					
25					
26					
27					
28					
29					
30					
31					
32					
33					
34					
35					

FIGURE C-3

PLOTTING BOARD SET FOR ORBIT 2097

APT TRACKING WORKSHEET
(DRIR)

STATION WALLOPS
SPACECRAFT ESSA
ORBIT 2097 DATE 4/26

CAMERA SHUTTER TIME = TONE CHANGE + 2 1/2 SEC. EQ.XING LONG. 42:85W
TIME 00:31:01Z

1. TIME AAN.	2. TIME (Z)	AZIMUTH	ELEV.	3. GREAT CIRCLE DIST.	HEIGHT
4	00:35:01	127	0	36.0	1470
5	36:01	124	2.3	33.5	1470
6	37:01	122	6.2	30.0	1470
7	38:01	118	8.7	28.0	1470
8	39:01	115	12.0	25.5	1460
9	00:40:01	110	15.6	23.0	1460
10	41:01	105	19.7	20.5	1460
11	42:01	098	23.4	18.5	1460
12	43:01	088	27.6	16.5	1460
13	44:01	078	30.9	15.0	1460
14	00:45:01	068	31.3	14.5	1450
15	46:01	052	31.3	14.5	1450
16	47:01	041	30.1	15.0	1450
17	48:01	030	26.7	16.5	1450
18	49:01	021	23.6	18.0	1450
19	00:50:01	014	18.7	20.7	1450
20	51:01	008	15.0	23.0	1440
21	52:01	004	12.5	24.7	1440
22	53:01	360	8.4	27.8	1440
23	54:01	357	3.9	31.5	1440
24	00:55:01	353	1.8	33.5	1440
25	56:01	352	0	36.0	1440

DATA LINES
1 00:37:01
2 00:41:01
3 00:45:01
4 00:51:01

4. PICTURE TIMES NOT APPLICABLE

1. TONE CHANGE Z
PLUS _____ 2 1/2 SEC.

PICTURE TIME _____ Z

MINUS: EQ. CROSSING TIME _____ Z

PICTURE TIME AAN*

2. TONE CHANGE Z
PLUS _____ 2 1/2 SEC.

PICTURE TIME _____ Z

MINUS EQ. CROSSING TIME _____ Z

PICTURE TIME AAN*

3. TONE CHANGE Z
PLUS _____ 2 1/2 SEC.

PICTURE TIME _____ Z

MINUS EQ. CROSSING TIME _____ Z

PICTURE TIME ____ AAN*

EQUATOR CROSSING TIME REFERS TO ASCENDING NODE.
AAN -- AFTER ASCENDING NODE.

APPENDIX D

GRIDDING EXERCISE

1. APT Pictures

The following exercise uses data and information found in Appendix A (Daily Predict) and Appendix C (Tracking). The Tracking Worksheet on page 126 indicates that pictures were taken at 15:34:58Z; 15:40:50Z and 15:46:42Z. For purpose of this exercise, picture # 2 (15:40:50Z; 44:15 AAN) will be chosen for gridding.

Preliminary preparation included preparation of the spacecraft ephemeris extrapolation shown on page 131. This particular tabulation was found useful to the author. Users may find other methods more to their liking; these naturally should be used.

1.1 Exercise: Picture Gridding

Picture #2

Time: 15:40:50 GMT

Time: 44 minutes 15 seconds AAN (after equator crossing from tracking worksheet page 126).

1.1.1 Subpoint and Height Interpolation

From worksheet: Orbit #2092

		Longitude	Latitude	Height
Minute	44	79.7°	40.5°	1410 KM
Minute	46	82.3°	34.3°	1410 KM
Difference	120 seconds	+2.6°	6.2°	0

Latitude: 44 minutes & 15 seconds after ascending node

= Latitude, minute 44 + $\frac{15}{120}$ x Difference

= $40.5 + \frac{15}{120} \times (-6.2) =$ 39.7°N

Longitude minute 44:15 =

Longitude minute 44 + $\frac{15}{120}$ x Difference

= $79.7 + \frac{15}{120} \times 2.6 =$ 80.0°W

Height = 1410 KM

The APT Plotting Board may be used to obtain an approximate check of these computations. It may be seen in Figure C2 that the spacecraft location at 44 minutes and 15 seconds after the ascending node is near

40°N and 80°W thus approximately verifying the computations.

1.2 Grid Choice

The grid with central latitude of 39 degrees is chosen as being closest to 39.7 degrees latitude of those grids available.

1.3 Grid Magnification (Column E, page 34)

Height 1410 KM

1400 KM = 10.7 " For an 8" picture

1450 KM = 10.4 "

-0.3 Difference

1410 KM - $10.7 + \frac{10}{50}(-0.3) =$ **10.6"** Between T'S.

2. DRIR Pictures:

The accompanying orbital tabulation provides data (for illustrative purposes) that are not actually required in the gridding procedure when using the overlay method. The orbit from which data are to be acquired is #2097 with an equator crossing (ascending node) of 00:31:01Z at 42.85 degrees west. Note that although the reference orbit is #2091, the computations of equator crossing longitude and time begin with data from orbit 2095 since this minimizes cumulative "round-off" errors. Orbital Height will be 1470 KM at acquisition decreasing to 1440 KM at signal fade. The 800 nautical mile grid is the appropriate one to use in this case. Figure D3b and D3c show this grid with appropriate annotation based on the equator crossing longitude 42.85 degrees west.

Figure D4 is a DRIR picture strip assumed to have been acquired from orbit #2097. Note that data lines at 6, 10, 14 and 20 minutes after ascending node were indicated during data acquisition.

From the Data Sheet (or directly from the Predict Message)

	TIME	SUBPOINT	
AAN	GMT	Latitude	Longitude*
6	00:37:01	18.3	48.3W
10	00:41:01	30.5	52.4W
14	00:45:01	42.6	57.6W
20	00:51:01	60.3	69.8°W

* Used to check grid accuracy - Figures D5 and 6 show the picture with grid overlay and the final gridded picture.

DATA ACQUISITION 4/25/1968

NODAL INCREMENT 1 Hr. 54 Min. 53 Sec.

NODAL LONGITUDINAL INCREMENT 28.71

REFERENCE ORBIT

ASCENDING NODE 129.44°E

REF ORB # & DATE 4/25	NODES TO ACQ. ORBIT	DATA ACQ. ORBIT #	REF. ORBIT ASC. NODE TIME	INCR. TO ACQ. ORBIT (TIME)	ACQ. ORBIT ASC. NODE TIME	INCR TO ACQ. ORB. LONG.	ACQ. ORBIT ASC NODE LONG.
2091	0	2091	13:01:42	0	13:01:42	0	129.44°E
2091	+1	2092	13:01:42	1:54:53	14:56:35	28.71	100.73 E
2091	+2	2093	13:01:42	3:49:46	16:51:28	57.42	72.02 E

REF.- Reference INCR.- Increment ORB. - Orbit

ACQ.- Acquisition LONG.- Longitude LAT. - Latitude

ASC.- Ascending AAN - After Ascending Node # - Number

TIME AAN	REF ORB LONGITUDE	INCR.	1ST ACQ. ORB. (# 1091) LONGITUDE	INCR.	2ND ACQ. ORB. (# 2092) LONGITUDE	INCR.	3RD ACQ. ORB. (# 2093) LONGITUDE	LAT.	HEIGHT
32	9.9W	0	9.9	28.7	38.6	57.4	67.3	74.1	1420
34	24.2	-	24.2	28.7	52.9	57.4	81.6	69.4	1420
36	33.3	-	33.3	28.7	62.0	57.4	90.7	64.1	1420
38	39.6	-	39.6	28.7	68.3	57.4	97.0	58.4	1410

TIME AAN	REF ORB. LONGITUDE	INCR.	1ST ACQ. ORB (#1091) LONGITUDE	INCR.	2ND ACQ. ORB. (#2092) LONGITUDE	INCR.	3RD ACQ. ORB (#2093) LONGITUDE	LAT.	HEIGHT
40	44.3	-	44.3	28.7	73.0	57.4	101.7	52.6	1410
42	47.9	-	47.9	28.7	76.6	57.4	105.3	46.6	1410
44	51.0	-	51.0	28.7	79.7	57.4	108.4	40.5	1410
46	53.6	-	53.6	28.7	82.3	57.4	111.0	34.3	1410
48	55.9	-	55.9	28.7	84.6	57.4	113.3	28.2	1410
50	58.0	-	58.0	28.7	86.7	57.4	115.4	22.0	1410
52	60.0	-	60.0	28.7	88.7	57.4	117.4	15.8	1410

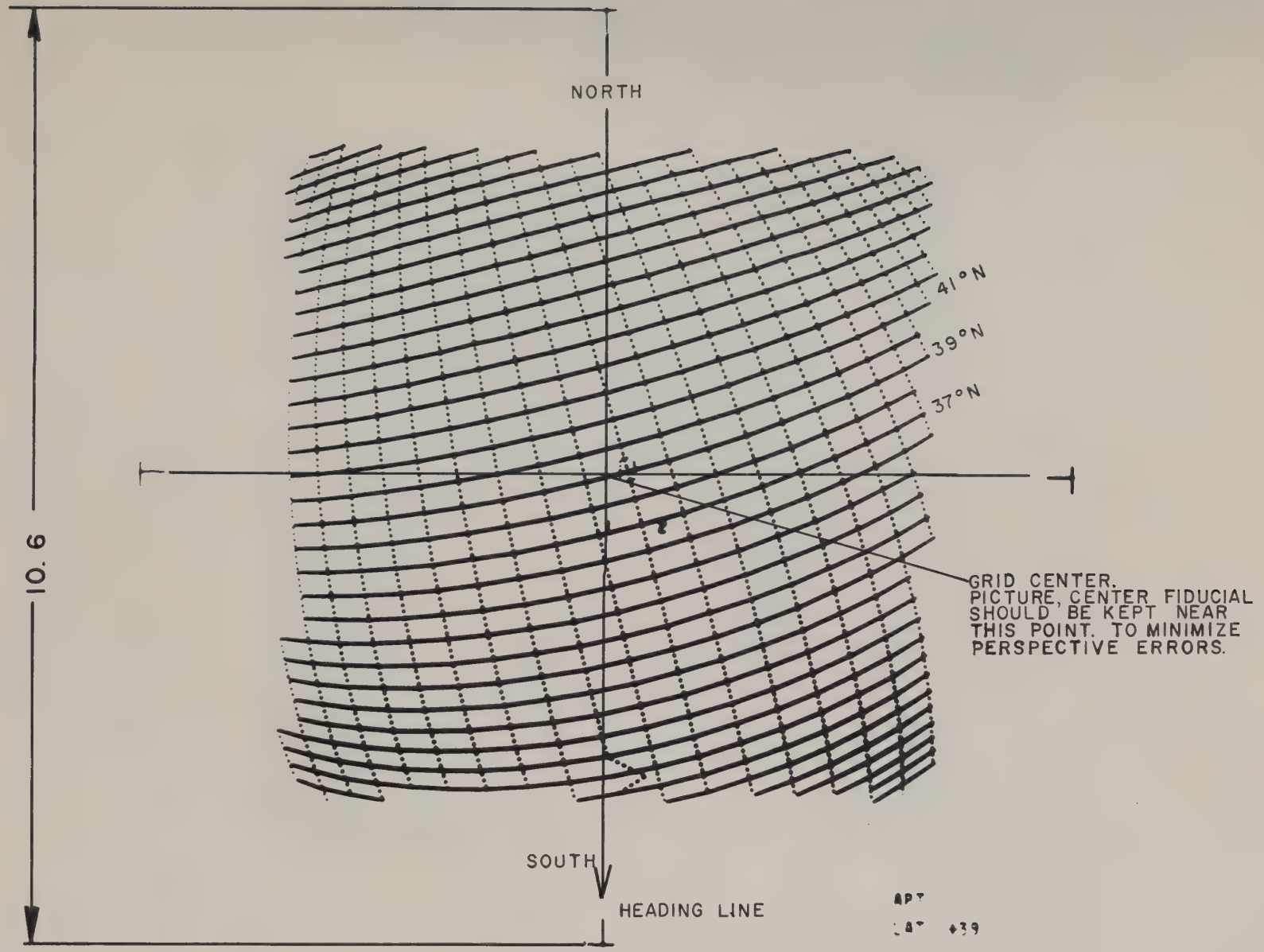
NORTH
41°N
39°N
37°N
GRID CENTER.
PICTURE CENTER FIDUCIAL
SHOULD BE KEPT NEAR
THIS POINT. TO MINIMIZE
PERSPECTIVE ERRORS.
SOUTH
HEADING LINE
9.01

FIGURE D I

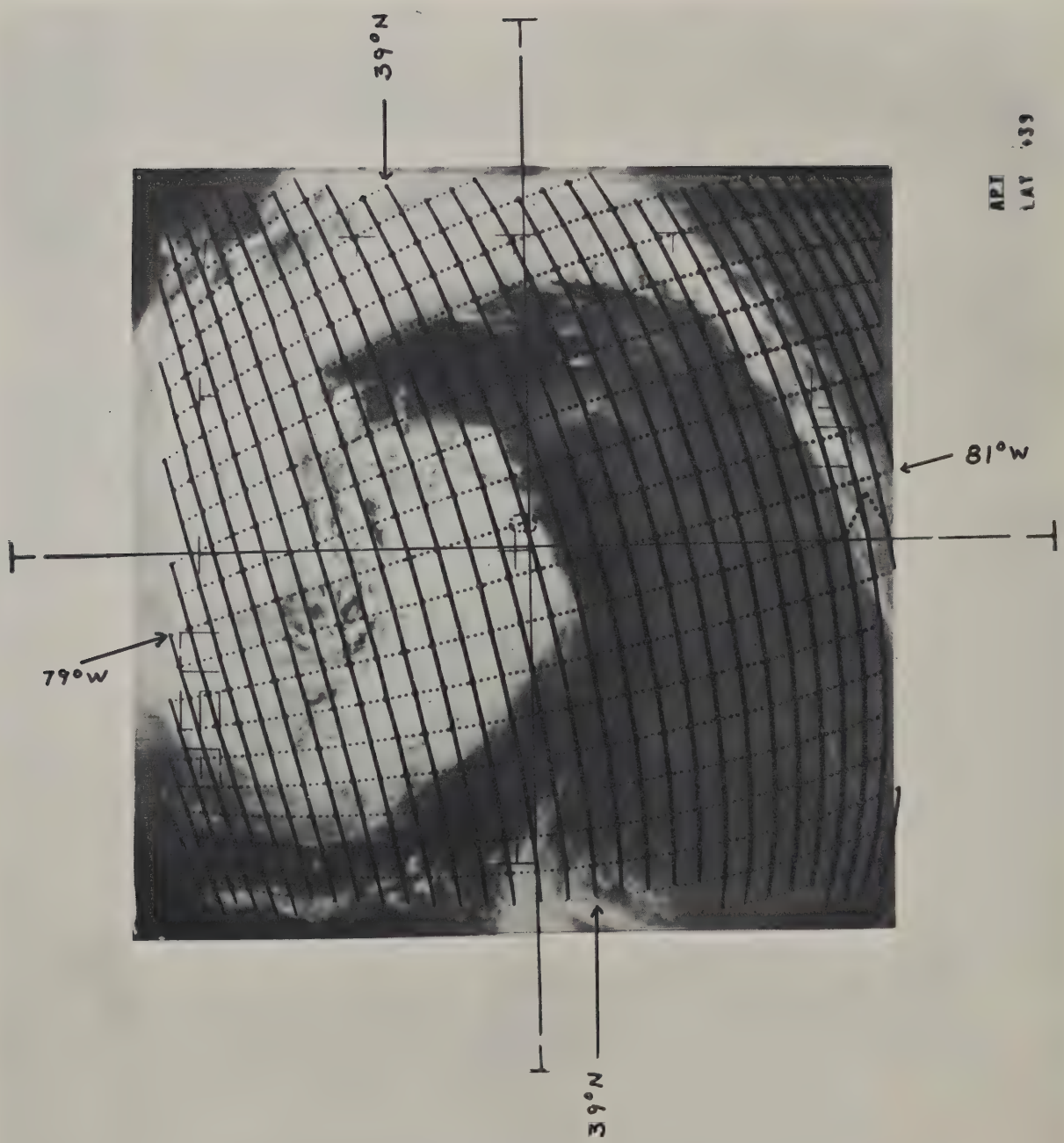

FIGURE D2
APT PICTURE WITH GRID OVERLAY

DATE OF ACQUISITION

NODAL INCREMENT 1:54:53

NODAL LONGITUDINAL INCREMENT 28.71

ORBIT 2095 ASCENDING NODE 14.57°E*

REF. ORB.# & DATE	NODES TO ACQ. ORBIT	DATA ACQ. ORBIT #	(REF.) ORBIT ASC. NODE TIME	INCR. TO ACQ.ORBIT TIME	ACQ ORBIT ASC NODE TIME (Z)	INCR TO ACQ ORB LONG.	ACQ ORBIT ASC NODE LONGITUDE
2091	5	2096	2095* 20:41:15Z	1:54:53	4/25 22:36:08	28.71	14.14W
2091	6	2097	20:41:15Z	3:49:46	4/26 00:31:01	57.42	42.85
2091	7	2098	20:41:15Z	5:44:39	4/26 02:25:54	86.13	71.56

* Part 1, Line 2

TIME AAN	REF ORB LONG.	INCR 5x 28.7	1ST ACQ ORB (#2096) LONGITUDE	INCR 6x 28.7	2ND ACQ ORB (#2097) LONGITUDE	INCR 8x 28.7	4TH ACQ ORB (#2099) LONGITUDE	LAT	HEIGHT
02	127.7E	143.5	15.8W	172.2	44.5	229.6	101.9	6.1	1480
04	125.3	143.5	18.2	172.2	46.9	229.6	104.3	12.3	1470
06	123.9	143.5	19.6	172.2	48.3	229.6	105.7	18.3	1470
08	121.9	143.5	21.6	172.2	50.3	229.6	107.7	24.4	1460

354-645 O - 69 - 10

TIME AAN	REF. ORB. LONGITUDE	INCR.	1ST ACQ. ORB. (2096) LONGITUDE	INCR 6x 28.7	2ND ACQ ORB (#2097) LONGITUDE	INCR 8x 28.7	4TH ACQ ORB (2099) LONGITUDE	LAT.	HEIGHT
10	119.8	143.5	23.7	172.2	52.4	229.6	109.8	30.5	1460
12	117.3	143.5	26.2	172.2	54.9	229.6	112.3	36.6	1460
14	114.6	143.5	28.9	172.2	57.6	229.6	115.0	42.6	1440
16	111.4	143.5	32.1	172.2	60.8	229.6	118.2	48.6	1450
18	107.5	143.5	36.0	172.2	64.7	229.6	122.1	54.5	1450
20	102.4	143.5	41.1	172.2	69.8	229.6	127.2	60.3	1440
22	95.4E	143.5	48.1	172.2	76.8	229.6	134.2	65.9	1440

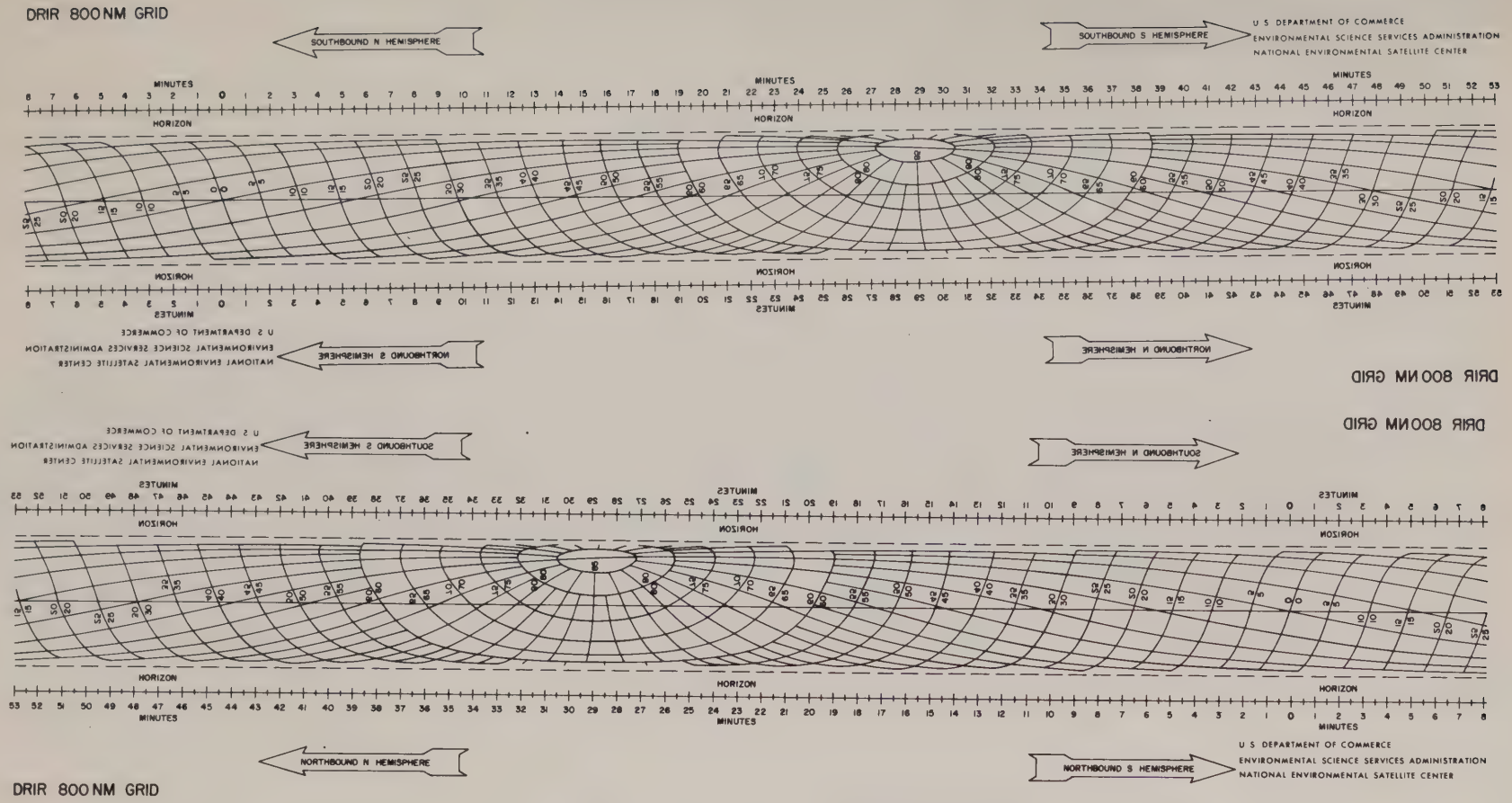

FIGURE D 3A

DRIR GRID 800 NAUTICAL MILES

DRIR 800NM GRID
SOUTHBOUND N HEMISPHERE
MINUTES
HORIZON
HORIZON
MINUTES
HORIZON
HORIZON
MINUTES
NORTHBOUND S HEMISPHERE
U S. DEPARTMENT OF COMMERCE
ENVIRONMENTAL SCIENCE SERVICES ADMINISTRATION
NATIONAL ENVIRONMENTAL SATELLITE CENTER

FIGURE D- 3B

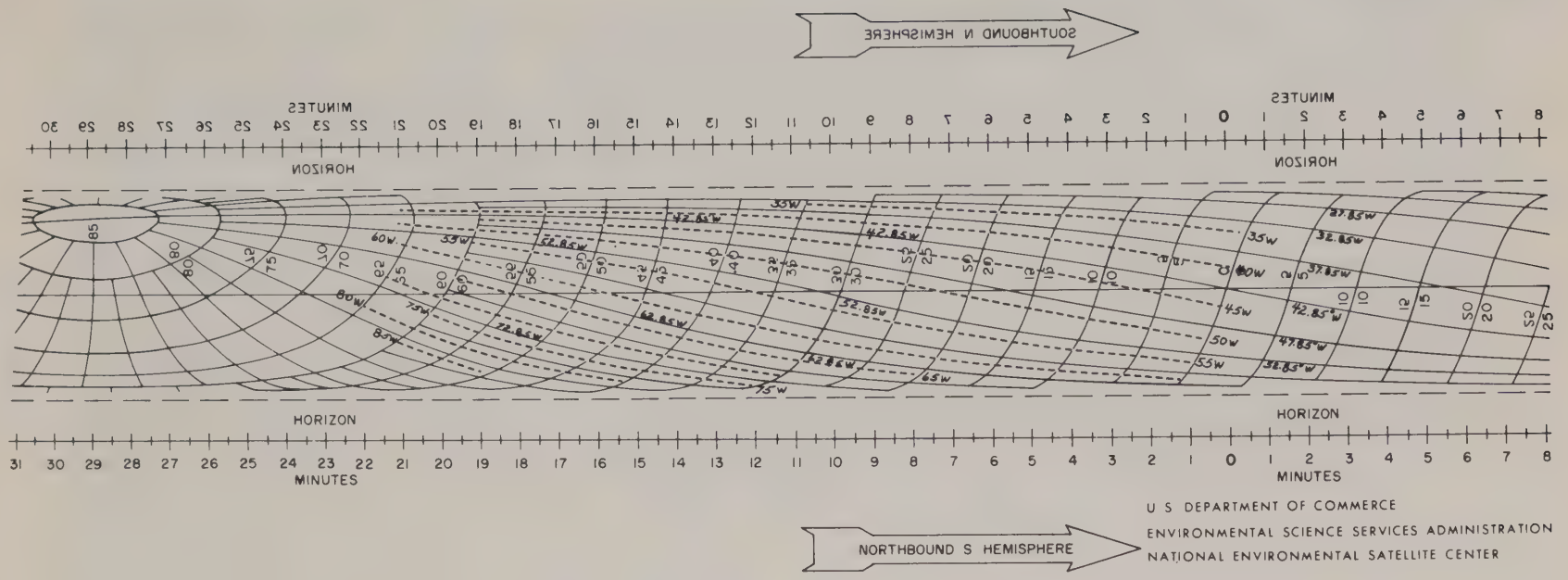
SOUTHBOUND N HEMISPHERE
HORIZON
MINUTES
HORIZON
MINUTES
NORTHBOUND S HEMISPHERE
U S DEPARTMENT OF COMMERCE
ENVIRONMENTAL SCIENCE SERVICES ADMINISTRATION
NATIONAL ENVIRONMENTAL SATELLITE CENTER

FIGURE D-3C

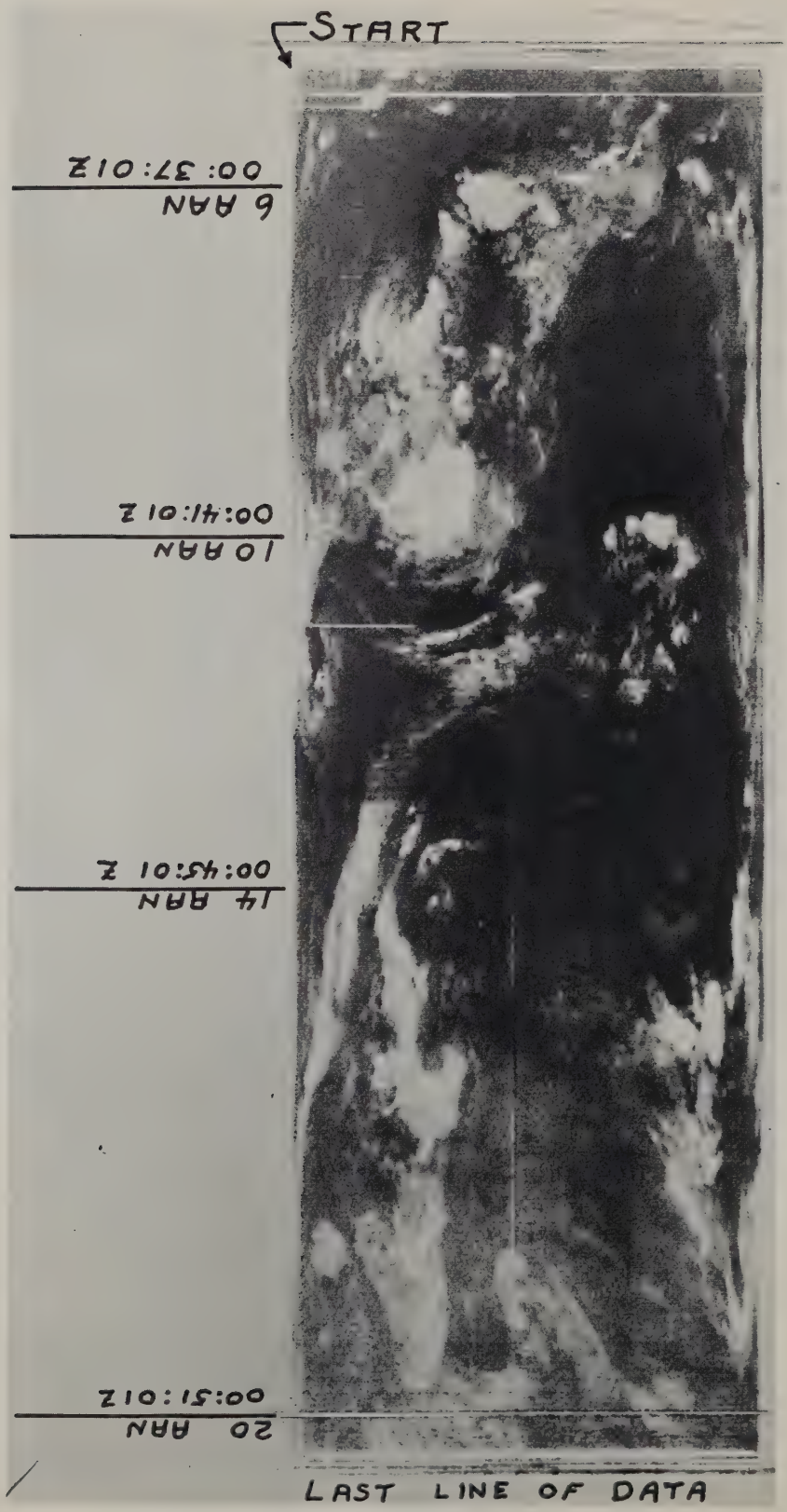
START
6 AM
00:37:01Z
10 AM
00:41:01Z
14 AM
00:45:01Z
20 AM
00:51:01Z
LAST LINE OF DATA

Figure D-4.

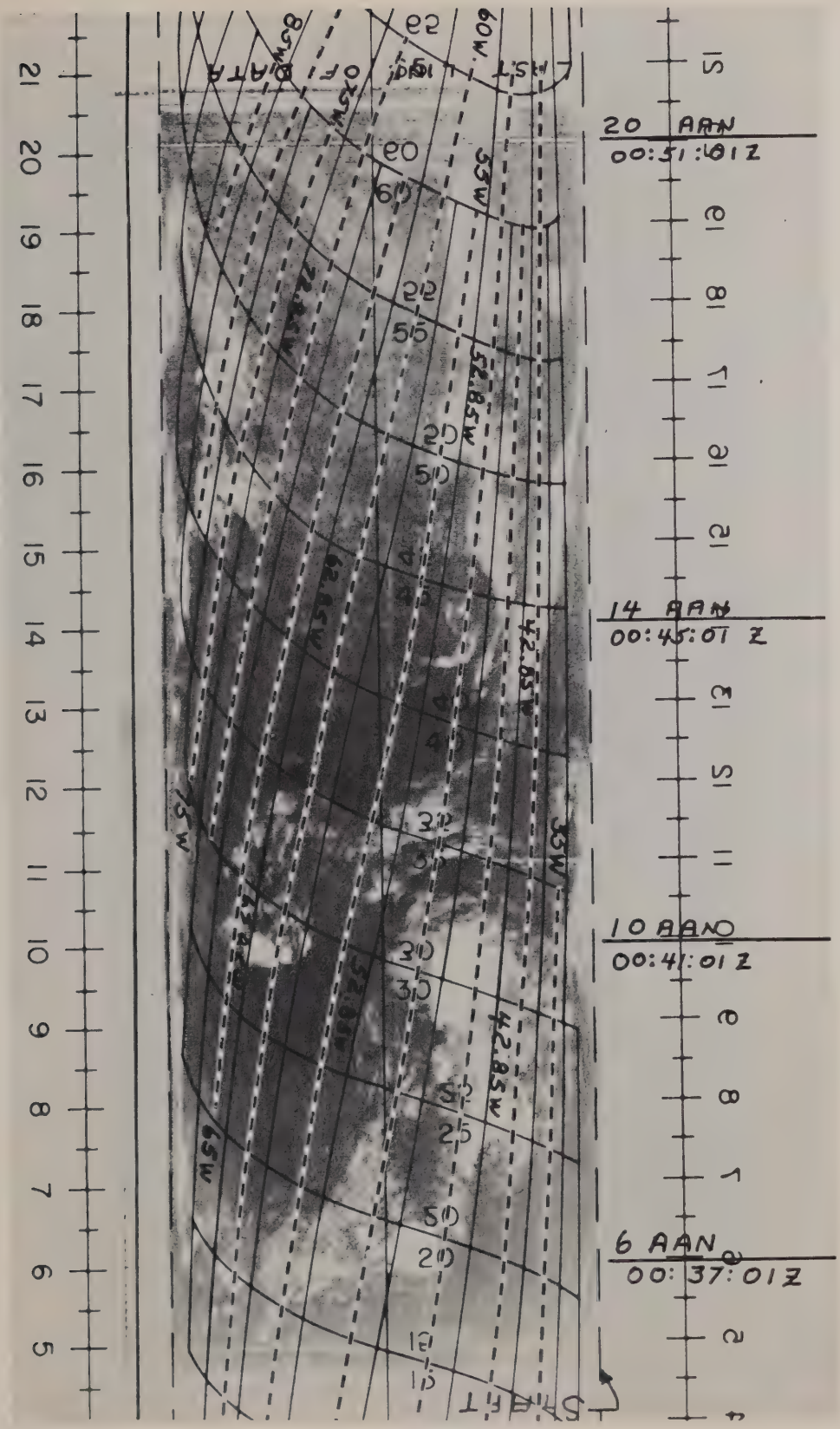
20 AAN
00:51:01Z
14 AAN
00:45:01Z
10 AAN
00:41:01Z
6 AAN
00:37:01Z
60W
55W
52.85W
42.85W
65W

Figure D-5.

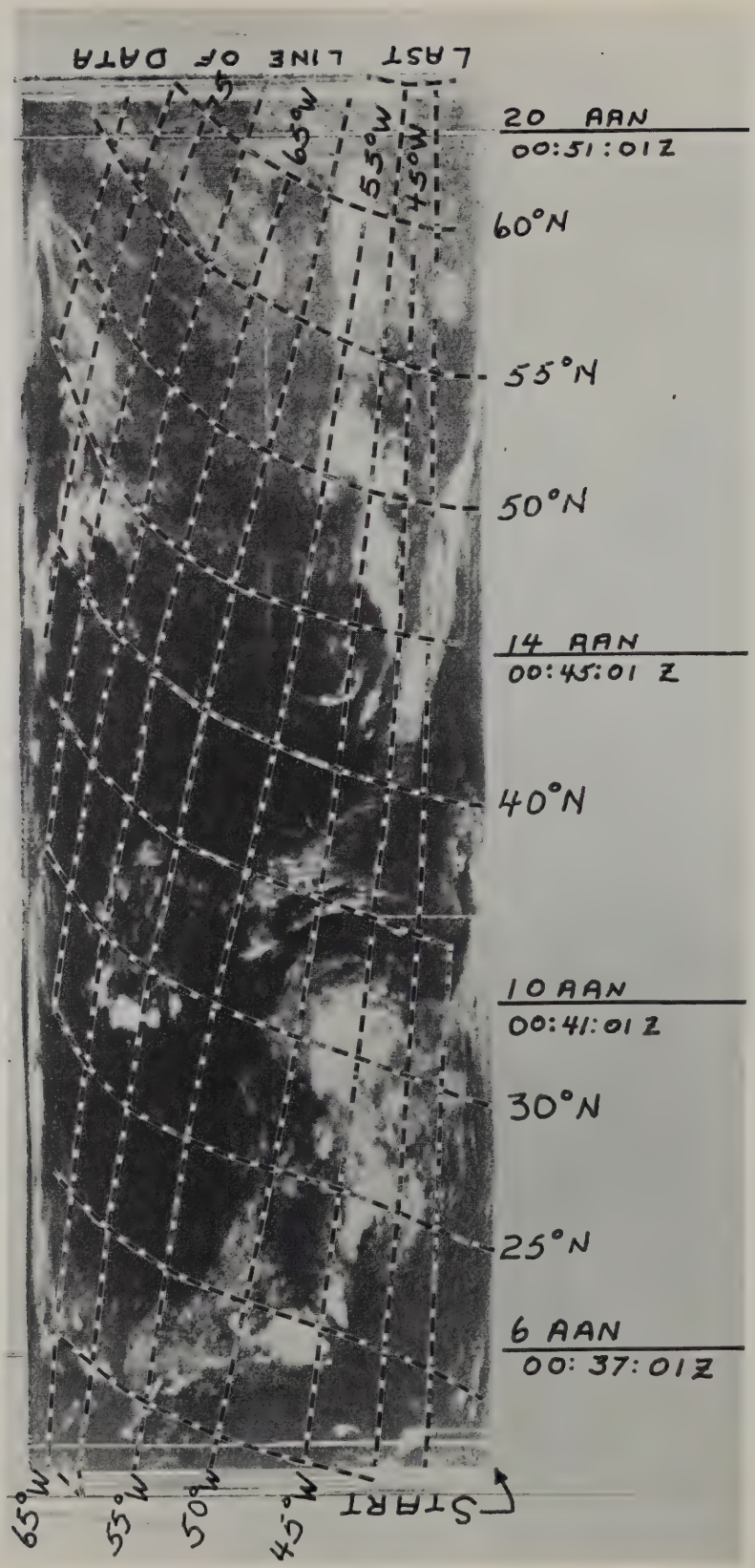
LAST LINE OF DATA
65°W
63°W
53°W
45°W
20 AAN
00:51:01Z
60°N
55°N
50°N
14 AAN
00:45:01 Z
40°N
10 AAN
00:41:01 Z
30°N
25°N
6 AAN
00:37:01Z
START
65°W
55°W
50°W
45°W

Figure D-6.

ANOMALISTIC PERIOD OF SATELLITE: The time elapsing between successive passages of a satellite through the perigee.

APOGEE: The point in its orbit at which the satellite is farthest from the center of the earth.

APSIS: The points in an elliptic orbit at which the radius vectors reach a maximum or minimum (e.g., perigee and apogee of a satellite orbit). The line joining these two points is called the line of apsides.

APT: Automatic Picture Transmission System - a vidicon camera that "takes" and immediately transmits cloud pictures to all suitably equipped ground stations within range. This system is independent of the AVCS.

ARGUMENT OF PERIGEE: The geocentric angle of the perigee measured in the orbital plane from its ascending node in the direction of motion.

ARGUMENT OF SATELLITE: The geocentric angle of a satellite measured in the orbital plane from the ascending node in the direction of motion.

ARGUMENT OF SATELLITE AT MINIMUM (MAXIMUM) NADIR ANGLE: (See Argument of Satellite and Nadir Angle).

ASCENDING NODE (AN): The point at the equator at which the satellite in its orbital motion crosses from the southern to the northern hemisphere. Terrestrial Ascending Node (TAN) is given in degrees longitude. Celestial Ascending Node (CAN) is given on right ascension hours, minutes, etc.

ASCENDING NODE TIME: The time when the satellite passes the ascending node.

ATTITUDE (SATELLITE): The position of the axis of a satellite with respect to (a) its orbital plane, (b) the earth's surface, or (c) any fixed set of coordinates.

AVCS: Advanced Vidicon Camera System.

AZIMUTH (α): A horizontal direction expresses in degrees measured clockwise from an adopted reference direction, usually true north.

BULGE OF THE EARTH ($R_E - R_P$): The difference between the equatorial and the polar radii of the earth.

CDA: Command and Data Acquisition Station (see Data Acquisition Station).

CELESTIAL: The prefix to designate lines or points which have been projected onto the celestial sphere by means of the radials through the center of the earth.

CELESTIAL EQUATOR: The great circle along which the plane of the earth's equator intersects the celestial sphere.

CELESTIAL SPHERE: An imaginary sphere of infinite radius with its center located at the observer or at the center of the earth. In satellite meteorology the center of the celestial sphere is at the center of the earth. Lines or points are projected onto the celestial sphere using radials through the center of the earth.

CELESTIAL SUBSATELLITE POINT: A point on the celestial sphere the declination of which is identical to the geocentric latitude of TSP and the right ascension of that of TSP. (See SUBPOINT TRACK).

DATA ACQUISITION STATION (CDA): A ground station at which various functions to control satellite operations and to obtain data from the satellite are performed. The CDA transmits programming signals to the satellite, and commands transmission of data to the ground.

DECLINATION (δ): The angular distance of an object north (+) or south (-) from the celestial equator measured along the hour circle passing through the object.

DEGRADATION: The lessening of picture image quality because of "noise", or any optical, electronic, or mechanical distortions in the image-forming system.

DESCENDING NODE (DN): The southbound equator crossing of the satellite; given in degrees longitude, date, and time for any given orbit or pass.

DIRECT ORBIT: The orbit with inclination between 0° and 90° measured counterclockwise from the equator. Same as the prograde orbit.

DISTORTION: An apparent warping and twisting of a picture image received from a satellite. This distortion has two causes: electronic and optical. "Electronic Distortion" is caused by imperfections in the circuitry, the tape recorder, the vidicon tube structure, the transmission system , or the signal characteristics. "Optical Distortion" is caused by the characteristics of the lens and optical alignment.

DRIR: Direct Readout Infrared.

ECLIPTIC: The great circle in which the plane of the earth's orbit intersects the celestial sphere.

ESSA: Abbreviation for Environmental Science Services Administration.

ESSA: Acronym for Environmental Survey SAtellite.

EQUATORIAL ORBIT: Orbit with zero degree inclination.

FIDUCIAL MARKS: Index marks rigidly connected with the camera optical system so that they form images on the negative.

GAMMA: Gamma is the angle at the satellite between the satellite spin-axis and the satellite-sun line.

HEADING LINE: The instantaneous projection of the spacecraft velocity vector on the earth's surface.

HRIR: High Resolution InfraRed.

IMAGE PRINCIPAL LINE: (See Principal Line).

IMAGE RASTER LINE: One line of raster on an image plane. (See Raster).

INCLINATION (OF SATELLITE ORBIT): (See Orbit Inclination).

LATITUDE-LONGITUDE GRID: A latitude-longitude grid is a form of perspective grid in which the quadrilaterals are latitudes and longitudes.

LOCAL VERTICAL: A line perpendicular to the surface of the earth.

MHZ: Abbreviation for Megahertz (million cycles per second).

NADIR ANGLE: The angle measured at the satellite between a specific axis or ray and the local vertical.

NASA: Abbreviation for National Aeronautics and Space Administration.

NODE: The points at the equator at which the satellite in its orbital motion crosses the equator. The line connecting the ascending and the descending nodes is called the line of nodes.

NODAL PERIOD: The time elapsing between successive passages of the satellite through successive ascending nodes.

NODAL INCREMENT: Degrees of longitude between successive ascending nodes.

NOISE: A voltage received through an antenna system or within the ground amplifier and other electronics that does not correspond to any intended signal. The "noise" seen on TIROS pictures is ordinarily in the form of small specks; occasionally noise appears in the form of bands or streaks along raster lines.

OBJECT SPACE ANGLE: The angle between two rays in space that intersect at the front nodal point of a camera lens.

OPTICAL AXIS: A straight line passing through the front and rear nodal points of a camera lens. The direction on the axis is considered positive from the rear to the front nodal points.

OPTICAL AND ELECTRONIC DISTORTIONS: (See Distortion).

ORBIT: The path which a celestial object follows in its motions through space, relative to some selected point.

ORBIT INCLINATION: The angle between the plane of the satellite orbit and the earth's equatorial plane. Inclination of retrograde orbit is expressed by 180 degrees minus the prograde inclination.

ORBIT NUMBER: In satellite meteorology orbit number refers to a particular circuit beginning at the satellite ascending node. The orbit number from launch to the first ascending node is designated zero, thereafter the number increases by one at each ascending node.

ORBITAL PLANE: The plane, or two dimensional space which contains the path of an orbiting satellite.

ORBIT, POLAR: An orbit which passes directly over both the geographic poles of the earth.

ORBIT, SUN-SYNCHRONOUS: (See Sun-Synchronous Orbit).

PERIGEE: The point in its orbit at which the satellite is closest to the center of the earth.

PERIGEE RATE: Rate of change of the argument of perigee. It is usually measured in degrees per day.

PRECESSION RATE ($\dot{\Omega}$): The fixed space angular motion of the orbital line of nodes; positive to the East, negative to the West. Precession rate for a sun-synchronous orbit is -0.986 degrees per day.

PITCH: Angular deviation of the camera axis from the vertical along the orbital plane at the time of picture taking.

PRINCIPAL DISTANCE: The distance measured along the optical axis either from the nodal point or the interior perspective center to the image or target plane.

PRINCIPAL LINE: A line of intersection between the principal plane and the image plane (Image Principal Line), or principal plane and the earth.

PRINCIPAL PLANE: The plane which includes the optical axis of a camera and the local vertical through the front nodal-point of a satellite camera lens.

PRINCIPAL POINT: The point of intersection of the optical axis of the camera with the image plane, or with the earth.

PROGRADE ORBIT: (See Direct Orbit).

R/O: Abbreviation for readout orbit.

RASTER: The pattern followed by the electron-beam exploring-element scanning the screen of a television transmitter or receiver. The scanning pattern or raster of the vidicon used in ESSA satellites is, theoretically, a series of straight parallel lines.

RASTER LINE: One scan line of a TV system.

READ-OUT STATION: (See Data Acquisition Station).

RESOLUTION: The ability of a film, a lens, a combination of both, or a vidicon system to render barely distinguishable a standard pattern of black and white lines. When the resolution is said to be 10 lines per millimeter, it means that the pattern whose line-plus-space width is 0.1 mm is barely resolved, the finer patterns are not resolved, and the coarser patterns are more clearly resolved.

RETROGRADE ORBIT: The orbit with inclination between 0° and 90° measured clockwise from the equator.

RIGHT ASCENSION: The arc measured eastward along the celestial equator from the vernal equinox to the great circle passing through the celestial poles and the object projected onto the celestial sphere. This angle is frequently given in hours and minutes ---24 hours equivalent to 360 degrees.

ROLL: Angular deviation of the satellite axis from the plane tangent to the orbital plane.

SUBPOINT TRACK: Locus of subsatellite points on the earth (TSP), on image, or on a celestial sphere.

SUBSATELLITE POINT: Intersections of the local vertical passing through the satellite with the earth's surface, with the image plane and with the celestial sphere.

SUBSOLAR POINT (SS): Intersection of the local vertical through the sun with the surface of the earth.

SUN-SYNCHRONOUS ORBIT: Nominally a retrograde, quasi-polar orbit such that the satellite crosses the equator on ascending node always at the same local solar time.

SYNCHRONOUS SATELLITE: A satellite in a west to east orbit of the earth at an altitude of 22,300 statute miles. At this altitude it circles the axis of the earth once in 24 hours. Thus its speed in orbit is synchronous with the earth's rotation.

TERRESTRIAL: The term to designate a line or a point on the earth's surface.

TIME PAST ASCENDING NODE: The amount of time for a body in orbit to advance from the last ascending node to an arbitrary position.

TIME PAST PERIGEE: The amount of time for a body in orbit to advance from the last perigee to an arbitrary position.

TIROS: Acronym for Television InfraRed Observation Satellite.

TRACK: A line connecting successive positions of a moving point.

VERNAL EQUINOX: (Also called the first of Aries). The point of intersection of the celestial equator with the ecliptic, at the point where the sun crosses from the south to the north side of the equator.

VERTICAL ANGLE: The angle between the local vertical and an oblique plane. The direction of the vertical plane, which is perpendicular to the oblique plane, defines the orientation of the vertical angle.

VIDICON: A photoconductive image pickup or television type tube. Each television camera in the satellite consists of a set of optics, a focal plane shutter and a vidicon tube. The image is focused on the vidicon screen by the lens, and the vidicon scanner transforms the image to an electric signal which can be transmitted or recorded on magnetic tape.

YAW: Angular deviation of satellite axis from the orbital path in the plane tangent to the orbital path.

U. S. GOVERNMENT PRINTING OFFICE : 1969 O - 354-645


DEPARTMENT OF COMMERCE
UNITED STATES OF AMERICA